2-5-2004

Evaluation of interlayer bonding in hot mix asphalt pavements

Stephen M. Gomba
Rowan University

EVALUATION OF INTERLAYER BONDING

IN HOT MIX ASPHALT PAVEMENTS

by
Stephen M. Gomba

A Thesis

Submitted in partial fulfillment of the requirements of the
Master of Science Degree
of
The Graduate School
at
Rowan University
February 5, 2004

EVALUATION OF INTERLAYER BONDING

IN HOT MIX ASPHALT PAVEMENTS

Prepared by:

Stephen Gomba

Approved by:

Yusuf Mehta
Assistant Professor, Rowan University
Thesis Advisor

Douglas Cleary
Associate Professor, Rowan University
Thesis Committee Member

Beena Sukumaran
Associate Professor, Rowan University
Thesis Committee Member

Ralph Dusseau
Civil & Environmental Engineering Chair, Rowan University
Thesis Committee Member

ABSTRACT

Stephen M Gomba
EVALUATION OF INTERLAYER BONDING IN HOT MIX ASPHALT PAVEMENTS
2003/04
Dr. Yusuf Mehta
Master of Science in Civil Engineering

This study investigates the potential of falling weight deflectometer (FWD) data for use in quantifying the level of interlayer bonding achieved in pavements. Data was obtained and used from the Federal Aviation Administration's (FAA) National Airport Pavement Test Facility located in Atlantic City, New Jersey. In this test facility, a section of the pavement had encountered a loss of bond between lifts of the surface hot mix asphalt (HMA) layer. FWD tests had been performed at locations throughout the pavement, on a monthly basis for the duration of the loading period. The FWD data, along with detailed material property data, was available through the FAA Airport Technology Research and Development Branch's web page.

The material properties and FWD data were used to calculate the stiffness moduli for each layer in the pavement using forward calculations. It was determined that calculated stiffness moduli for surface layers can be used as a parameter to determine the quality of interlayer bonding. To further investigate the level of bonding, a tack failure ratio was determined for each section, by modifying an equation for the equivalent modulus of two combined asphalt layers, and that was correlated to the slip between layers. This study developed a framework for the application of FWD data in identifying and quantifying interlayer slippage in HMA pavements.

ACKNOWLEDGEMENTS

I would like to thank my thesis committee members for reviewing my thesis and for offering guidance in my work. I would also like to thank my fellow graduate students, who have offered encouragement throughout this project. A special thank you goes to Jeremy Stevenson, a graduate student whose research also involved hot mix asphalt. He helped me in overcoming obstacles in my project during several brainstorming sessions, and was always willing to review my writing and presentations.

Most especially, I would like to thank my advisor, Yusuf Mehta. I was fortunate enough to have worked with him during my last two semesters of engineering clinic as an undergraduate, and then to have him as my thesis advisor as a graduate. From our first day of clinic together, he has challenged me, always pushing for a higher level of effort and results of higher quality. During this particular project, his challenges have been particularly important to me, as they have taught me many valuable lessons and have helped me grow as an engineer. Lastly, perhaps his greatest help to me has been his endless enthusiasm, which was a great driving force for me throughout this project.

TABLE OF CONTENTS

LIST OF FIGURES

LIST OF TABLES

CHAPTER ONE

INTRODUCTION

1.1. Problem

The Federal Aviation Administration's (FAA) National Airport Pavement Test Facility (NAPTF), located in Atlantic City, New Jersey, is a fully enclosed pavement test track. In this facility, nine sections of different pavement structures are evaluated under accelerated aircraft loading. One of the sections experienced extensive slipping between layers. Similar failures have been observed on highways in various states, such as Florida, Louisiana, Minnesota, New Jersey, and Wisconsin. This slippage can cause secondary failures like cracks and potholes, resulting in extensive failure of the pavement structure.

The slippage may be caused by poor bonding, which in turn may be caused by: improper amount of tack coat, improper tack coat type, poor lower layer condition, tack coat application in cold or wet weather, inadequate structural design of the surface course, and non-uniform application of tack.

In order to prevent such failures, poor bonding should be identified immediately after construction. If interlayer bonding failure can be detected in a new pavement, then steps could be taken to prevent such failures by modifying construction methodology.

The purpose of this study is to form a framework to use nondestructive Falling Weight Deflectometer (FWD) data to identify the lack of bonding in hot mix asphalt pavements. In particular, this study will address the lack of bonding between lifts in

asphalt layers with the same material properties. The intent is that eventually interlayer bonding will be evaluated during the construction of pavements. The ability to identify bonding failures directly after construction will save money by minimizing future rehabilitation caused by the interlayer bonding failures.

1.2. Hypothesis

The hypotheses of this study are:

1. Surface layer moduli calculated from FWD data can be used to identify a lack of interlayer bonding in pavements.
2. The effect of slip between two asphalt layers of similar properties can be determined by the ratio of moduli of the top layer and the moduli of the bottom layer.

1.3. Significance of Research

This study will provide a tool for state agencies to detect interlayer bonding failure from widely used FWD data. State agencies could use this methodology to detect failures immediately after construction of a given section and rectify, if necessary, any construction procedure to prevent them in the future. This methodology could also be used as a pavement management and rehabilitation tool, provided that the agencies have material data independently available. This methodology could reduce expenses for all, due to less pavement maintenance costs on the part of the roadway owners and less vehicle maintenance costs for the roadway users.

1.4. Study Objectives

The objectives of this study were:

1. To identify bonding failure, based on comparisons between surface layer moduli of failed and unfailed pavement sections calculated from FWD data.
2. To calculate the slip at the interlayer in the failed section.
3. To correlate the ratio of failed to unfailed pavement layer moduli with the effect of slip at the interlayer.
4. To develop a framework for using FWD data to identify interlayer bonding failures.

1.5. Research Approach

The following approaches were taken to accomplish each objective of this study:

Objective 1

1. Use pavement material data and established correlations to determine values of expected layer moduli for all layers in the pavement being analyzed.
2. Backcalculate layer moduli of the failed and unfailed pavement sections, assuming full bonding in both sections.
3. Check for reasonableness of backcalculated layer moduli.
4. If unreasonable backcalculated moduli are derived, forward calculate layer moduli of the failed and unfailed pavement sections, assuming full bonding in both sections.
5. If forward calculations are used, check for reasonableness of forward calculated layer moduli.

6. Using an established correlation, normalize the forward calculated surface layer moduli of failed and unfailed sections to a common temperature.
7. Compare the normalized calculated surface layer moduli of the failed and unfailed sections to determine if the failed sections can be identified by comparisons of failed and unfailed calculated surface layer moduli.

Objective 2

1. Calculate the stresses and vertical displacements in the failed section for each FWD test.
2. Calculate the effect of slip in the failed section for each FWD test by defining the effect of slip as being a function of the difference in radial stress at points directly above and below the failed interlayer.

Objective 3

Correlate the effect of slip with the ratio of surface moduli of failed and unfailed sections, considering the effect of slip calculated for each of the FWD tests in failed pavement sections.

Objective 4

Summarize each of the above steps so as to create a framework for using FWD data to identify interlayer bonding failures.

1.6. Scope of Study

This study utilized data obtained from the databases on the FAA's NAPTF website. All analyses were performed with data from the Medium subgrade strength Flexible pavement Conventional base (MFC) section within the "Medium Strength

Subgrade" section of the test pavement (as described in a later chapter). The MFC pavement section was composed of two sections, both of which were used for this study:

1. Unfailed section: a pavement section in which the interlayer bond was intact.
2. Failed section: a pavement section in which delamination occurred at the interlayer.

The data used in the study was of two types:

1. Material data: various material properties for the materials used in all layers of the pavement in the MFC section.
2. FWD data: 116 individual FWD tests within the MFC section, 60 of which were in the unfailed section, and 56 of which were in the failed section. Loads used in the tests included the following nominal loads: 9,000lb, 14,000lb, 25,000lb, 12,000lb, 24,000lb, and 35,000lb. Tests were conducted over a time span of 12 months.

CHAPTER TWO

LITERATURE REVIEW

2.1. Introduction

This chapter discusses the typical failures that occur due to poor interlayer bonding and the mechanism causing poor performance. This section is followed by a detailed explanation of factors that lead to poor bonding between layers and methods of detecting poor bonding.

2.2. Background

Many studies, as will be discussed below, have been and are continuing to be done on tack coats, proper use of tack coats, and their effects on interlayer strength. Through review of these studies, many things have been noted regarding tack coats, interlayers, and the various effects on pavement.

The first item of note from the literature review is what type of problems interlayer bonding failures cause. The typical signal that a pavement is experiencing interlayer bonding failure is slippage cracking, an example of which may be viewed in Figure 2.1.

This slippage cracking consists of crescent shaped cracks that develop at the pavement surface and are the direct result of a slippage of the upper asphalt layer over the lower layer (Shahin, et al., 1987b; Uzan, et al., 1978). The slippage between the layers is

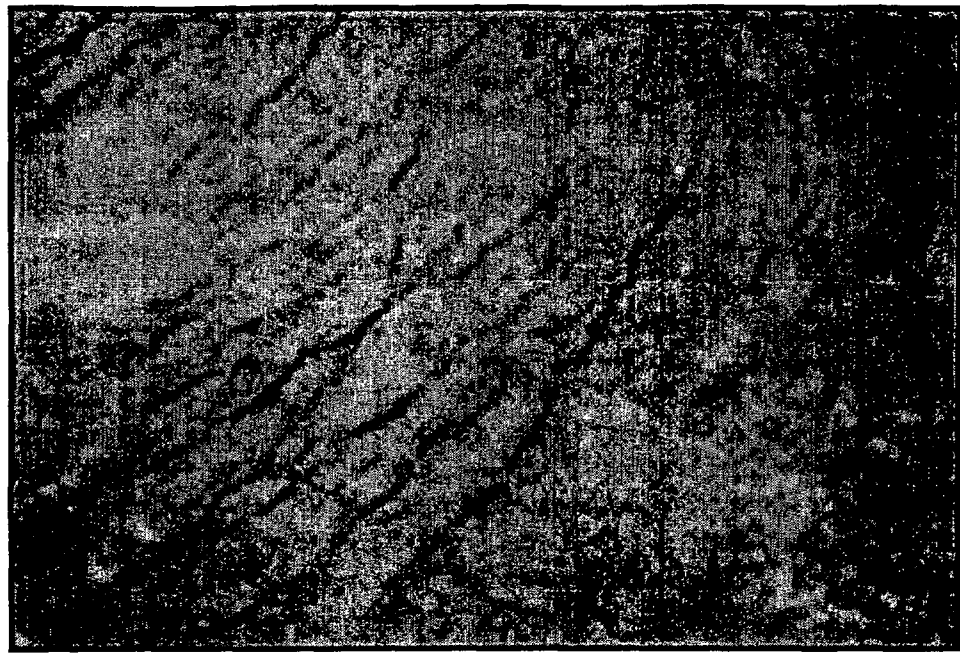

Figure 2.1. Slippage Cracking

the result of a weak interlayer bond. The crescent cracks, while certainly a problem themselves, are not the only problem resulting from slippage. As the interlayer bond is weakened and broken as the upper layer slips, the pavement system as a whole is weakened. This is because the broken bond reduces the stiffness of the system as a whole and loads may no longer be supported and distributed by the system as designed (Shahin, et al., 1987b).

2.3. Effect of Poor Bonding on Pavement Performance

Studies have provided insight on the failure mechanism in interlayer bonding failures (Uzan, et al., 1978, Shahin, et al., 1987b). In a pavement system in which the layers are fully bonded, a tensile strain occurs at the bottom of the second layer, as shown in Figure 2.2(a). If the bond between layers decreases, however, a tensile strain also occurs at the bottom of the top layer. As the interlayer bond is weakened, the pavement system begins to act as two separate systems- one system above the slippage and another below the slippage- as shown in Figure 2.2(b). This being so, as the bottom of the top layer develops more tensile strain, the top of the lower layer develops compressive strain. These strains at the interface further develop slippage, since the interlayer is distorted by the stresses between the two layers (Shahin, et al., 1987a). If the bond is completely broken, the pavement system is no longer a complete system, but becomes two separate systems. The upper slipped layer must now be able to handle all loads and resulting strains on its own or further failures occur. This indicates that the upper layer should be sufficiently stiff and/or thick for two reasons: to minimize the strains at the interlayer and to enable the layer to resist applied strains if the layer slips and is separated from the

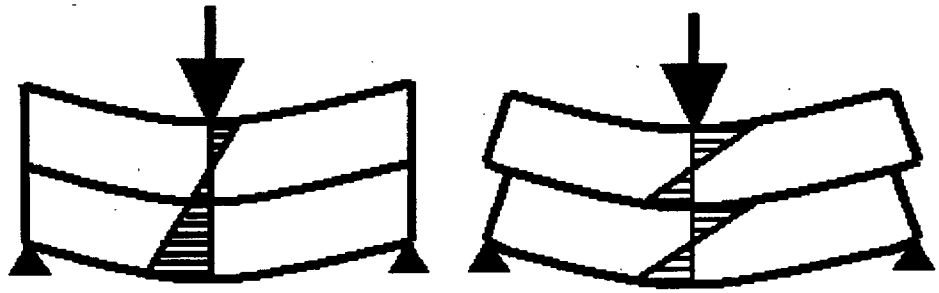

Figure 2.2. Failure Mechanism:
(a) Fully Bonded Pavement Acting as One System
(b) Fully Slipped Pavement Acting as Two Systems

lower layer(s).

2.4. Causes of Poor Bonding

The factors that affect bonding are:

- Type of tack coat.
- Amount of tack coat used.
- Pavement temperatures during service life.
- Gradations of pavement mixtures.
- Condition of surface being tacked.
- Moisture being present at time of tacking.

Each of these factors are briefly discussed below.

Several studies (Hachiya, et al., 1997; Mohammad, et al., 2002; Uzan, et al., 1978) have looked at the effect of different tack coats on interlayer bonding. In these studies, it was found that at high temperatures the type of tack has little effect on the shear strength of the interlayer, but at lower temperatures the types have varying strengths, though not significantly different.

The amount of tack coat in the interlayer affects the strength of the interface as well. The strength of the bond has been found to increase as the rate of application of tack coat increases, up to an optimum amount of tack (Hachiya, et al., 1997; Mohammad, et al., 2002; Uzan, et al., 1978). This may be seen in Figure 2.3, which is a figure from Mohammad, et al., 2002. After the optimal amount the strength decreases with an increase in rate of application, since beyond the optimum amount, the excess tack introduces a slip plane to the interlayer. However, the effect of the application rate is also

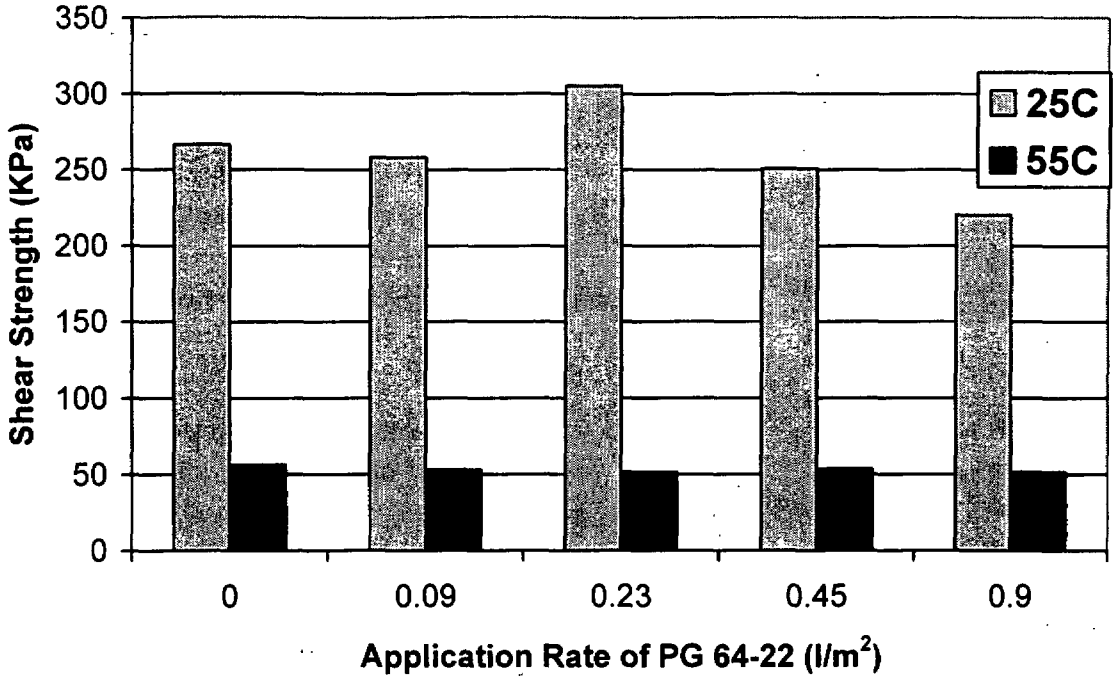

Figure 2.3. Tack Application Rates vs Strength, (Mohammad et al., 2002)

largely dependent on the air and pavement temperatures. At lower temperatures, an increased rate decreases the strength, however at higher temperatures the rate does not cause significant changes in the strength (Mohammad, et al., 2002). Also, the rate does not cause significant changes when placed on fresh pavement (Uzan, et al., 1978). Figure 2.4 shows an example of excess tack, while Figure 2.5 shows an appropriate application amount. Figures 2.6 and 2.7 show proper spraying and the results of poor spraying, respectively.

Different application rates are required for maximum effectiveness, based on the conditions of the surface being tacked and on the gradation of the asphalt mixtures used in the pavement. It has been found that milled surfaces provide a higher shear strength than do smooth and worn surfaces (Sholar, et al., 2002). Similarly, it has been found that coarse asphalt mixes provide a higher strength than fine mixes, because of aggregate interlock (Sholar, et al., 2002). Figure 2.8 shows a milling operation, which is recommended for effective bonding.

Finally, since weather is always a concern in construction, studies have been done on the effect of moisture on the strength of the interlayer. It was found that when moisture is on the interlayer plane at the time of paving, the strength of the interlayer decreases due to stripping (Sholar, et al., 2002).

2.5. Detection of Poor Bonding

At the current time, if poor interlayer bonding was to be identified before failures occurred, this would be done through destructive testing. The destructive method used

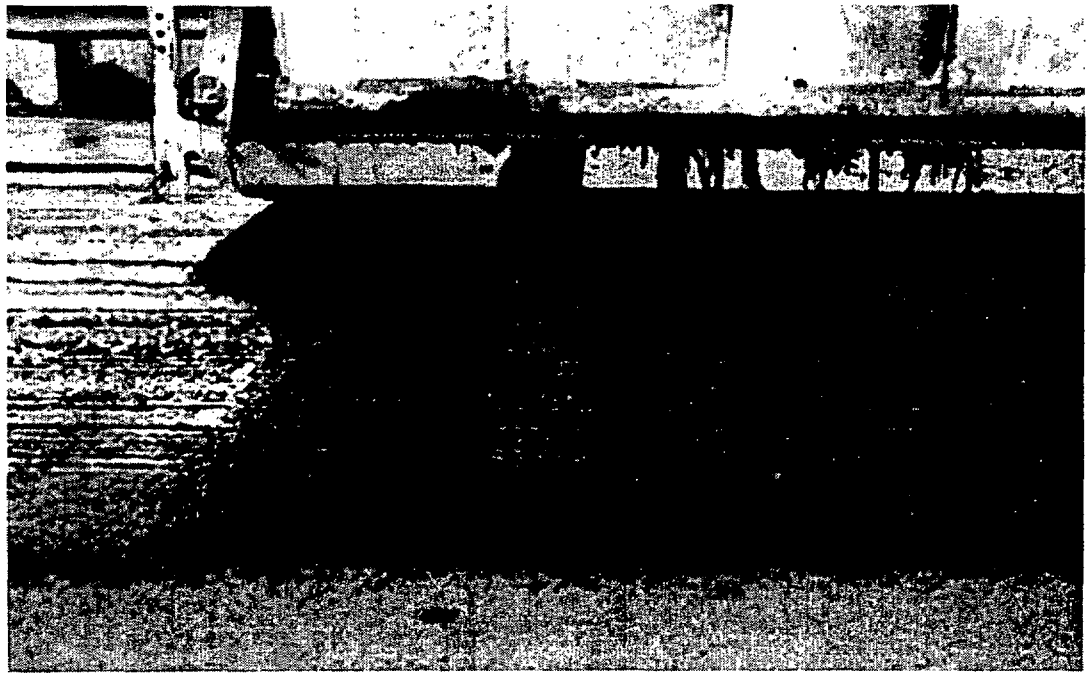

Figure 2.4. Excess Application

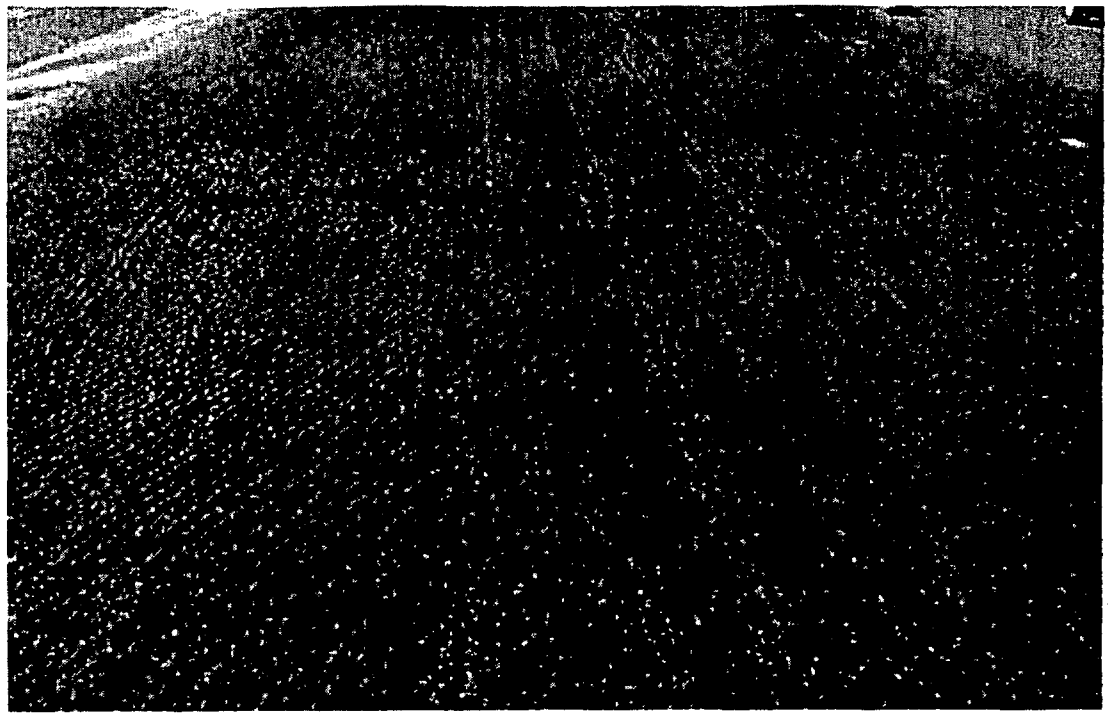

Figure 2.5. Appropriate Application Amount

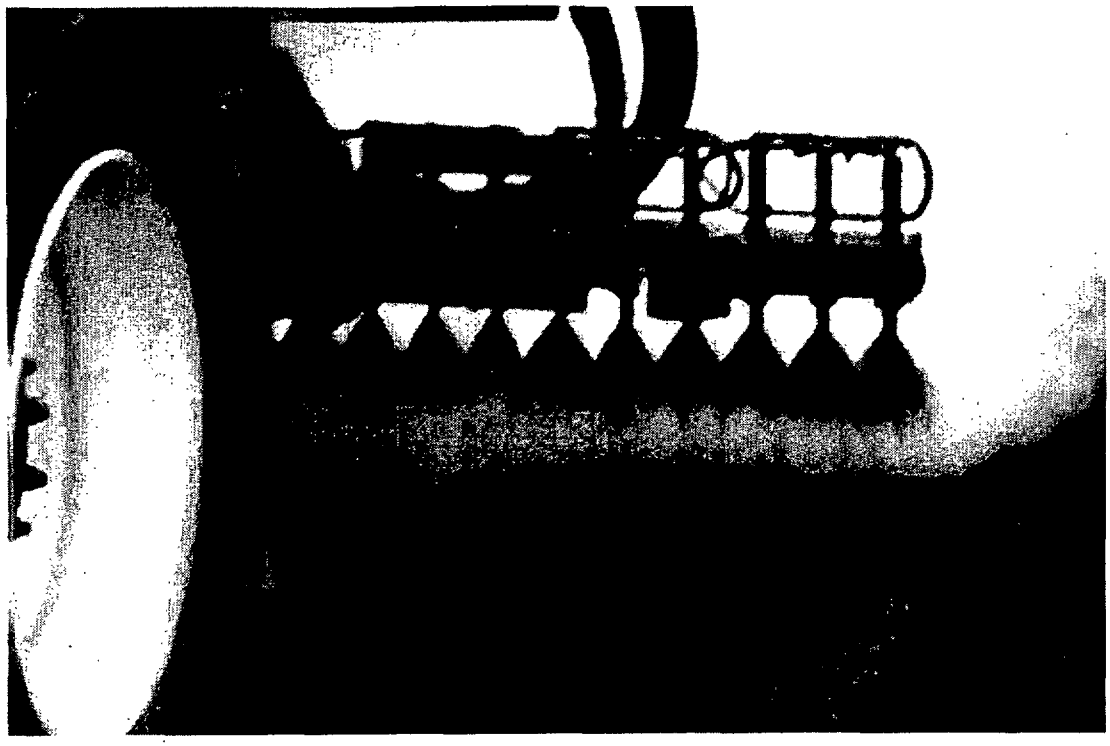

Figure 2.6. Proper Spraying

Figure 2.7. Result of Poor Spraying and Application Rate

Figure 2.8. Milling Operation

would be coring. Cores would be taken at locations along the length of pavement being tested, and the lack of bond would be identified by testing the core in shear. While this method is effective, it has the downfall of being destructive. This study looks at the potential of using a nondestructive test to identify poor interlayer bonding.

The Falling Weight Deflectometer (FWD) is a tool used in non-destructive testing of pavements. The FWD device (Figure 2.9) is mounted on a trailer, which can be towed by a truck and easily transported between testing locations. Since it is a mobile testing device, complete road closures are not necessary when the FWD test is being performed.

In an FWD test, a weight is dropped onto the pavement, applying a dynamic load to the pavement to mimic loading by traffic. The loads used range from 3000 to 33000 pounds, but a commonly used load is 9000 pounds. As the load is applied, sensors on the FWD machine measure the deflection of the pavement as it reacts to the load. Most FWD machines have seven sensors located in positions similar to those shown in Figure 2.10.

The data obtained from the FWD test are the measured deflections of the pavement at each testing location. The deflections at each location form a deflection basin: a large deflection at the point of loading and decreasing deflections as the distance from the load increases. A typical deflection basin is shown in Figure 2.11. The FWD data is used for pavement analysis. Programs are utilized to calculate the stiffness moduli of the pavement layers based on the measured deflections. The calculated in-situ moduli are typically used to evaluate the structural condition of pavements. This study investigates the use of FWD data to analyze the bonding within pavements.

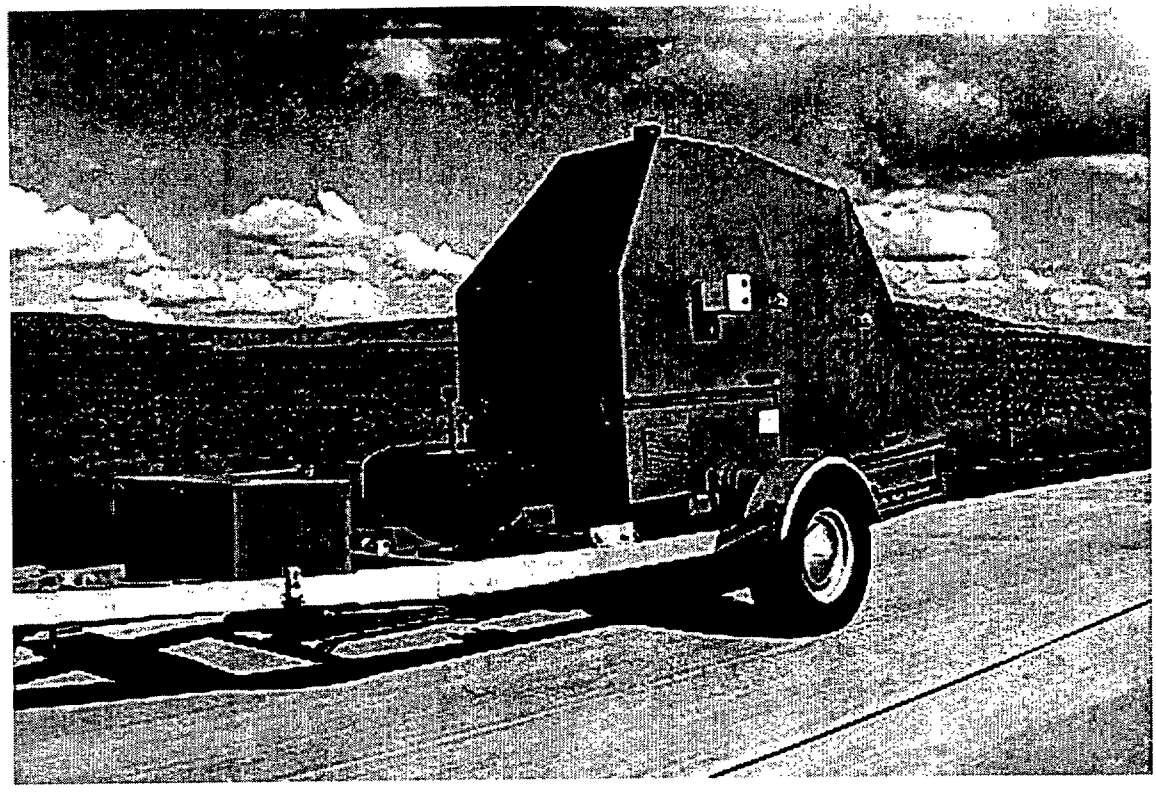

Figure 2.9. FWD Machine

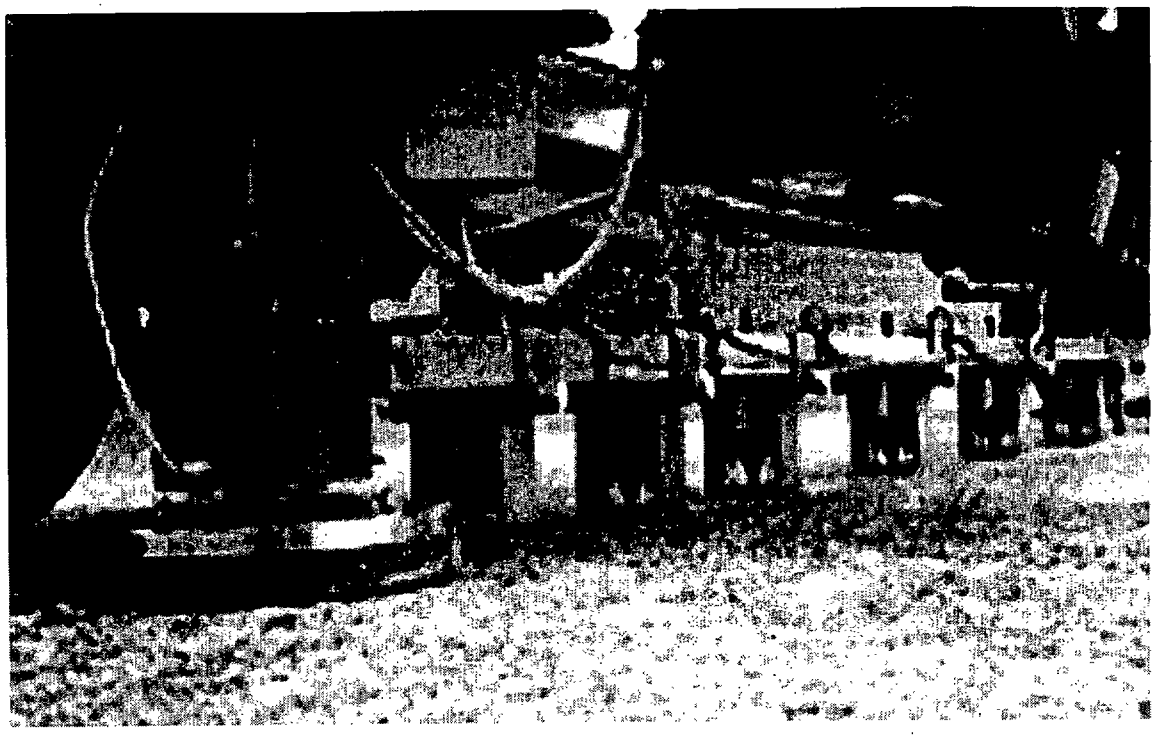

Figure 2.10. FWD Loading Plate and Sensors

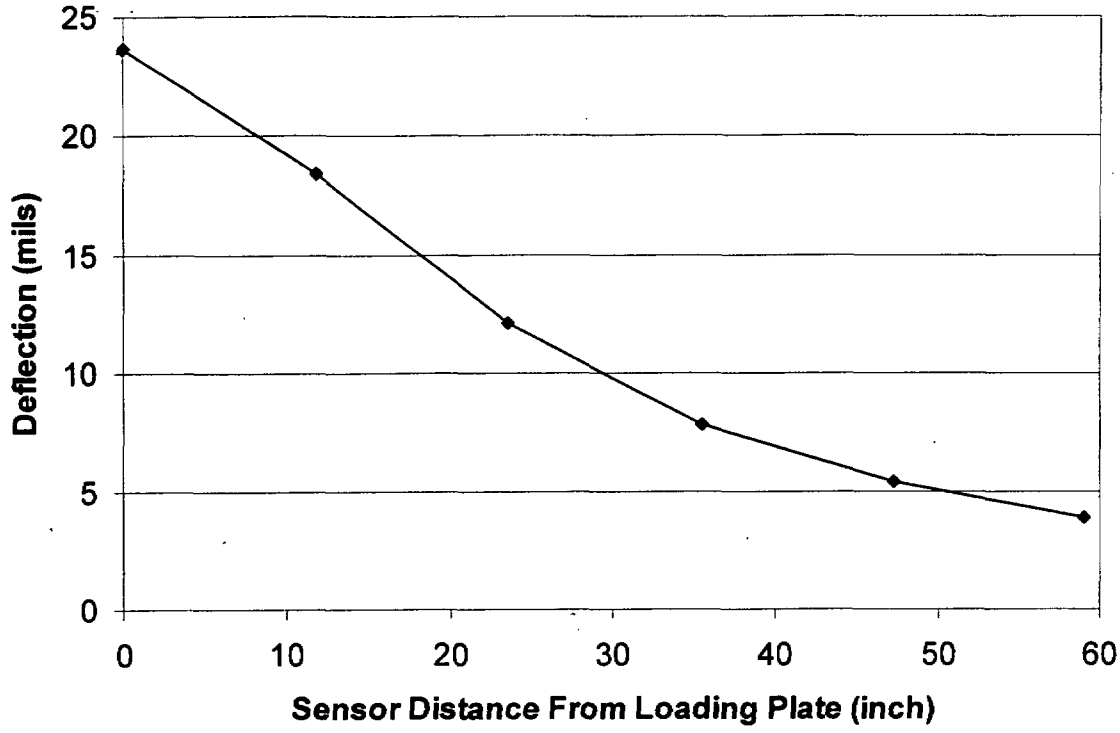

Figure 2.11. Typical Deflection Basin

2.6. Summary

This chapter discussed interlayer bonding failures, the mechanics of such failures, the causes of poor bonding, and the detection of poor bonding. These are all important topics in studies of interlayer bonding. However, for this study, the most critical topic discussed in this chapter is the detection of poor bonding. The use of FWD data to detect poor bonding is the focus of this study, and so it is discussed throughout the following chapters.

CHAPTER THREE

DATA

3.1. Introduction

Chapter Two discussed the results and causes of interlayer bonding failures and the identification of poor bonding. As indicated at the end of the chapter, the use of FWD data in identifying poor bonding is the focus of this study. While FWD data was the primary set of data used, other data used included pavement section and pavement material data. This chapter discusses each set of data utilized in this study.

3.2. Federal Aviation Administration's National Airport Pavement Test Facility

The source utilized for this study was the Federal Aviation Administration's (FAA) National Airport Pavement Test Facility (NAPTF), located in Atlantic City, New Jersey. The facility is a fully enclosed test track that is 900 feet long and 60 feet wide. The test track, as shown in Figure 3.1, is composed of nine different pavement structures, with three different strength subgrades. The pavement was loaded, with a 45,000 lb load, using various airplane landing gear configurations traveling along the pavement. During the loading period, which was roughly fourteen months, FWD tests were performed monthly at various locations on the pavement. At the end of the loading period, one section of pavement was investigated in detail since it had experienced rather severe rutting. In the investigation, a trench was dug perpendicular to the centerline of the

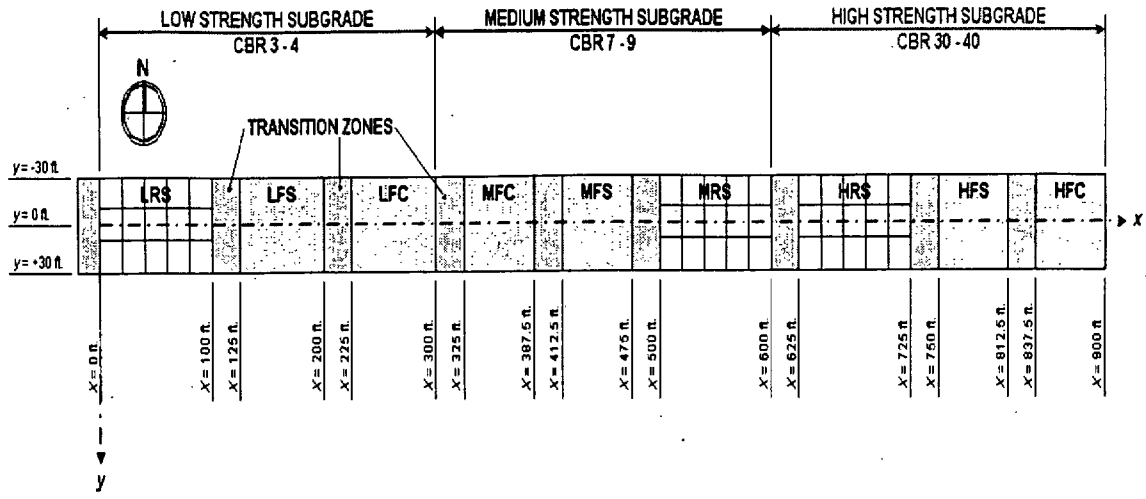

Figure 3.1. FAA NAPTF Site Layout (FAA NAPTF, 2003)

pavement to view the pavement cross-section. During these investigations, which included taking cores of the pavement, it was found that there had been delamination of the surface asphalt layer between lifts. A thin layer of dust was observed between the two lifts, which may have been the cause of the delamination (Garg, 2001). This section was within the medium strength section, which is shown in Figure 3.1, and is shown in more detail in Figure 3.2.

3.3. Section Details

The section in which delamination was found is the "Medium strength subgrade, Flexible pavement, Conventional base" (MFC) section (labeled as "Item 2-2" in Figure 3.2), which occupies stations 3+25 to 3+87 of the test track (stations start at the west end of the track and measure the x-distance shown in Figure 3.1). More particularly, the delamination was found in the area of 3+65 to 3+76. This MFC section was analyzed in this study. Figure 3.3 shows the pavement structure of the MFC section. The FAA NAPTF website at the address listed in the reference section of this report contains details on the loading of the test facility and the other pavement structures tested (FAA, 2003).

3.4. Material Data

Quality control during construction of the facility was strict, and material tests were performed on all materials used. Fairly extensive material property data are available in the database on the FAA NAPTF website listed in the reference section (FAA, 2003). This data was used in the FWD data analyses as discussed in a later

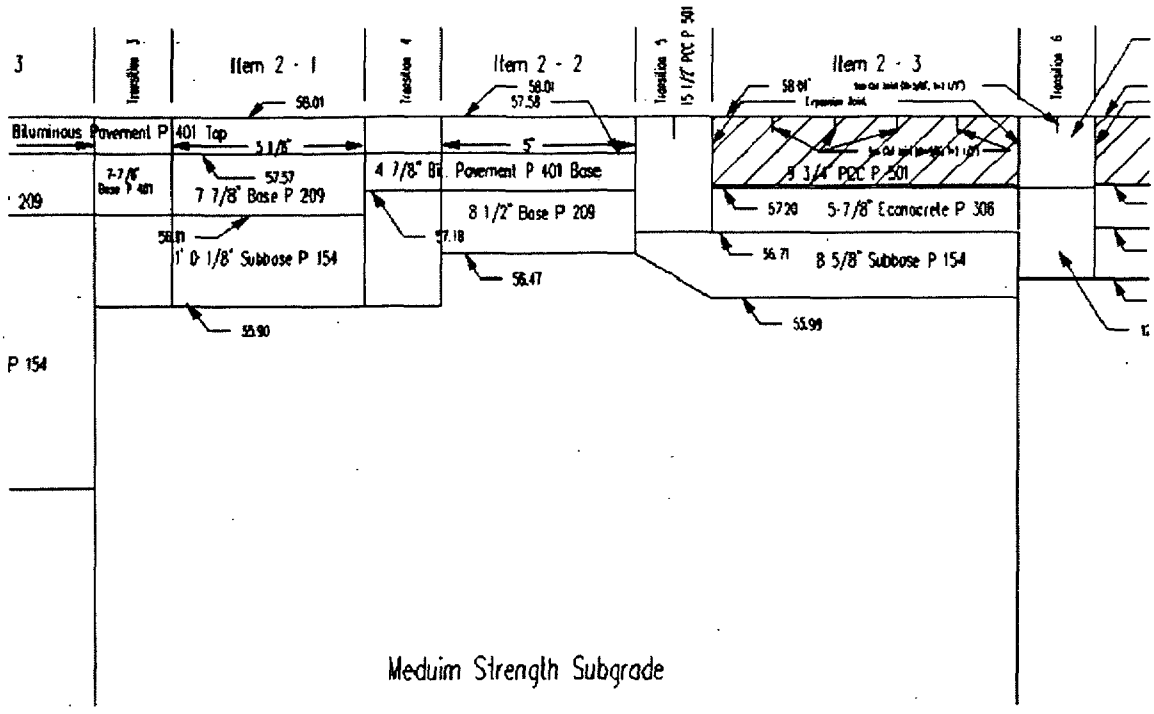

Figure 3.2. Medium Strength Subgrade Section (FAA NAPTF, 2003)

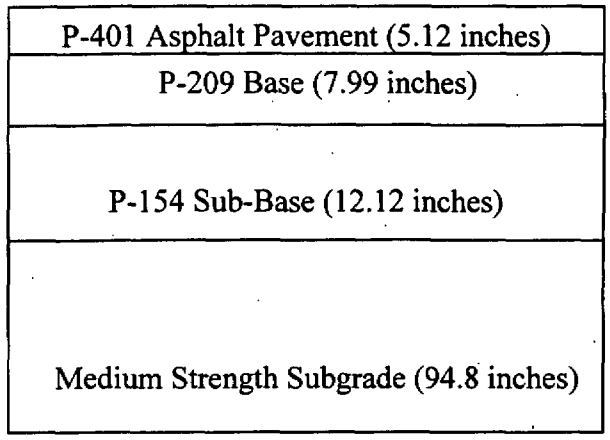

Figure 3.3. MFC Section Pavement Structure

section. Table 3.1 shows available material property data. Detailed material properties of all materials in the MFC section are shown in Appendix A.

3.5. Falling Weight Deflectometer Data

FWD tests were performed at regular time intervals during the life of the pavement tests. Tests were performed in Lanes 2 and 5, along with the centerline of the facility (lane designations are shown in Figure 3.4). The raw deflection data may be viewed in the Appendix B. Information on the FWD data used in this study is given in Table 3.2.

3.6. Summary

This chapter provided an overview of all of the data utilized in this study. The pavement section being analyzed was presented, and both the material data available and the FWD tests used in the analysis were identified. The use of the material data and the analysis of the FWD data are discussed next.

Table 3.1. Available Material Property Data

Property	Layer / Material			
	P-401	P-209	P-154	Subgrade
CBR	N/A	√	√	√
Moisture Content		√	√	√
Dry Density		√	√	√
Resilient Modulus		√	√	√
Aggregate Gradations	√	Not Applicable		
% Asphalt	√			
% Voids	√			
% VMA	√			
% VFA	√			
Stability	√			
Flow	√			
Maximum Specific Gravity	√			
Bulk Specific Gravity	√			
% Compaction	√			

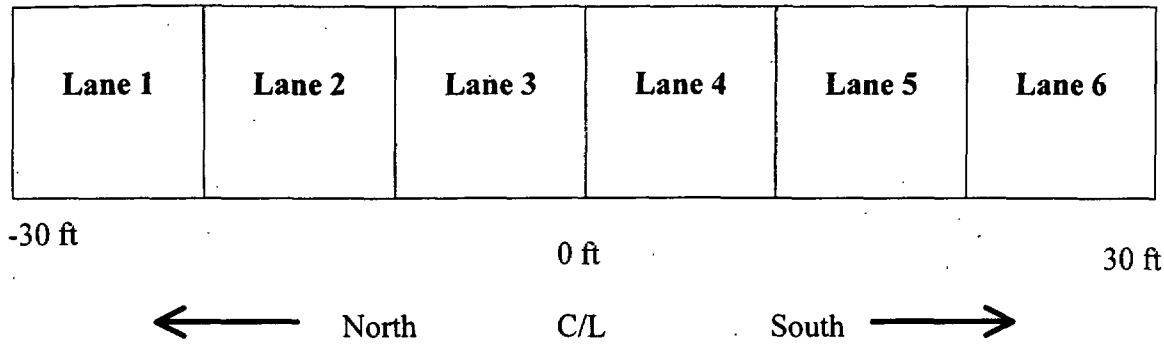

Figure 3.4. FAA NAPTF Lane Designations

Table 3.2. Locations and Dates of FWD Tests Used in Analysis

FWD Drop Numbers *	Location of Test **	Date of Test	Condition of Interlayer
24855 - 24858	3+45: Lane 5	2/16/00	Unfailed
24859 - 24862	3+55: Lane 5	2/16/00	Unfailed
24863 - 24866	3+65: Lane 5	2/16/00	Failed
24867 - 24918	3+75: Lane 5	2/16/00	Failed
24919 – 24922	3+45: C/L	2/25/00	Unfailed
24923 – 24926	3+55: C/L	2/25/00	Unfailed
24927 – 24930	3+65: C/L	2/25/00	Failed
24931 - 24934	3+75: C/L	2/25/00	Failed
24959 – 24962	3+45: C/L	3/20/00	Unfailed
24963 – 24966	3+55: C/L	3/20/00	Unfailed
24967 – 24970	3+65: C/L	3/20/00	Failed
24971 - 24974	3+75: C/L	3/20/00	Failed
25303 – 25306	3+45: C/L	6/22/00	Unfailed
25307 – 25310	3+55: C/L	6/22/00	Unfailed
25311 – 25314	3+65: C/L	6/22/00	Failed
25315 - 25318	3+75: C/L	6/22/00	Failed

* Each FWD test performed was numbered with a 5 digit number. Refer to the Appendix for further information on each FWD drop.

** Stations indicated are distances from the west end of the facility, i.e. 0+00 = the start of the Low Strength Subgrade section.

CHAPTER FOUR

FALLING WEIGHT DEFLECTOMETER ANALYSES

4.1. Introduction

This chapter discusses in detail the analysis conducted to obtain moduli of all layers in the pavement structure from FWD deflection data. This analysis was conducted using various programs and is explained below.

4.2. Backcalculation of Pavement Layer Moduli

Once FWD data is obtained, it can be utilized to estimate the pavement layer moduli. This is done through a method called backcalculation. All backcalculation programs determine the pavement layer moduli based on the measured surface deflections. The general idea in backcalculation is to match the measured surface deflections with estimated surface deflections, accomplished by adjusting the layer moduli to change the shape of the estimated surface deflection basin.

4.2.1. Backcalculation Analysis of FAA NAPTF MFC Section

Analysis of this section was ideal, since the test facility is in a controlled environment facility. Material properties were recorded for all materials used, and FWD data is available for each month that the pavement was loaded. Material properties and

FWD data may be viewed in the Appendix. With extensive material and deflection data available, calculations involving the pavement may be made with greater confidence.

To begin the study of the MFC section, anticipated ranges of layer moduli were calculated from the available material properties for each layer shown in the Appendix. These calculations were performed using correlations found in *Pavement Analysis and Design* (Huang, 1993). For the base, subbase, and subgrade layers, expected resilient modulus values were determined from tested CBR values. For the hot mix asphalt (HMA) layer, the expected range of resilient modulus was determined from the percent binder, stiffness modulus of binder, and percent aggregate for the mix. The expected layer moduli based on the material properties are shown in Table 4.1. The expected layer moduli values were a yardstick to evaluate the reasonableness of backcalculated moduli.

Before investigating the slippage issue, the backcalculations were first validated by backcalculating the layer moduli for an unloaded or relatively unloaded section of pavement. The reason for this is that within such a pavement section, backcalculation should provide reasonable results, since loads may cause distresses in pavements which would affect backcalculated moduli. The centerline of the pavement facility is unloaded, so theoretically all FWD tests performed on the centerline would produce similar backcalculated layer moduli for different locations. This being the case, the backcalculations were initially performed on the centerline to determine the unfailed sections for validation purposes.

Two backcalculation programs were utilized: EVERCALC 5.0 (Washington State DOT, 2001) and BAKFAA (FAA, 2000). Both programs were used to analyze FWD data from the beginning of the loading period (drop numbers 24919 to 24934 and 24959

Table 4.1. Expected Layer Moduli

Layer	Minimum Expected E (psi)	Maximum expected E (psi)
P-401 HMA	145,000*	2,600,000*
P-209 Base	15,000	30,000
P-154 Subbase	10,000	20,000
Subgrade	8,000	23,000

* Assuming less aging of the asphalt than usual, since it is in an enclosed facility.

to 24974) and the end of the loading period (drop numbers 25303 to 25318). These drop numbers were chosen because they represented times near the beginning and ending of the loading period. Dates and locations of these drops were shown in the previous chapter in Table 3.2. Two rounds of backcalculations were done for the above locations and are discussed below.

4.2.2. Backcalculation Results

The results of each round are discussed separately below.

4.2.2.1. Backcalculation Round 1 Results

For the first round of backcalculations, a stiff layer below the subgrade, with an infinite depth and a modulus of 1,000,000 psi, was added to the structure in Figure 3.3. This stiff layer represents the native soil below the constructed subgrade, since the in-situ soil is assumed to be stiff as described in a study of FWD calculations on the FAA NAPTF subgrades (McQueen, et.al., 2001). The structure details are shown in Table 4.2. It was assumed that all layers were fully bonded for all sections.

In Round 1, it was discovered that the programs grossly over-estimated the moduli of the subbase layer and under-estimated the moduli of the base layer. However, the calculated HMA layer and subgrade moduli were in the expected range. The pavement structure was thus slightly modified in the following round. The results of Round 1 may be viewed in Appendix C in Tables C.1-C.2.

Table 4.2. Pavement Structure

	Round 1 (Original)			Round 2 (Modification)		
Layer	**Material**	**Thickness (in)**	**Poisson's Ratio**	**Material**	**Thickness (in)**	**Poisson's Ratio**
1	HMA	5.12	0.35	HMA	5.12	0.35
2	Base	7.88	0.35	Merged Base/Subbase	20	0.35
3	Subbase	12.12	0.35	Subgrade	94.8	0.45
4	Subgrade	94.8	0.45	Stiff Layer	Infinite	0.45
5	Stiff Layer	Infinite	0.45	---	---	---

4.2.2.2. Backcalculation Round 2 Results

In the second round of backcalculations, the structure was similar to that of the first round, but the base and subbase layers were merged into one layer. There were two reasons for this: 1) the programs were under-estimating the base layer and over-estimating the subbase layer, and 2) there was poor reliability on the calculated moduli for both layers. Table 4.2 shows the structure details for both Round 1 and 2. Once again it was assumed that all layers were fully bonded.

The results of this round provided more reasonable moduli for the combined layer, keeping in mind that the combined moduli would be a weighted average of the individual layer moduli. The HMA layer and subgrade moduli were again in the expected range. However, there was no statistically significant difference between failed and unfailed sections. The results of Round 2 may be viewed in Appendix C in Tables C.3(a) – C.4(b).

4.2.3 Discussion of Backcalculation Results

The backcalculated moduli did not reflect a lack of bond because of the linear elastic analysis that was used. Linear elastic analysis may be an over-simplification that is affecting the calculated moduli, since it is well known that materials do not always behave in the linear range. This analysis did not allow for calculation of reasonably accurate layer moduli for all layers, which is critical, especially for the surface layer.

Since the linear elastic analysis did not provide reasonable results, a more extensive non-linear elastic analysis that would accurately model the material behavior was necessary. This non-linear elastic analysis is discussed in the next section.

4.3. Forward Calculation Analysis of FAA NAPTF MFC Section

Since reliable non-linear analysis backcalculation tools were not available, a forward calculation program that allowed non-linear analysis was used. The forward calculation program used was KENLAYER.

In forward calculations, like backcalculations, the FWD data is used to calculate layer moduli. The difference is that in forward calculations the programs calculate deflections based on the inputs of layer moduli and FWD loads. The layer moduli are changed manually by the user so that the calculated deflection basins match the measured deflection basins.

Forward calculations have been performed on both Lane 5 and the centerline (C/L), with FWD data from times 1 day (FWD drop numbers 24855 to 24918 and 24919 to 24934) and 8 weeks of loading (FWD drop numbers 25303 to 25318). The dates and locations of these drops are shown in Chapter 3 in Table 3.2.

The structure analyzed in KENLAYER was slightly different from the structures used in the backcalculations. The main reason for this is that the program allows the use of nonlinear elastic materials. The base, subbase, and subgrade were all considered as nonlinear layers.

Since moduli values change with stress and hence depth, the principle of finite element analysis was used to accurately model the pavement behavior, and the base and subbase layers were subdivided into smaller layers. As non-linear material layers, the moduli values depend on the stress invariant, which varies with depth (as discussed in the next section). Since the subgrade was considered to be sufficiently far from the surface, it was considered as one layer with nonlinear material properties. Again, a stiff layer was

Table 4.3. Structure used in Forward Calculations

Layer #	Material	Thickness (in)	Poisson's Ratio	Unit Weight (lb/in^3)
1	HMA	5.12	0.35	0.088
2	Base	1.315	0.35	0.088
3	Base	1.315	0.35	0.088
4	Base	1.315	0.35	0.088
5	Base	1.315	0.35	0.088
6	Base	1.315	0.35	0.088
7	Base	1.325	0.35	0.088
8	Subbase	2.02	0.35	0.074
9	Subbase	2.02	0.35	0.074
10	Subbase	2.02	0.35	0.074
11	Subbase	2.02	0.35	0.074
12	Subbase	2.02	0.35	0.074
13	Subbase	2.02	0.35	0.074
14	Subgrade	94.8	0.45	0.0537
15	Stiff Layer	Infinite	0.45	0.0537

included below the subgrade. The structure used in the forward calculations is shown in Table 4.3.

4.3.1. Material Modeling

4.3.1.1. Base and Subbase

The program calculated the nonlinear layer moduli for the base and subbase by using equations that include constants derived from material property tests: the unconfined or triaxial compression tests. For granular materials, i.e. the base and subbase, the equation used was:

$$E = K_1 * \theta^{K_2} \qquad (4.1)$$

where:

E = Stiffness modulus of material

K_1 = Material constant, derived through material testing

θ = Stress invariant, which is the sum of the three principle stresses derived through material testing

K_2 = Material constant, derived through material testing

The program also used K_0, which was the coefficient of earth pressure and was assumed to be 0.6, as recommended by Huang, 1993. The values of K_1 and K_2 for each material were determined by fitting the above equation using the material data of the respective layer. Each respective layer had data from two samples that were tested, and so for each layer there were two data plots and two equations, as shown in Figures 4.1 and 4.2. The average K_1 and K_2 of the two samples for each layer's material was used. For the base, K_1 and K_2 were 4088 and 0.6, respectively. For the subbase, K_1 and K_2 were 3729 and 0.56, respectively.

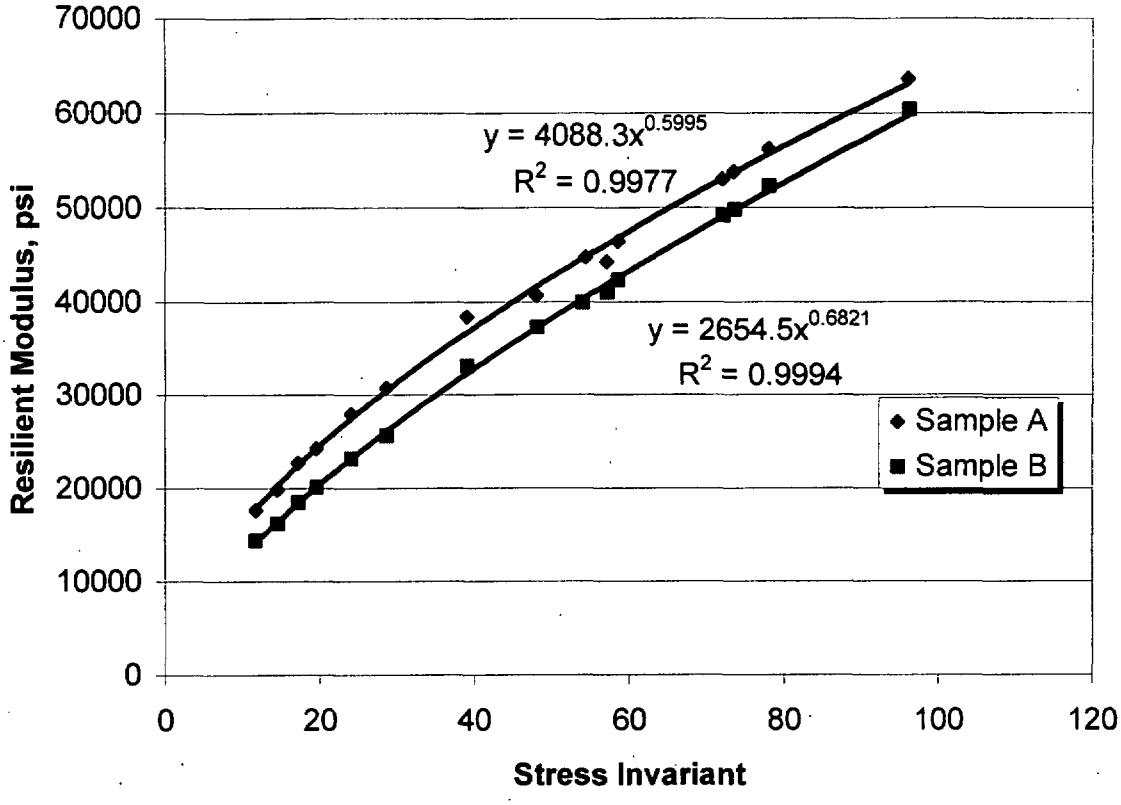

Figure 4.1. Calculation of K_1, K_2 for Base (P-209)

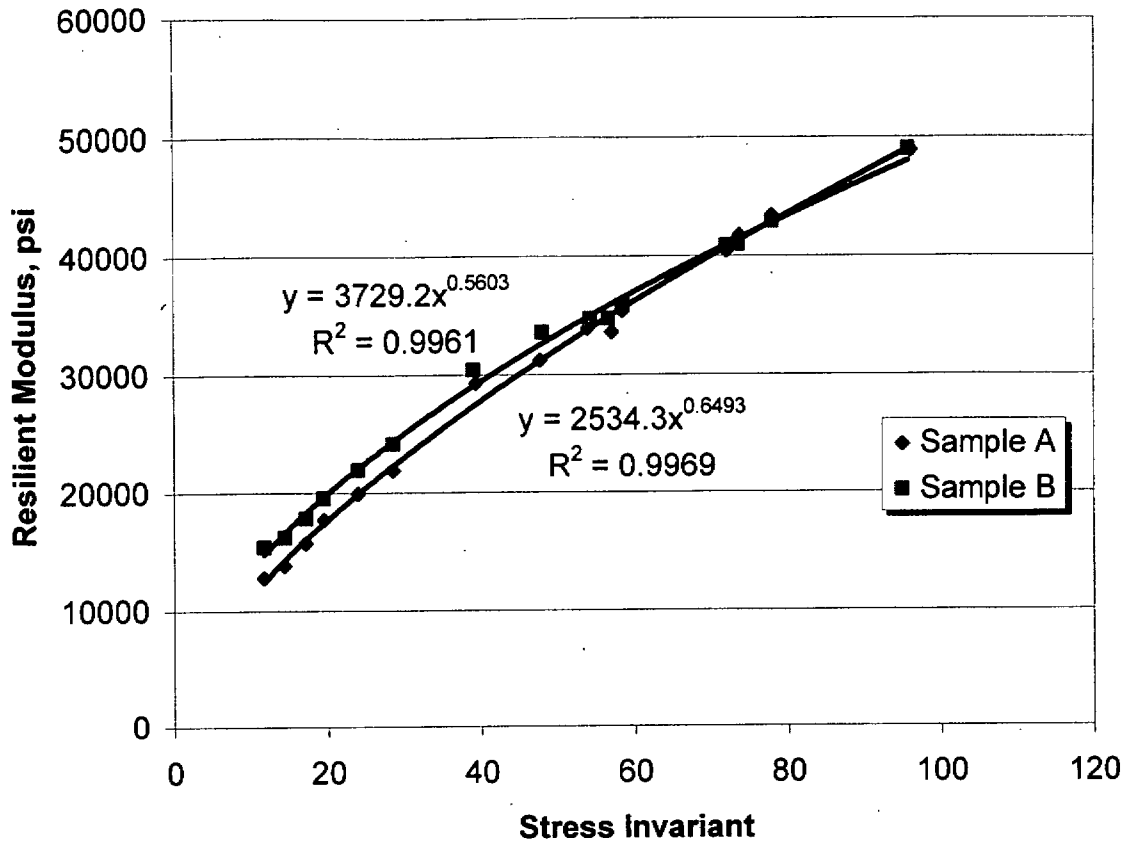

Figure 4.2. Calculation of K_1, K_2 for Subbase (P-154)

4.3.1.2. Subgrade

For the nonlinear clay materials, i.e. the subgrade, the equations used were:

$$E = K_1 + K_3(K_2 - \sigma_d), \text{ when } \sigma_d < K_2 \qquad (4.2)$$

$$E = K_1 + K_4(\sigma_d - K_2), \text{ when } \sigma_d > K_2 \qquad (4.3)$$

where:

E = Stiffness modulus

K_1, K_2, and K_3 = Material constants, determined through laboratory testing

σ_d = Deviator stress, derived from triaxial test

For this study, the values used were as recommended by Huang: $K_2 = 6.2$, $K_3 = 1110$, and $K_4 = 178$ (Huang, 1993), while K_1 was changed so that the calculated deflection basin matched the measured deflection basin.

4.3.2. Factors Affecting Forward Calculation Analysis

Many factors influenced the deflections of the pavement under applied loads. This is especially true since FWD data is being analyzed from tests performed at different times over a span of a year, during which the pavement was heavily trafficked. Some of the main factors that were found to influence the calculated E values were: time, load, and temperature. Additionally, since two lanes were involved in the analysis, the lanes were also a factor to be considered, along with the sections of each lane. Each of these factors is briefly discussed below.

Time

The time of the tests, that is the date on which the tests were taken, is an important factor. This is because as the pavement is loaded, its condition deteriorates. There were fifteen different dates in which FWD testing was performed. However, the pavement was not loaded between all of these dates, so in this paper the FWD tests are identified by both the FWD number and by the number of days or weeks of loading to date. The dates of FWD tests and the "time loaded to date" information for FWD tests of the MFC section are shown in Table 4.4. Those that were used in the forward calculation analysis are shown in bold. More detailed information on trafficking between FWD test dates may be viewed in Appendix D.

Load

The load applied by the FWD machine is an important factor because the base, subbase, and subgrade were all modeled as non-linear materials. The calculated moduli of these non-linear layers were thus different for each load.

Lane

In this study, two lanes have been analyzed. These are Lane 5, which is loaded, and the C/L, which is not loaded. The difference in loading between lanes makes a difference in the calculated moduli for each lane. For this reason, the results of each lane may not be compared with those of other lanes.

Table 4.4. Dates and Loading Information for FWD Tests [*1]

Date of FWD Test	Days Loaded to Date [*2]	Weeks Loaded to Date [*3]	Traffic Repetitions to Date
6/14/1999	0	0	0
11/17/1999	0	0	0
1/11/2000	0	0	0
2/11/2000	0	0	0
2/16/2000	**1**	**0.14**	**28**
2/25/2000	**1**	**0.14**	**28**
3/20/2000	1	0.14	28
4/7/2000	8	1.14	931
4/14/2000	12	1.71	1892
4/20/2000	15	2.14	2746
4/26/2000	19	2.71	3556
5/6/2000	26	3.71	5015
5/23/2000	37	5.29	8040
6/22/2000	**54**	**7.71**	**11948**
8/31/2000	58	8.29	12952

*1 Those tests in bold indicate data used in forward calculation analysis.

*2 1 Day = 1 day of traffic repetitions.

*3 1 Week = 7 days of traffic repetitions (not 7 consecutive calendar days).

Section

Each lane consisted of two sections. An unfailed section, at stations 3+45 and 3+55, where there was no delamination, and a failed section at stations 3+65 and 3+75, where delamination was found.

Temperature

The pavement temperature at the time of the FWD tests is very important, since asphalt stiffness is significantly affected by temperature. In order to make any comparison between FWD tests performed at different temperatures, it was necessary to make adjustments to all calculated asphalt moduli to adjust them to a common temperature. The average temperature, 13°C (55°F), was used as the common temperature to minimize error through having large adjustments. This adjustment was made with the temperature adjustment factor, recommended by Briggs, et.al., 2000. This adjustment factor, for adjusting backcalculated asphalt moduli, is given by:

$$ATAF = 10^{slope(T_r - T_m)} \qquad (4.4)$$

where:

ATAF = Asphalt temperature adjustment factor

slope = slope of the log modulus versus temperature equation

(-0.0195 used for Lane 5 and –0.021 used for the C/L)

T_r = Reference mid-depth of HMA layer (13°C used)

T_m = Mid-depth temperature of HMA layer at time of FWD test

The temperatures and adjusted calculated surface layer moduli may be viewed in Appendix G in Table G.1(a) – G.1(b).

4.4. Results of Forward Calculations

4.4.1. Forward Calculation Results of All Layers

The P-401 and P-154 layer moduli were mostly in the expected ranges. Several P-209 moduli, for FWD loads of 35,000 pounds, were over the expected values by up to 16,000 psi. This is likely attributed to the fact that a larger load was applied. However, most were in the expected range. Only 29% were greater than 5% over the maximum expected, and only 17% were greater than 10% over the maximum expected. The calculated subgrade moduli were mostly in the expected range, though towards the high end. A few were slightly higher than expected, but minimally so (+1000 psi). The calculated layer moduli of all layers for Lane 5 and the C/L are shown in Table 4.5(a) and Table 4.5(b), respectively. The author had confidence in these values because the deflection basins matched very well (typical deflection basin match shown in Figure 4.3) and the calculated layer moduli were all in or reasonably close to the expected range. Deflection basins for Lane 5 and the C/L are shown in Appendix E and Appendix F, respectively.

4.4.2. Comparison of Forward Calculated Surface Layer Moduli

With the calculated P-401 moduli adjusted to a single reference temperature, the forward calculated moduli were compared between failed and unfailed sections. The comparison was made by first sorting the results by lane, contact pressure, and time. The average modulus and 95% confidence interval were calculated for each data set. The average surface layer moduli of the failed sections were compared with those of the

Table 4.5(a). Forward Calculation Results (Lane 5)*

FWD #	FWD Load (lb)	$E_{P\text{-}401}$ (psi)	$E_{P\text{-}209}$ (psi)	$E_{P\text{-}154}$ (psi)	$E_{subgrade}$ (psi)
24856	11,000	1,700,000	16,600	12,902	22,800
24857	23,000	1,510,000	23,655	16,142	20,580
24858	35,000	1,200,000	**30,130**	18,512	19,220
24860	11,000	1,625,000	16,717	12,917	22,080
24861	23,000	1,470,000	23,767	16,147	20,230
24862	35,000	1,150,000	**30,380**	18,517	19,010
24864	11,000	1,500,000	16,978	13,025	22,210
24865	23,000	1,050,000	25,090	16,635	20,830
24866	35,000	700,000	**33,448**	19,200	19,600
24916	11,000	1,525,000	16,972	13,050	22,710
24917	23,000	1,150,000	24,813	16,567	20,910
24918	35,000	775,000	**32,875**	19,200	20,010

* Values in bold designate values that were outside the expected range.

Table 4.5(b). Forward Calculation Results (C/L) *

FWD #	FWD Load (lb)	E_{P-401} (psi)	E_{P-209} (psi)	E_{P-154} (psi)	$E_{subgrade}$ (psi)
24920	11,000	1,700,000	16,528	12,922	**24,320**
24921	23,000	1,600,000	23,705	16,337	22,260
24922	35,000	1,310,000	**30,008**	18,808	20,710
24924	11,000	1,800,000	16,617	13,003	**24,790**
24925	23,000	1,612,000	23,748	16,358	22,240
24926	35,000	1,230,000	**30,378**	18,892	20,700
24928	11,000	1,571,000	16,875	13,053	**23,730**
24929	23,000	1,300,000	24,497	16,592	22,110
24930	35,000	820,000	**32,520**	19,177	20,220
24932	11,000	1,550,000	16,888	13,073	**24,330**
24933	23,000	1,000,000	25,577	17,007	22,680
24934	35,000	515,000	**35,385**	19,845	21,030
25304	11,000	450,000	19,667	13,870	22,160
25305	23,000	**141,400**	**33,175**	18,193	20,880
25306	35,000	**72,000**	**46,082**	**21,595**	19,870
25308	11,000	500,000	19,670	13,963	**23,130**
25309	23,000	155,000	**32,865**	18,225	21,380
25310	35,000	**65,000**	**46,645**	**21,745**	20,160
25312	11,000	525,000	19,518	13,915	**23,160**
25313	23,000	275,000	**30,355**	17,668	20,930
25314	35,000	**73,000**	**45,875**	**21,482**	19,580
25316	11,000	460,000	19,902	14,092	**24,080**
25317	23,000	148,000	**32,935**	18,255	21,580
25318	35,000	**64,000**	**46,770**	**21,707**	19,860

* Values in bold designate values that were outside the expected range.

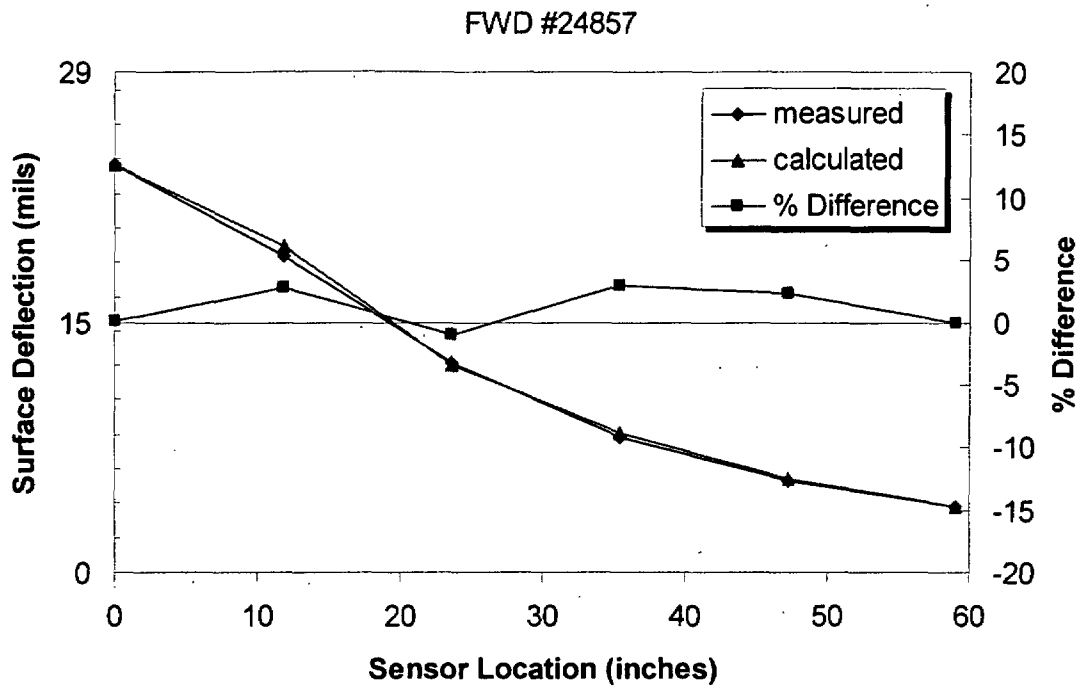

Figure 4.3. Typical Match of Measured and Calculated Deflection Basins

unfailed sections, for both Lane 5 and the C/L, as discussed below. Additionally, a statistical analysis of the calculated P-401 moduli was conducted using SPSS to identify what factors (time, load, temperature, lane, section) significantly affected the calculated P-401 moduli. These results may be seen in Appendix H in Table H.1.

4.4.2.1. Center Line Surface Layer Moduli

Figures 4.4 – 4.6 compare the average surface layer moduli between failed and unfailed section in the C/L. It is seen that at 1 Day, the difference between the failed and unfailed sections is clear. Irrespective of the load, the unfailed section has higher moduli than the failed section and the 95% confidence intervals for each do not overlap, indicating a statistically significant difference. At 8 Weeks, the moduli of both sections were much lower than the moduli at 1 Day. The moduli for both sections at 8 Weeks were essentially equal, with no statistically significant difference between sections.

4.4.2.2. Lane 5 Surface Layer Moduli

The loading period of 8 Weeks was not analyzed for Lane 5, due to the results found for the C/L. The C/L was not directly loaded, yet the moduli decreased dramatically and there was no statistically significant difference between sections. Since this occurred on the unloaded C/L, similar results were expected for the loaded Lane 5, but with even more dramatic decreases in moduli. Therefore, Figures 4.7 – 4.9 compare the average surface layer moduli between failed and unfailed section in Lane 5, at the loading period of 1 Day. For each load, the moduli of the unfailed section are

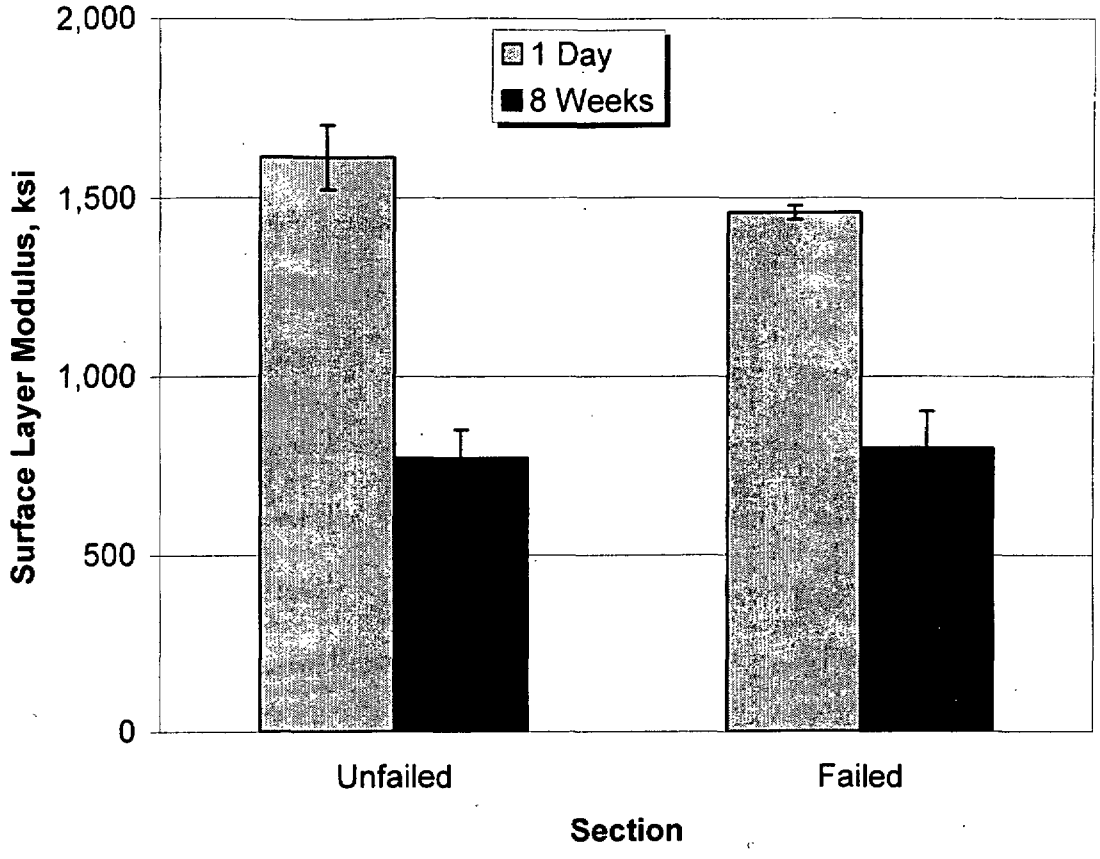

Figure 4.4. Surface Layer Moduli of Failed and Unfailed Sections (C/L, 12 kip load)

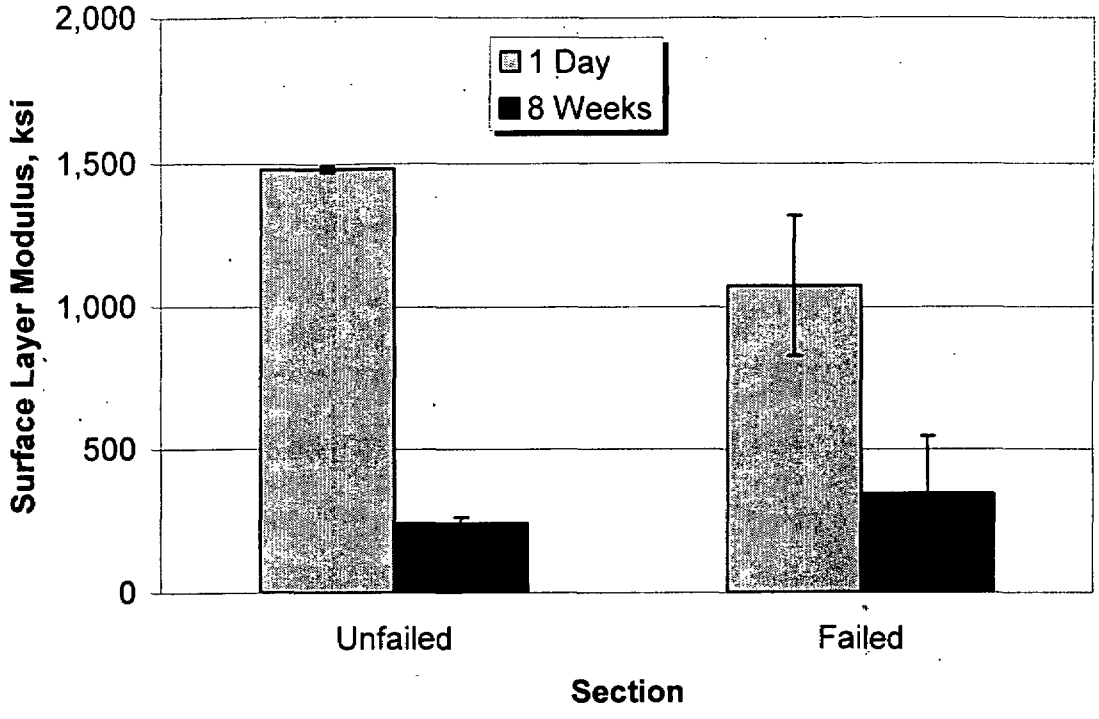

Figure 4.5. Surface Layer Moduli of Failed and Unfailed Sections (C/L, 24 kip load)

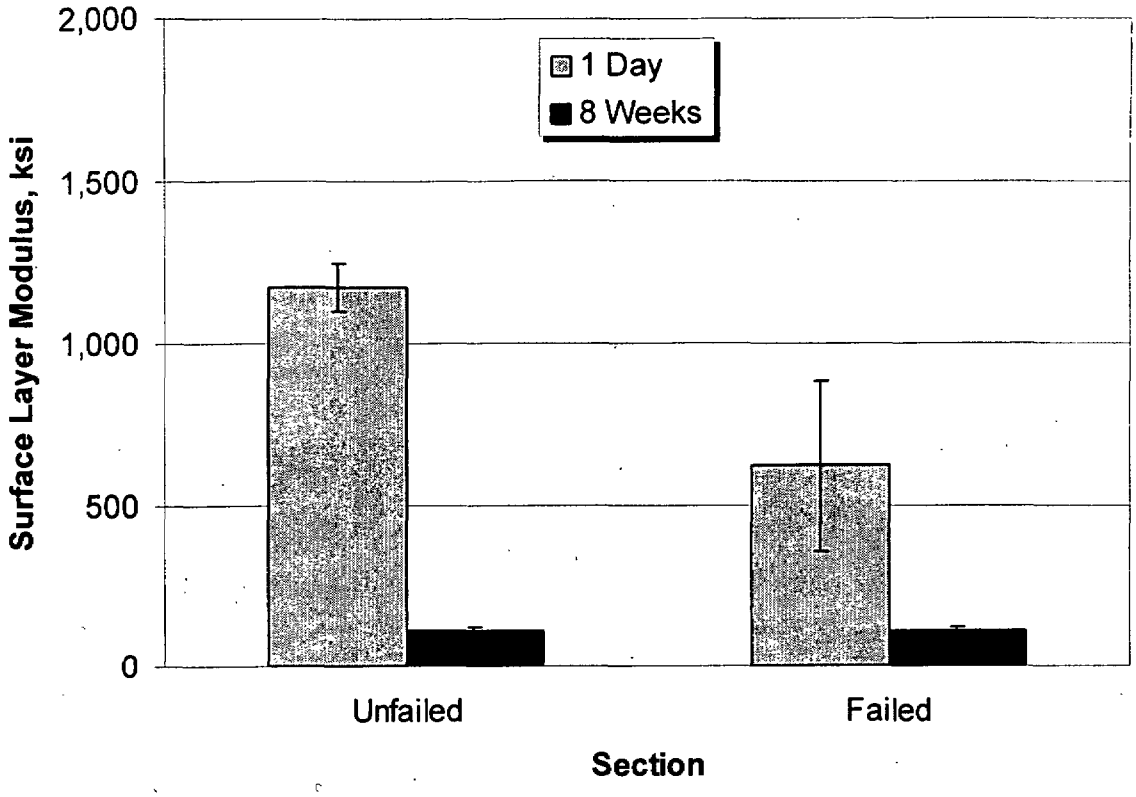

Figure 4.6. Surface Layer Moduli of Failed and Unfailed Sections (C/L, 35 kip load)

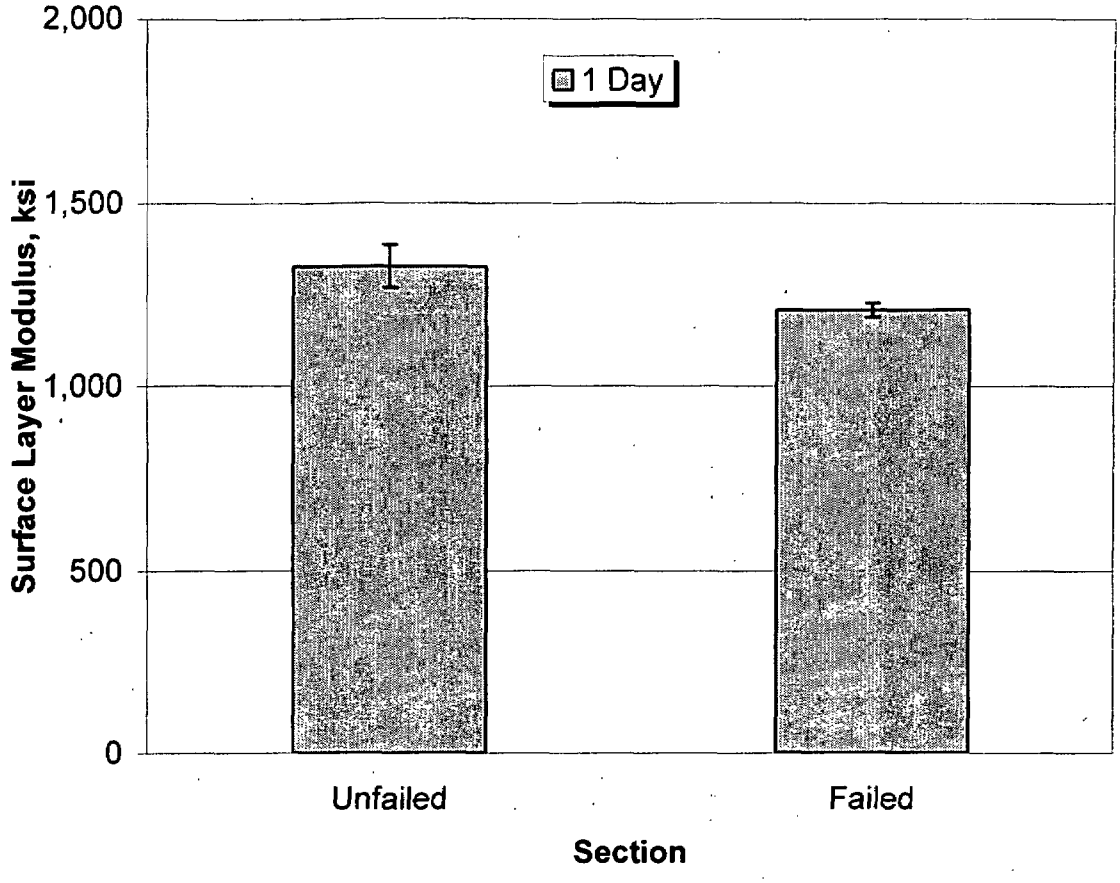

Figure 4.7. Surface Layer Moduli of Failed and Unfailed Sections (Lane 5, 12 kip load)

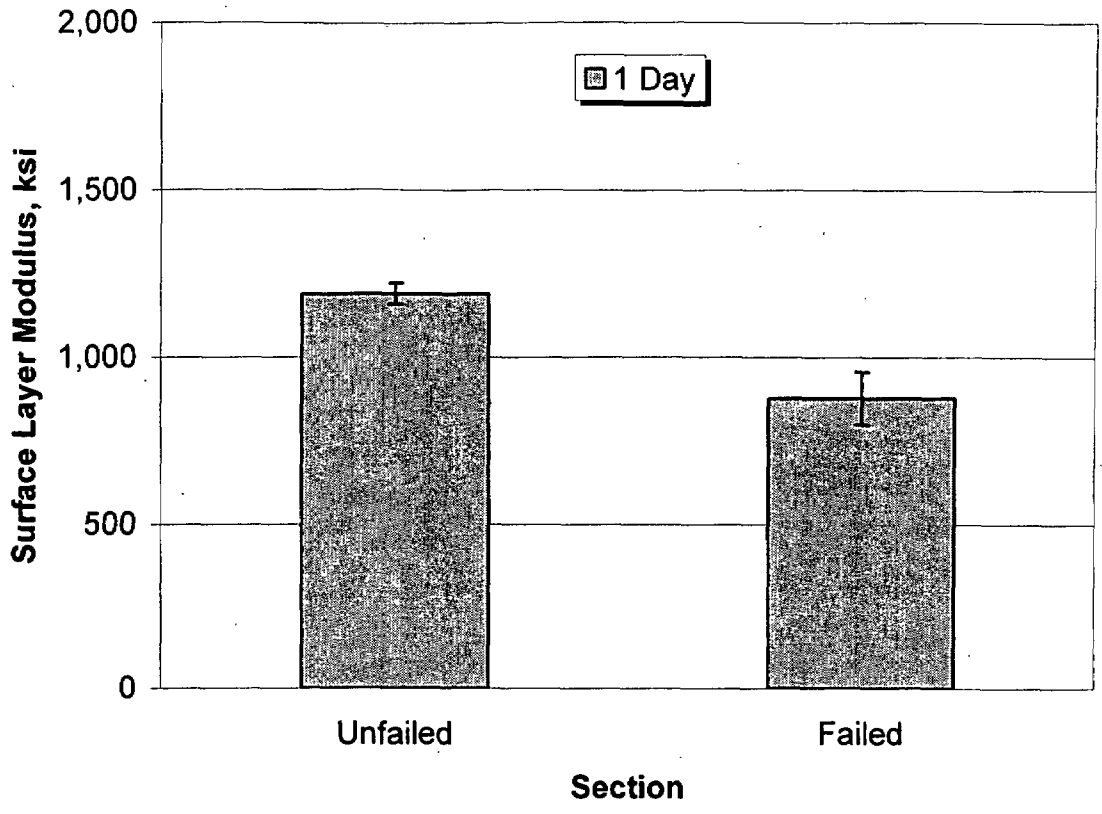

Figure 4.8. Surface Layer Moduli of Failed and Unfailed Sections (Lane 5, 24 kip load)

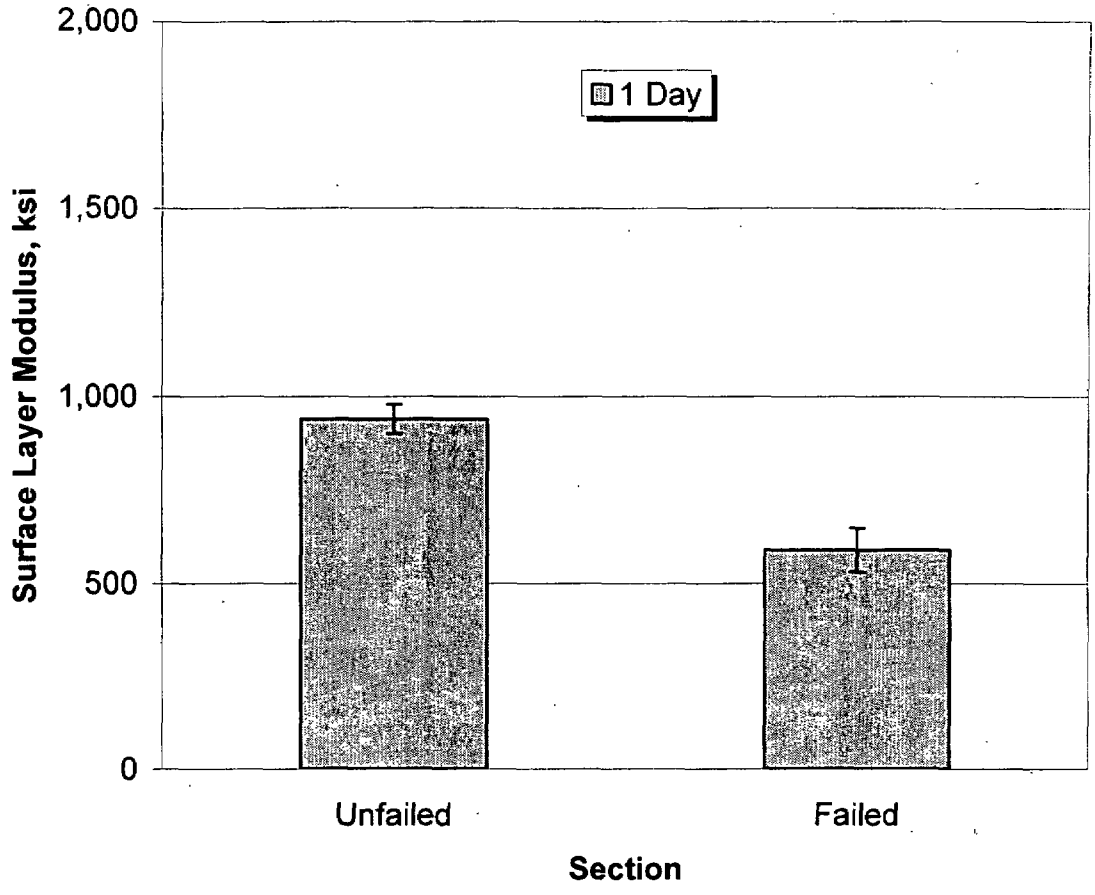

Figure 4.9. Surface Layer Moduli of Failed and Unfailed Sections (Lane 5, 35 kip load)

consistently higher than the moduli of the failed section. The 95% confidence intervals for each section do not overlap, indicating a statistically significant difference.

4.5. Discussion of Forward Calculation Results

4.5.1. Centerline

Figures 4.4 – 4.6 clearly indicate a statistically significant difference between failed and unfailed sections at 1 Day. Irrespective of the load, the failed section has lower moduli than the unfailed section. This seems to indicate that where interlayer bonds are poor, surface layer moduli are lower. Similarly, this seems to indicate that where interlayer bonds are intact, the surface layer moduli are higher. This is also an indication that any load may be able to identify sections with poor interlayer bonds.

At 8 Weeks, there is no statistically significant difference between sections. This may be because of structural deterioration. At that time, the pavement loading had been nearly completed and the pavement may have experienced a structural failure, which would mask the interlayer bonding as seen from FWD data. The results for 8 Weeks indicate the importance of testing pavements early in the pavement's life, so that other pavement distresses do not mask potential interlayer bond problems.

4.5.2. Lane 5

Figures 4.7 – 4.9 clearly show a statistically significant difference between failed and unfailed sections at 1 Day, for each load. Irrespective of the load, the failed section has lower moduli than the unfailed section. As in the C/L results, this seems to indicate that sections with poor interlayer bonds will exhibit lower surface layer moduli than

sections with good interlayer bonds. This also indicates that there is no certain load magnitude required for identifying poor interlayer bonds.

The loading period of 8 Weeks was not analyzed for Lane 5, because as indicated in the results for the C/L, the pavement may have experienced structural deterioration. Since this was found for the C/L, which was not directly loaded, the structural condition of Lane 5, which was directly loaded, was expected to be worse. With the structural deterioration, as shown in the C/L results, there would be no statistically significant difference between failed and unfailed sections, since the structural failure masks the interlayer bonding failure.

4.5.3. Results Summary

The failed and unfailed sections were assumed to be fully bonded during the FWD analysis. The surface deflections, however, are influenced by the lack of bonding in the failed section. This phenomenon was observed by the difference in forward calculated moduli of failed and unfailed sections. It is emphasized that both the sections were constructed at the same time and exposed to similar environmental and loading conditions. Therefore, the moduli are similar for both sections, and so the difference in forward calculated moduli can be attributed to the lack of bonding.

CHAPTER FIVE

INTERLAYER SLIP ANALYSIS

5.1. Introduction

This chapter discusses the effect of slip within the MFC pavement section. Section 5.2 provides background information on the analysis of the effect of slip. Section 5.3 discusses the calculation of pavement mechanical responses in the failed sections of the MFC pavement. Section 5.4 discusses the determination of the effect of slip occurring in the failed pavements.

5.2. Analysis of Slip

5.2.1. Background

As explained in the previous chapter, the surface moduli were significantly different between failed and unfailed sections. This indicated that the FWD data was able to identify the lack of interlayer bonding. However, simply knowing that a lack of bonding exists is not enough. In some pavements, a lack of bond may be present, but if the surface layer is sufficiently thick, the effect of slip due to that lack of bond may be negligible. Therefore, the effect of slip that occurs as a result of the lack of bonding needs to be found, since the effect of slip will vary with pavement structure and loading.

To determine the effect of slip that was occurring, radial stresses at the interlayer were used as the basis of comparison. The effect of slip was defined by the algebraic difference between radial stresses directly above and directly below the interlayer.

However, in earlier calculations, the asphalt was considered as one layer. Since the slippage occurred between lifts of the asphalt layer, the layer was split into two layers for stress/slip calculations. After splitting the asphalt layer, stresses were calculated in the pavement for each FWD drop on failed sections, to eventually find the effect of slip in each FWD drop. This process is explained in detail below.

5.2.2. Asphalt Layer Moduli

5.2.2.1. Splitting of Asphalt Layer

In the forward calculation process, the asphalt layer was considered as one single layer. Technically, since the interlayer failure at the FAA NAPTF occurred in between lifts of the asphalt layer, the asphalt was divided into two layers. This was not a concern as far as the forward calculations were concerned, since FWD calculations are unable to accurately distinguish between thin layers. However, in order to analyze the slip, the asphalt layer needed to be split into two (shown in Figure 5.1).

This splitting was done with the use of an equation for the equivalent modulus of a combined asphalt layer with different thicknesses and/or moduli, as presented by Huang, 1993:

$$E_1 = \left[\frac{h_{1a}(E_{1a})^{\frac{1}{3}} + h_{1b}(E_{1b})^{\frac{1}{3}}}{h_{1a} + h_{1b}} \right]^3 \qquad (5.1)$$

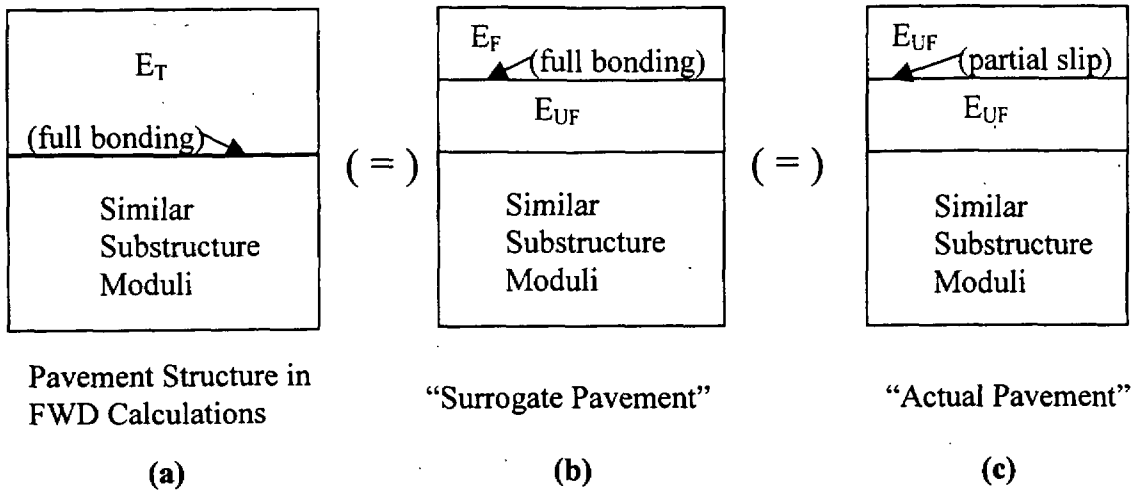

where:

E_F = Modulus of top 2.56 inch asphalt layer, as calculated with Equation 5.2.

E_T = Effective asphalt layer modulus, as calculated in FWD calculations with asphalt layer being equal to 5.12 inches (entire thickness of asphalt).

E_{UF} = Actual modulus of asphalt = average effective modulus (E_T) of asphalt layer in *unfailed* sections.

Figure 5.1. Splitting of Asphalt Layer in Failed Section

The equation was simplified since the asphalt layers are equal (2.56 inches each), and the equation's notation was changed to match the notation used in this project. The modified equation was:

$$E_F = \left[2(E_T)^{\frac{1}{3}} - (E_{UF})^{\frac{1}{3}} \right]^3 \qquad (5.2)$$

where:

E_F = Modulus of top 2.56 inch asphalt layer (Figure 5.1(b)), as calculated from this equation.

E_T = Effective asphalt layer modulus (Figure 5.1(a)), as calculated in FWD calculations with asphalt layer being equal to 5.12 inches (entire thickness of asphalt).

E_{UF} = Actual modulus of asphalt (Figure 5.1(b) and (c)) = average effective modulus (E_T) of asphalt layer in *unfailed* sections.

5.2.2.2. Implications and Applications of Splitting Asphalt Layer

The implication of the above equation is this: in sections that are fully bonded (no slippage), E_F will be equal to E_{UF}. In sections in which slippage occurred, E_F will be lower than E_{UF}. The reason for this is that the equation assumes full bonding. If there is actually slippage, then E_F is reduced to account for the worsened performance of the pavement system caused by the slippage.

The purpose of the equation was to determine the modulus of each asphalt layer, so that slip at the interlayer could be evaluated. The unfailed sections were assumed fully bonded, so the equation was only applied to the failed sections. Furthermore, since the

forward calculation analysis results indicated that statistically significant differences between failed and unfailed sections were only found at the loading period of 1 Day, the equation was only applied to the failed sections at 1 Day. The results of the asphalt layer moduli computations are shown in Tables 5.1 – 5.3 at the end of the next section.

5.2.3. Tack Coat Failure Ratio

A goal of this study is to determine a way to easily identify and quantify the effect of slip in a pavement under the design loads. In order to make this a simple procedure, a term called the Tack Coat Failure Ratio (TFR) was created. This term is simply the ratio of the calculated modulus of the top asphalt layer to the calculated modulus of the lower asphalt layer (E_F to E_{UF}), as they are defined above and shown in Figure 5.1. In equation form, the TFR is:

$$TFR = \frac{E_{topHMAlayer}}{E_{lowerHMAlayer}} = \frac{E_F}{E_{UF}} \qquad (5.3)$$

where: E_F and E_{UF} are as explained previously.

TFR = 1 for fully bonded interlayer

TFR = 0 for complete lack of interlayer bonding

The TFR was calculated for each of the FWD drops in the failed sections at 1 Day, as shown in Tables 5.1 – 5.2. These TFR's were later correlated with the effect of slip in the pavement section. The intent is that in the future, a TFR can be calculated from FWD calculations, and from the TFR/slip correlation the effect of slip in the pavement may easily be determined.

Table 5.1. Asphalt Moduli and TFR for the C/L, 1 Day

FWD ID	Station	Load (kip)	Section	FWD-Calculated E_T (ksi)	Average E_T (ksi)	E_T (ksi)	E_F (ksi) (Calculated from Equation)	E_{UF} (ksi) (Avg. E_T, UF Section)	TFR
24920	3+45	11	UF	1,700	1,750	-	-	-	-
24924	3+55	11	UF	1,800		-	-	-	-
24928	3+65	11	F	1,571	-	1,571	1,405	1,750	0.803
24932	3+75	11	F	1,550		1,550	1,366	1,750	0.780
24921	3+45	23	UF	1,600	1,606	-	-	-	-
24925	3+55	23	UF	1,612		-	-	-	-
24929	3+65	23	F	1,300	-	1,300	1,036	1,606	0.645
24933	3+75	23	F	1,000		1,000	570	1,606	0.355
24922	3+45	35	UF	1,310	1,270	-	-	-	-
24926	3+55	35	UF	1,230		-	-	-	-
24930	3+65	35	F	820	-	820	491	1,270	0.387
24934	3+75	35	F	515		515	141	1,270	0.111

Table 5.2. Asphalt Moduli and TFR for Lane 5, 1 Day

FWD ID	Station	Load (kip)	Section	FWD-Calculated E_T (ksi)	Average E_T (ksi)	E_T (ksi)	E_F (ksi) (Calculated from Equation)	E_{UF} (ksi) (Avg. E_T, UF Section)	TFR
24856	3+45	11	UF	1,700	1,662	-	-	-	-
24860	3+55	11	UF	1,625		-	-	-	-
24864	3+65	11	F	1,500	-	1,500	1,380	1,662	0.811
24916	3+75	11	F	1,525		1,525	1,395	1,662	0.839
24857	3+45	23	UF	1,510	1,490	-	-	-	-
24861	3+55	23	UF	1,470		-	-	-	-
24865	3+65	23	F	1,050	-	1,050	706	1,490	0.474
24917	3+75	23	F	1,150		1,150	866	1,490	0.581
24858	3+45	35	UF	1,200	1,175	-	-	-	-
24862	3+55	35	UF	1,150		-	-	-	-
24866	3+65	35	F	700	-	700	374	1,175	0.318
24918	3+75	35	F	775		775	477	1,175	0.407

5.3. Effect of Slip

5.3.1. Background

Pavements with poor interlayer bonding experience an effect of slip. The effect of slip experienced by the pavement varies with several different conditions. Different loads on the pavement will produce varied effects of slip: a small car driving on a road may not cause any effect of slip, but a heavily loaded tractor-trailer on the same road may cause a high effect of slip for the same interlayer. The pavement structure itself affects the effect of slip in the pavement. Structures with very stiff and/or very thick surface layers may experience low effects of slip. Alternatively, structures with soft and/or thin surface layers may experience high effects of slip. The reason for this is that stiff and/or thick surface layers are able to withstand much of the load itself, causing less of the load to be transferred to the lower pavement structure, and thus lower stresses and strains in the lower pavement structure, including the interlayer.

The effect of pavement structure on the effect of slip can be explained by the TFR, which was described and calculated in the previous section. The TFR, being a ratio of E_F to E_{UF}, is a direct indication of the stiffness of the surface layer, relative to the layer below the interlayer. This being the case, a high TFR (1.0) would indicate a relatively stiff surface layer and thus a lower effect of slip. A low TFR (0.0) would indicate a large difference in stiffness between the two top layers and thus a higher effect of slip.

The TFR's were previously determined for each of the failed locations, and so effect of slip needed to be determined for each location. As mentioned previously, the effect of slip was determined by comparing radial stresses directly above and below the interlayer under the FWD loads. This process is described in detail below.

5.3.2. Preliminary Calculations and Validations

The initial intent was to use the program KENLAYER to calculate the stresses for each location and FWD drop, since it was used to calculate the layer moduli. However, KENLAYER only computes slips of 0 and 1; that is, only full slip and full bond, and no intermediate degrees of slip. Since the pavement had some intermediate degree of slip, the program BISAR was used instead.

Some preliminary investigation was necessary before the program was used for the actual analysis though. BISAR uses two different numbers to account for the bonding in the modeled pavements: there is an unnamed input number (named in this paper as "BISAR slip number"), and a "spring compliance" number that appears in the output and is used to represent the degree of bonding within the program. In order to effectively use the program to determine the effect of slip, a correlation between the BISAR slip number and the output spring compliance number was necessary. Additionally, a correlation was made between BISAR's input/output and KENLAYER's output for both fully bonded and fully slipped pavements, in order to verify that BISAR was being used properly.

To calibrate the BISAR slip number, and to validate the BISAR calculations, a simple three-layer pavement structure was analyzed using both KENLAYER and BISAR. The system used was a simplified MFC system: two 2.56 inch asphalt layers over a 7.88 inch gravel layer (shown in Figure 5.2). The gravel layer was used since the only layers that were critical for this investigation were the two asphalt layers. If different sub-layers had been used, the results would have been the same. The values for the moduli and loading were those for FWD drop # 24864. The following mechanical responses were computed in KENLAYER and BISAR for the fully bonded and fully slipped interface

cases: vertical displacement, vertical stress, vertical strain, radial stress, and radial strain. These were computed directly under the load, at depths of 0, 1.28, 2.55, 2.57, 3.84, and 9.08 inches (as shown in Figure 5.2).

Through this analysis, it was determined that the range of BISAR slip number values was 0 to 1,000,000, with the 0 corresponding to the BISAR spring compliance number of 0.0 and the 1,000,000 corresponding to a spring compliance of 1.0. It was also found that the spring compliance of 0.0 matched the KENLAYER slip of 1(full bond), and the spring compliance of 1.0 matched the KENLAYER slip of 0 (full slip). These findings are shown in Table 5.3.

Slip was measured by the difference in radial stresses between points just above and just below the interface. Figure 5.3 shows the radial stresses for varied degrees of slip at the points directly above and below the interface, directly under the load. This demonstrates the increase of radial stress due to slip, and it also demonstrates the increase in radial stress difference between the two points with the increase in slip. Figure 5.4 shows the difference in radial stress versus the BISAR slip number.

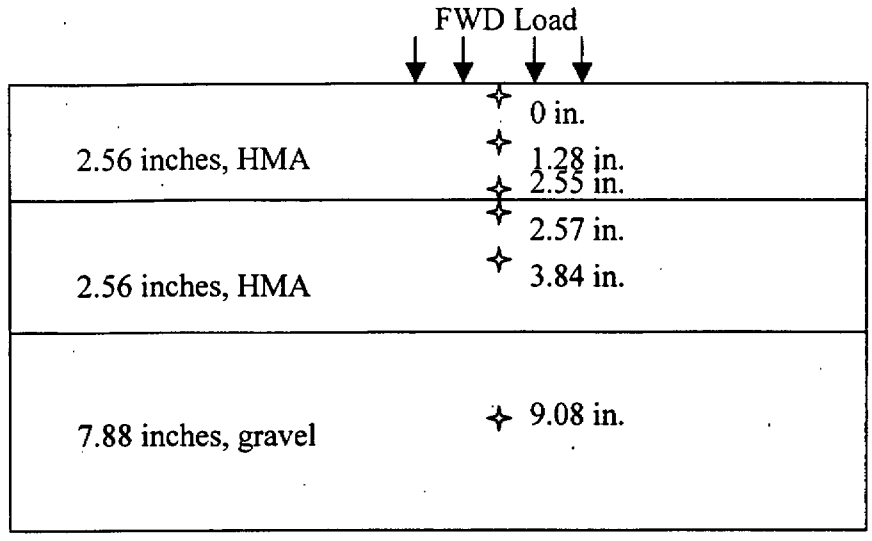

Figure 5.2. Structure and Evaluation Points Used for Preliminary Investigation

Table 5.3. BISAR / KENLAYER Interface Values

KENLAYER Interface Number	BISAR Slip Number	BISAR Interface Spring Compliance	Physical Meaning
1	0	0.0	Fully Bonded
0	1,000,000	1.0	Fully Slipped

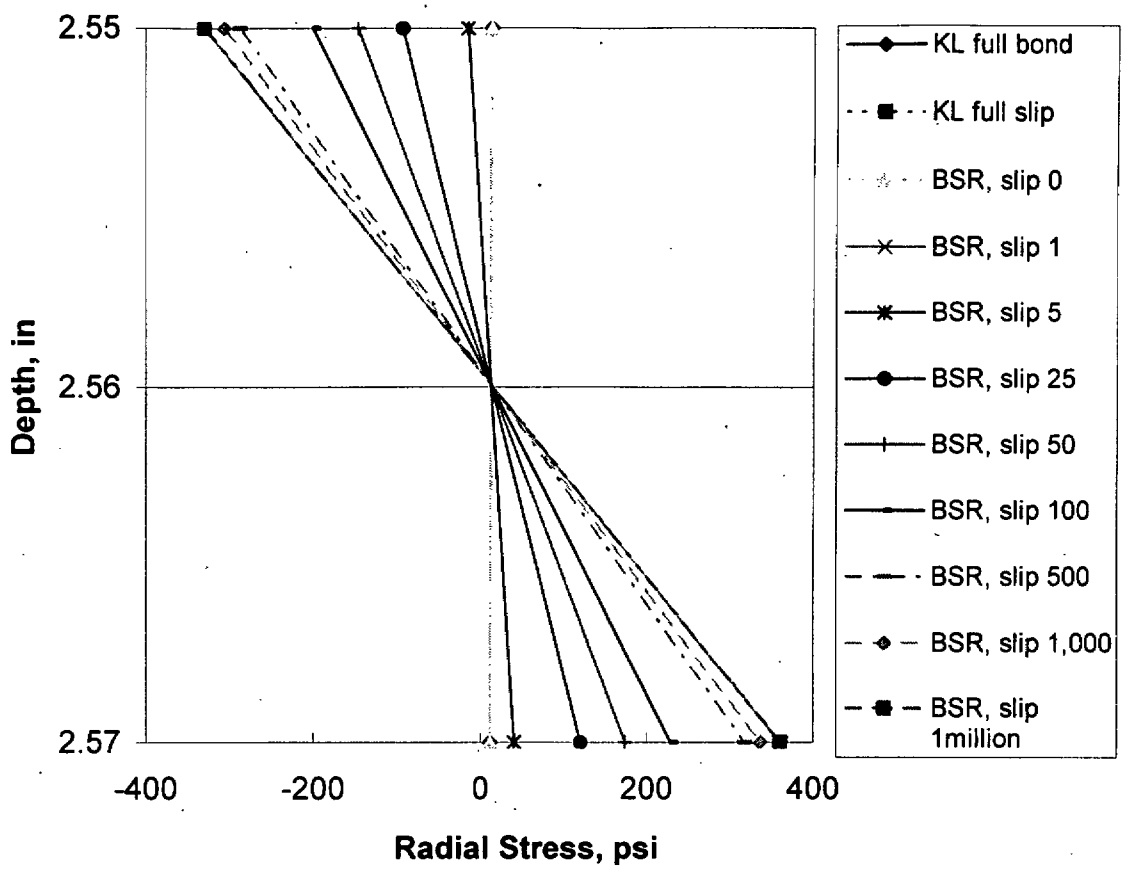

Figure 5.3. Radial Stresses at Points Above and Below Interface, for Varied Slip

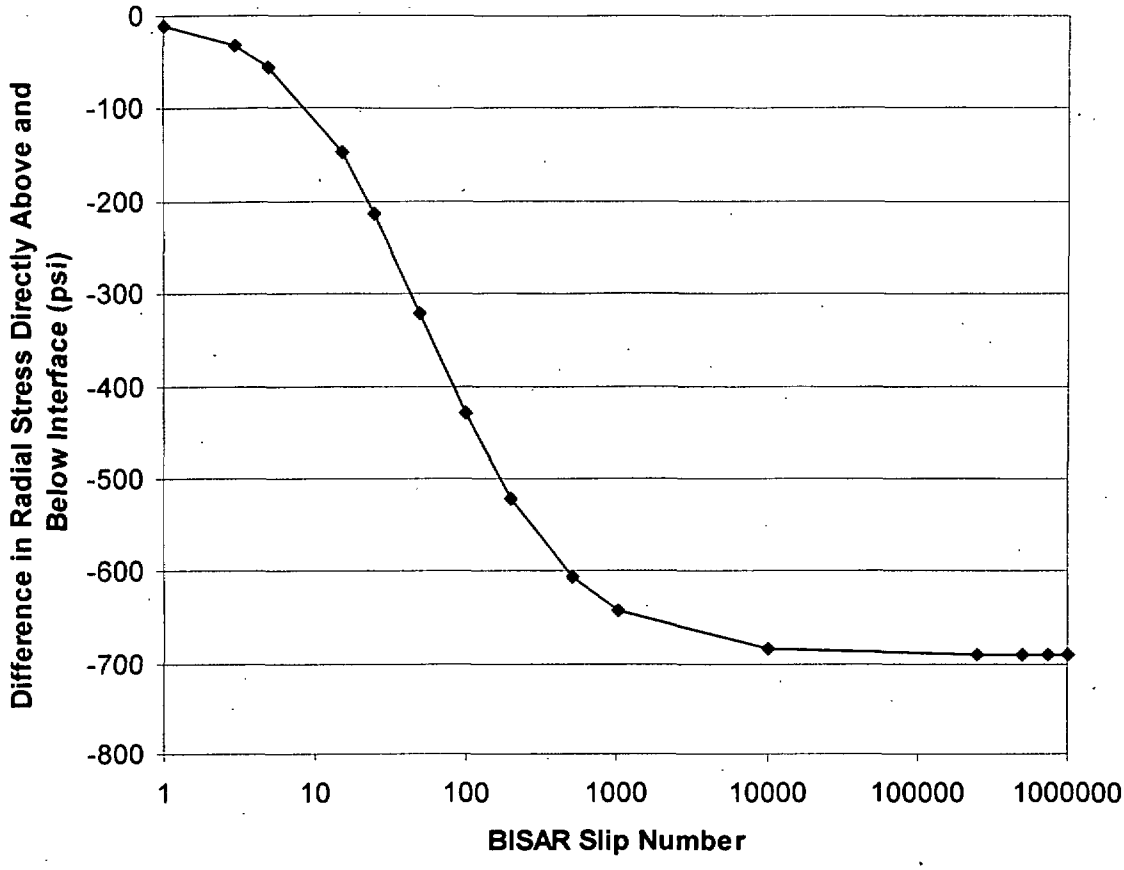

Figure 5.4. Radial Stress Differences vs. BISAR Slip Number in BISAR Investigation

5.3.3. Determination of Effect of Slip in MFC Failed Sections

The next step in the study was to determine the effect of slip in the failed sections. As explained before, backcalculation programs do not evaluate various degrees of slip. Thus this analysis was done indirectly, with the use of BISAR. This analysis was performed in four steps, as described below.

Step 1: Calculation of Mechanical Responses in "Surrogate Pavement"

Analysis of a "surrogate pavement" was conducted. The "surrogate pavement" is a representation of a failed section in which there is full bonding but the calculated moduli of the top asphalt layer (E_F) is lower than the moduli of the lower asphalt layer (E_{UF}), as described previously in Section 5.2.2. That is, the TFR < 1. Figure 5.5(a) shows the "surrogate pavement" analyzed. The asphalt moduli E_F and E_{UF} used are shown below in Table 5.4.

Mechanical responses, calculated at locations directly under the load, were: vertical displacement, vertical stress, and radial stress. Figure 5.6 shows the layer thicknesses and evaluation points that were used.

Step 2: Calculation of Mechanical Responses in "Actual Pavement"

Analysis was conducted on the "actual pavement". The "actual pavement", as described previously in Section 5.2.2, has both asphalt layer moduli of E_{UF}, as shown in Figure 5.5(b). The values of E_{UF} used are shown below in Table 5.4.

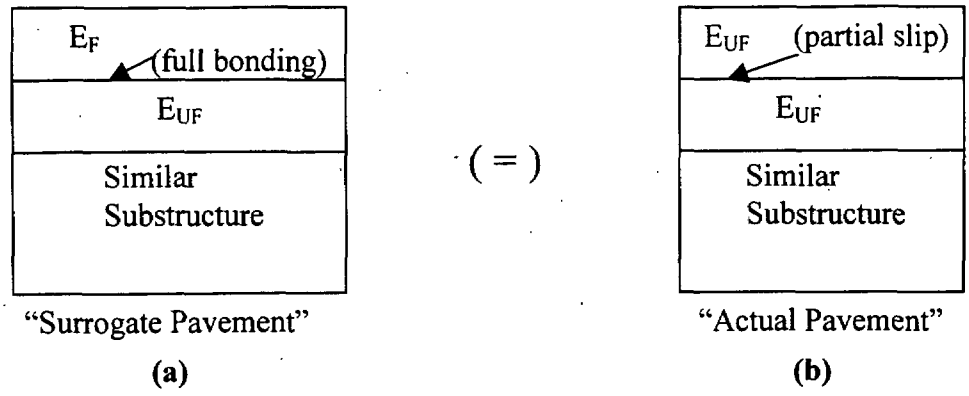

Figure 5.5. MFC Failed Section Analysis, Pavement Structure Cases

Table 5.4. Properties of Sections Analyzed

FWD ID	Load (lb)	Lane	Case *	E_F (ksi)	E_{UF} (ksi)	E_{P-209} (ksi)	E_{P-154} (ksi)	$E_{subgrade}$ (ksi)
24928	11592	C/L	Surrogate	1,405	1,750	16.875	13.053	23.730
			Actual	1,750				
24932	11492	C/L	Surrogate	1,366	1,750	16.888	13.073	24.330
			Actual	1,750				
24929	23244	C/L	Surrogate	1,036	1,606	24.497	16.592	22.110
			Actual	1,606				
24933	23315	C/L	Surrogate	570	1,606	25.577	17.007	22.680
			Actual	1,606				
24930	35055	C/L	Surrogate	491	1,270	32.520	19.177	20.220
			Actual	1,270				
24934	34869	C/L	Surrogate	141	1,270	35.385	19.845	21.030
			Actual	1,270				
24864	11726	5	Surrogate	1,380	1,662	16.978	13.025	22.210
			Actual	1,662				
24916	11726	5	Surrogate	1,395	1,662	16.972	13.050	22.710
			Actual	1,662				
24865	23367	5	Surrogate	706	1,490	25.090	16.635	20.830
			Actual	1,490				
24917	23424	5	Surrogate	866	1,490	24.813	16.567	20.910
			Actual	1,490				
24866	35190	5	Surrogate	374	1,175	33.448	19.200	19.600
			Actual	1,175				
24918	35153	5	Surrogate	477	1,175	32.875	19.200	20.010
			Actual	1,175				

*In the Surrogate Case, interlayer is fully bonded. In the Actual Case, the interlayer has varied degrees of slip.

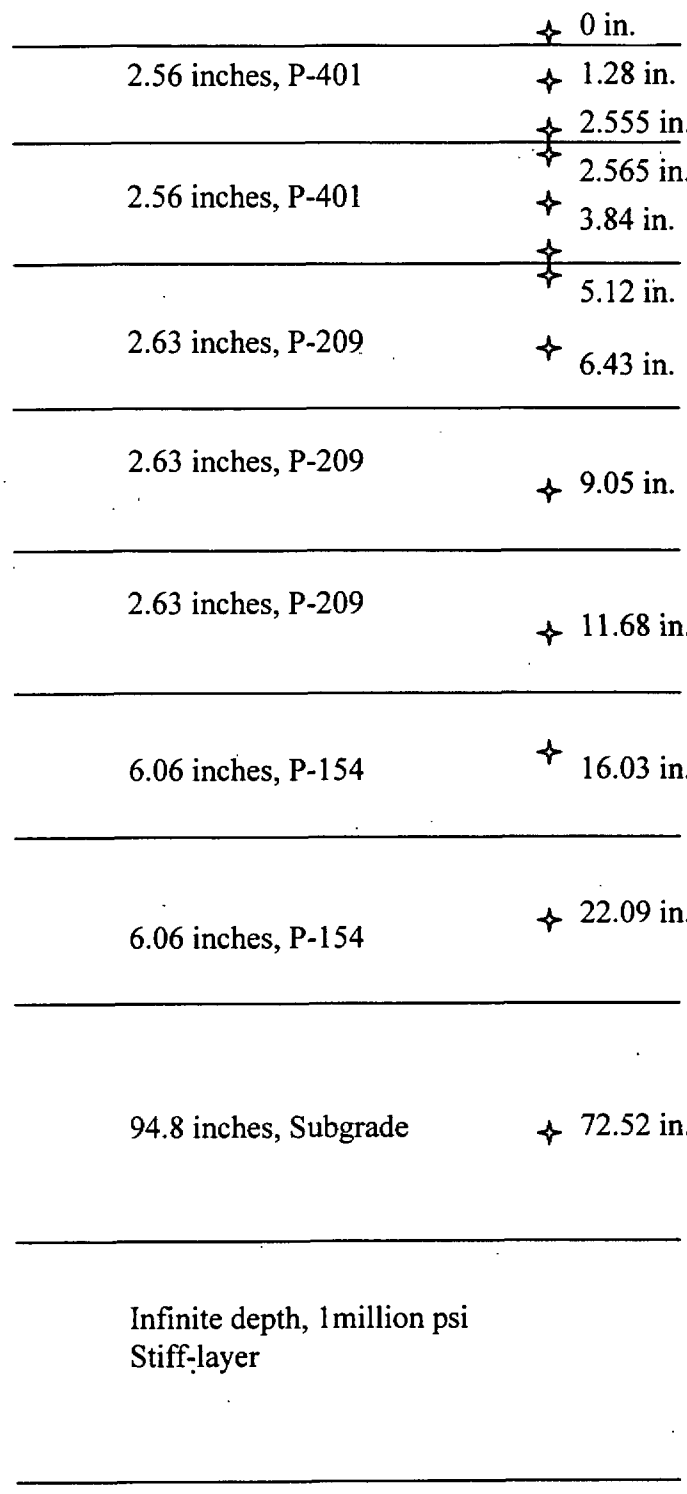

Figure 5.6. Layers and Evaluation Points Used in BISAR

As explained in the previous section, BISAR is able to calculate mechanical responses in pavements with various degrees of slip, which are designated by the BISAR slip number. In this analysis, therefore, the slip between asphalt layers was varied. Six different degrees of slip were analyzed, ranging from full bond (BISAR slip number = 0) to full slip (BISAR slip number = 1 million). The same mechanical responses were calculated as for the "surrogate pavement".

The results of both Step 1 and 2 were plotted together for each FWD number analyzed. Typical plots of vertical displacement, vertical stress, and radial stress may be viewed in Figures 5.7 – 5.9, respectively. These plots show the increase of vertical displacement, vertical stress, and radial stress, as the BISAR slip number increases (the mechanical responses all increase as slip at the interlayer increases). The results for each analyzed FWD drop number may be viewed in Appendix I. The mechanical responses calculated in Steps 1 and 2 were utilized in two stages: Step 3 used the vertical displacement and vertical stress results, and Step 4 used the radial stress results.

Step 3: Comparison of "Surrogate Pavement" and "Actual Pavement"

The vertical displacement and vertical stress results were used to determine the BISAR slip number that most accurately described the interlayer condition that existed for each of the sections mentioned previously in Table 5.4. The plots of vertical displacement and vertical stress (typical plots in Figures 5.7 and 5.8) were used in determining the slip in the pavement for each of the previously mentioned sections and cases. Comparisons were made between the "surrogate pavement", which reflects the existing pavement, and the "actual pavements" with varied slip. In the figures, the

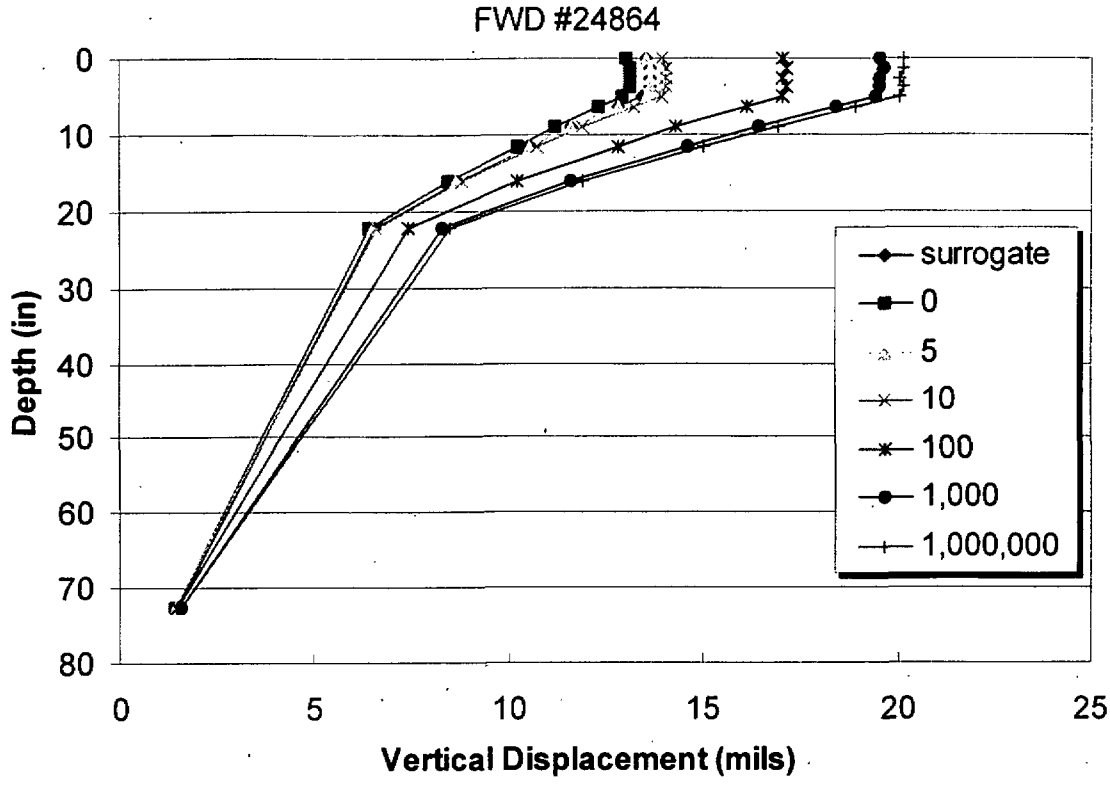

Figure 5.7. Typical Vertical Displacement Plot

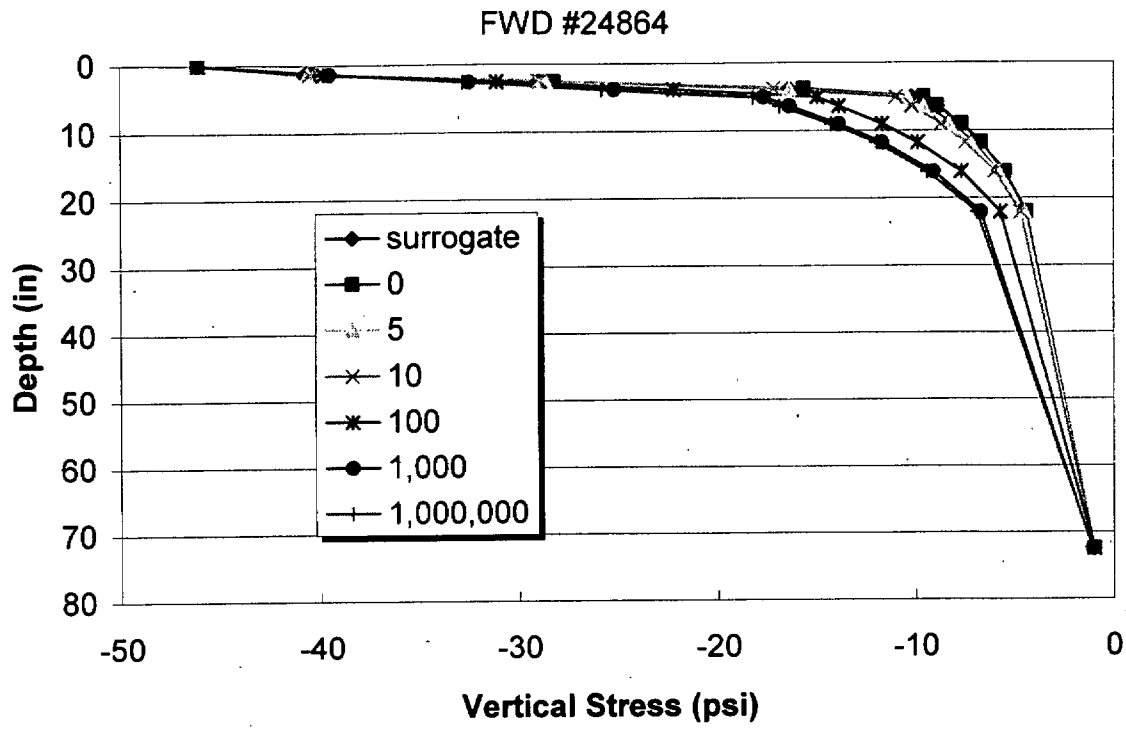

Figure 5.8. Typical Vertical Stress Plot

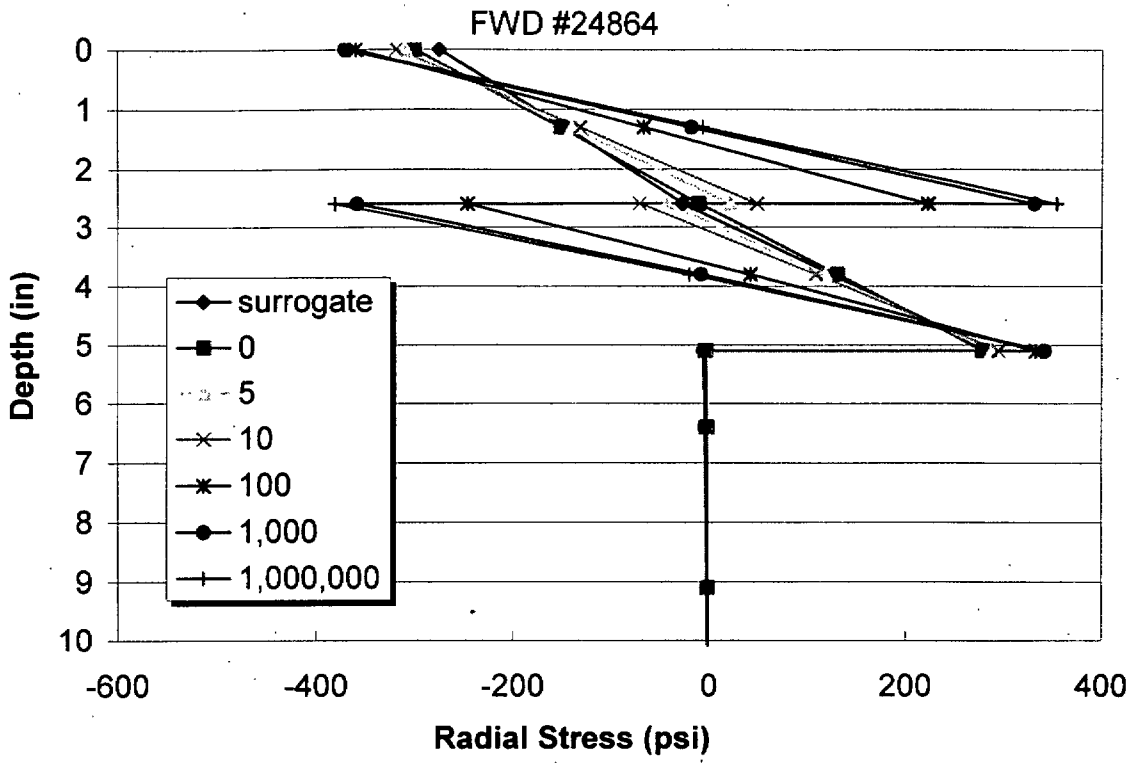

Figure 5.9. Typical Radial Stress Plot

"surrogate pavement" curve matched up with an "actual pavement" curve. The "actual pavement" curve that matched indicated the BISAR slip number that best described the interlayer at that particular section. For example, for FWD #24864, (the results for which are used in the typical plots shown in Figures 5.7 and 5.8), the curve corresponding to BISAR Slip Number 5 matches closely with the curve corresponding to the "surrogate pavement". Thus, for FWD #24864, the slip in the pavement was that which corresponds to the BISAR Slip Number 5. Now that a BISAR slip number was known for each section, the effect of slip was determined in Step 4.

Step 4: Determination of Effect of Slip

The effect of slip was now determined by using the radial stress results from Steps 1 and 2. Based on the preliminary investigations with BISAR (discussed previously), the radial stresses just above and below the interface were used to determine the effect of slip. Figure 5.10 shows a typical plot of radial stresses just above and below the interface. The difference in radial stress between depths 2.555 and 2.565 inches was calculated for each case (interlayer located at 2.56 inches). The differences were then plotted against the BISAR slip number. The resulting plots (shown in Appendix J) were similar to the typical plot shown in Figure 5.11.

Using the plot of "radial stress difference at interface", the radial stress difference at the interface in the actual pavement section was identified by identifying the radial stress difference that matched the BISAR slip number found in Step 3.

Finally, the effect of slip in the pavement was calculated as being the ratio of the difference in radial stress at interface (just identified) to the maximum difference in radial

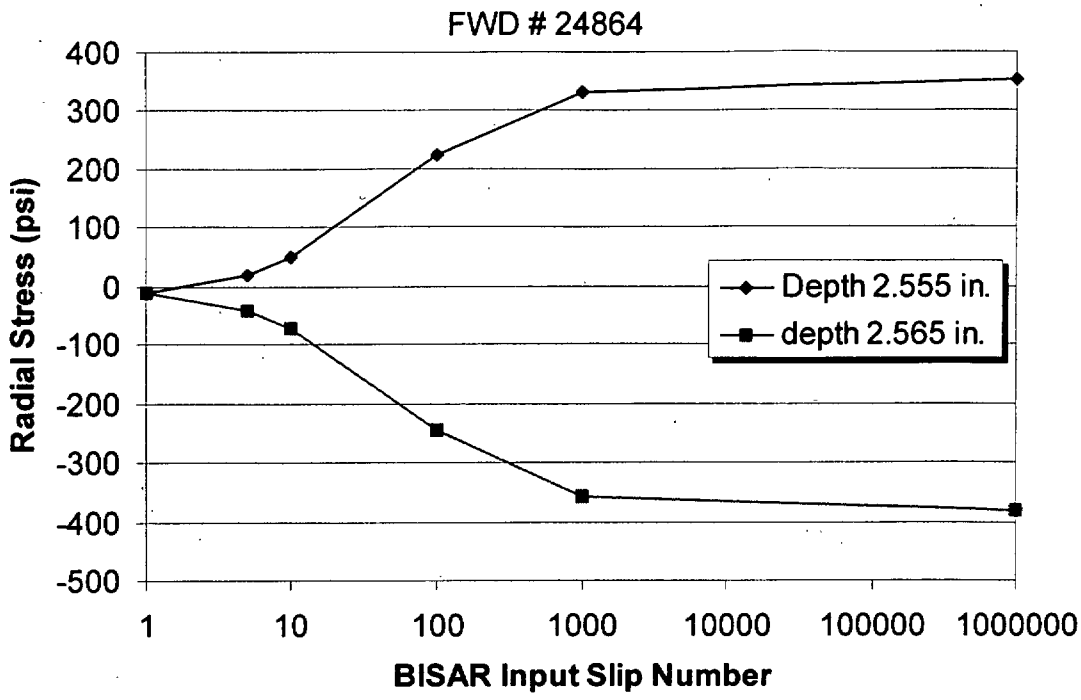

Figure 5.10. Typical Plot of Radial Stresses Just Above and Below the Interface

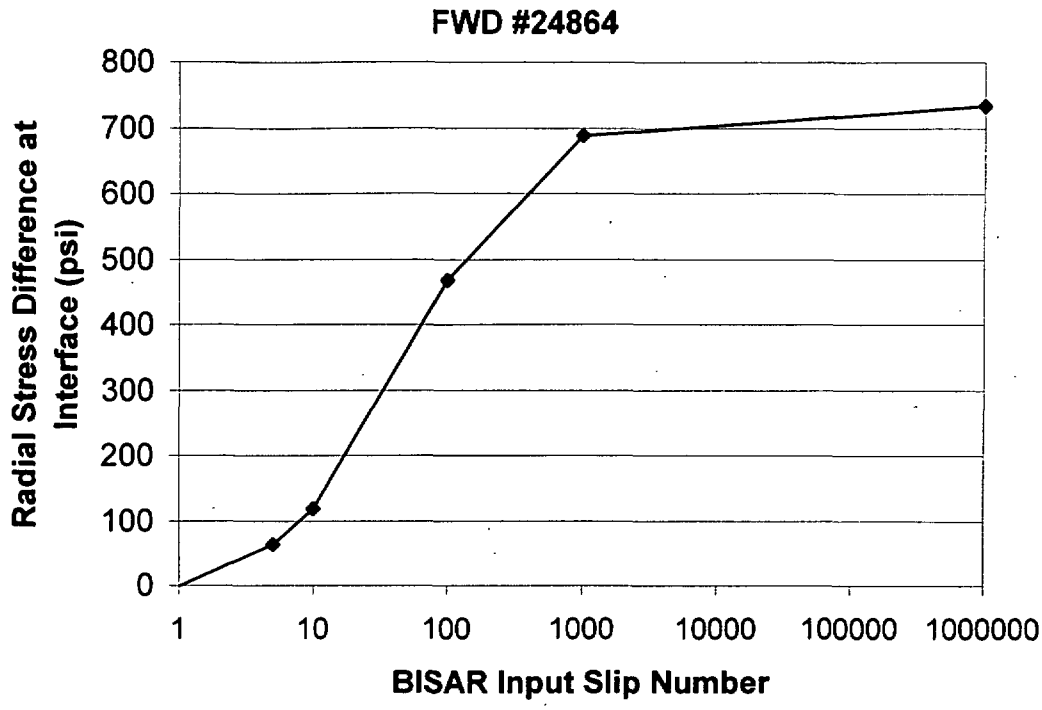

Figure 5.11. Typical Plot of Radial Stress Difference at Interface

stress at interface. The maximum difference in radial stress at the interface is that which occurs at full slip (BISAR slip number = 1 million), and was obtained from the same plot of "radial stress difference at interface" (typical plot, Figure 5.11). The resulting effect of slip values found are shown in the next section.

5.3.4. Results

The effect of slip, as calculated using the method described above, is shown for each FWD number in Table 5.5. These results were correlated to the previously determined TFR's. This correlation is discussed in the next section.

5.4. Correlation of Tack Coat Failure Ratio with Effect of Slip

The calculated TFR's were plotted against the calculated effect of slip values. For convenience, both the TFR and Effect of Slip values are repeated in Table 5.6. The plot of these is shown in Figure 5.12. A correlation was developed. The line is described by a trinomial equation, as shown in the figure. It is hypothesized that this equation is unique for this particular pavement, and that every pavement structure will have its own curve and equation. Therefore, if this is the case, then in order to determine the effect of slip in another pavement, one must follow the procedures outlined in this study to find the TFR/Effect of Slip correlation for that pavement, instead of using the correlation that resulted from this study. Also, it must be recognized that this result is valid only for situations similar to what existed at the FAA NAPTF: slippage between layers of a common material. In a situation where slippage occurs between layers of different

Table 5.5. Effect of Slip Results

FWD ID	Load (lb)	Lane	BISAR # Corresponding to Theoretical Pavement	Radial Stress Difference for Corresponding BISAR # (psi)	Maximum Radial Stress Difference at Interface (psi)	Corresponding Effect of Slip (%)
24928	11592	C/L	5	66.7	739	9
24932	11492	C/L	5	66.1	731	9
24929	23244	C/L	10	215.5	1281	17
24933	23315	C/L	60	552	1264	44
24930	35055	C/L	50	560	1543	36
24934	34869	C/L	800	1320	1524	87
24864	11726	5	5	63.8	734	9
24916	11726	5	5	63.8	733	9
24865	23367	5	30	331	1242	27
24917	23424	5	20	267	1248	21
24866	35190	5	70	693	1517	46
24918	35153	5	50	536	1521	35

Table 5.6. TFR and Effect of Slip

FWD ID	Load (lb)	Lane	TFR	Effect of Slip (%)
24928	11592	C/L	0.803	9
24932	11492	C/L	0.780	9
24929	23244	C/L	0.645	17
24933	23315	C/L	0.355	44
24930	35055	C/L	0.387	36
24934	34869	C/L	0.111	87
24864	11726	5	0.811	9
24916	11726	5	0.839	9
24865	23367	5	0.474	27
24917	23424	5	0.581	21
24866	35190	5	0.318	46
24918	35153	5	0.407	35

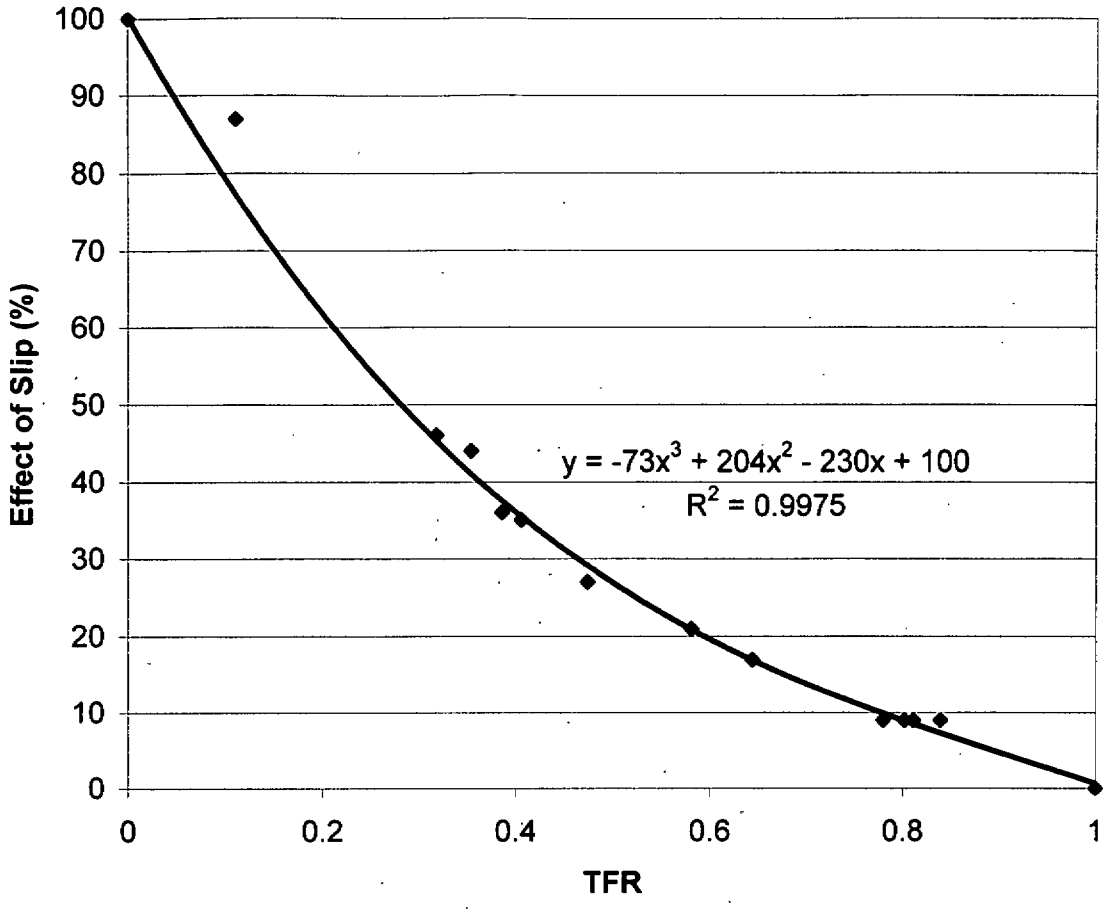

Figure 5.12. Effect of Slip / TFR Correlation

materials, such as between a surface course and base course, the outlined procedure may need to be modified to account for this difference.

5.5. Framework for Using FWD Data in Interlayer Slip Analysis

The above analysis, along with the preceding analyses in this study, may be summarized into a framework that outlines the application of FWD data in identifying poor interlayer bonding in a pavement and quantifying the effect of slip resulting from poor bonding. This outline is shown below in Figure 5.13. This outline would be followed to analyze the effect of slip at one or more locations along a given roadway. If more than one location were analyzed, an effect of slip / TFR correlation could be developed, similar to that which was developed in this study.

A state agency would be able to use this correlation to evaluate interlayer bonding in the same roadway or even different roadways of similar pavement structure. In this event, the agency would only have to compute the TFR's on a roadway and use the correlation to determine the effect of slip, instead of calculating the mechanical responses and determining the effect of slip manually for each location. For example, Figure 5.14 shows a typical correlation that a state agency may have developed for a pavement. The agency would calculate the TFR's of other locations using the above framework, and then use the correlation to determine the effect of slip. If a significant effect of slip is observed in a new pavement, then appropriate modifications to construction practices could be made to avoid future problems. Additionally, the effect of slip data may be used for pavement management, to help prioritize and schedule rehabilitation projects.

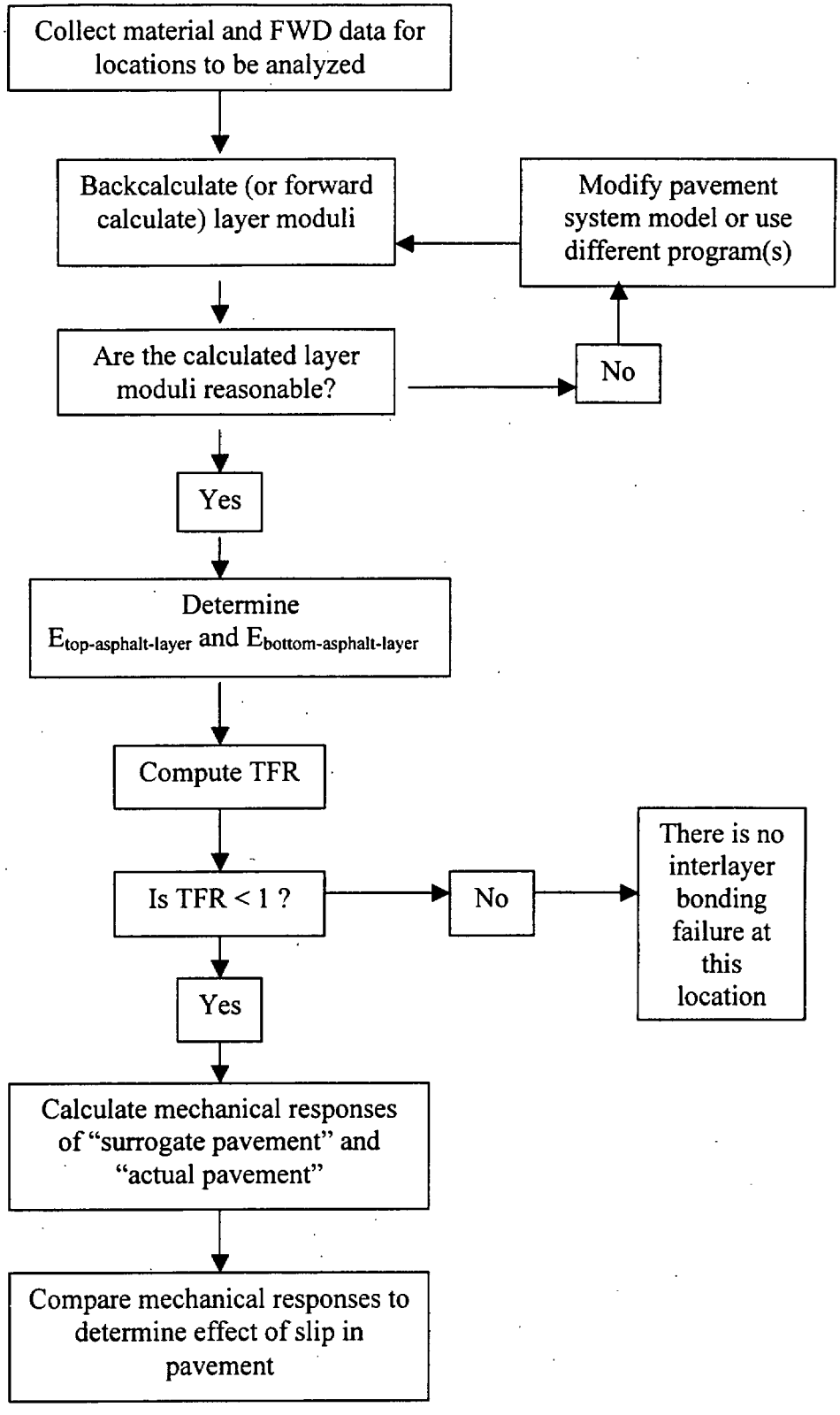

Figure 5.13. Framework of FWD Data Use in Interlayer Slip Analysis

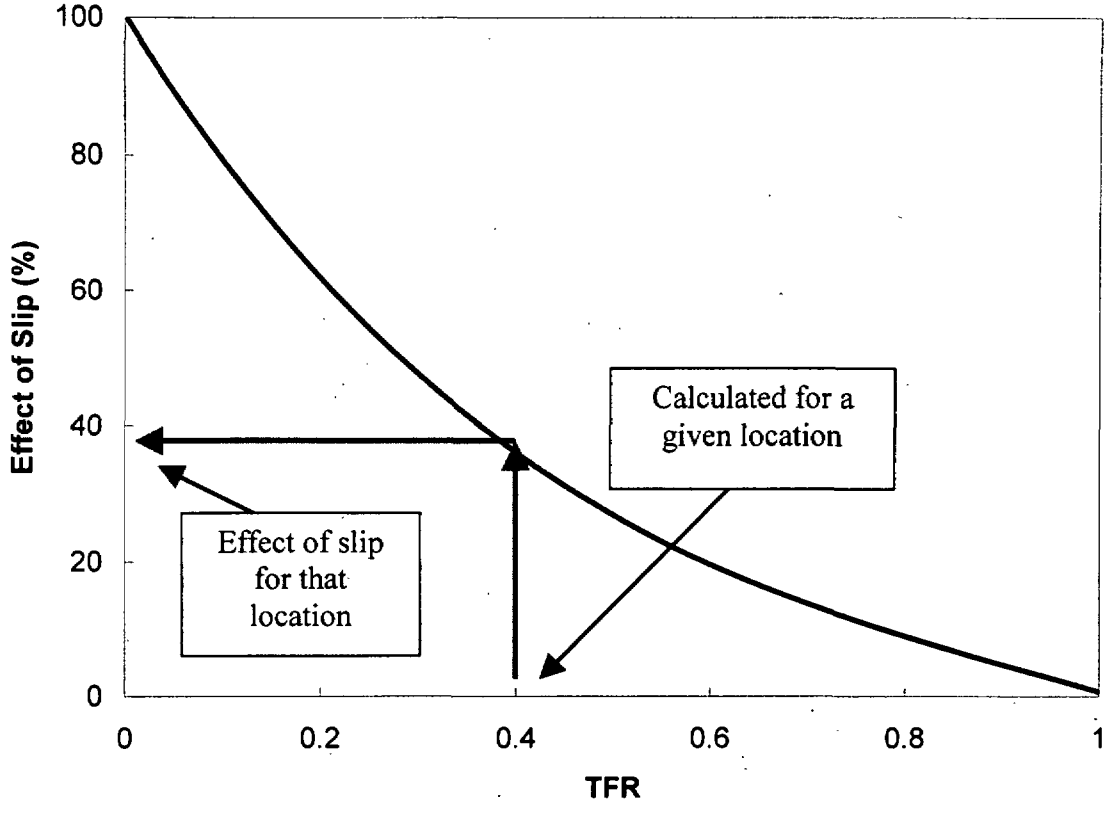

Figure 5.14. Agency Use of Effect of Slip / TFR Correlation

CHAPTER SIX

CONCLUSIONS AND RECOMMENDATIONS

6.1. Summary of Findings

In analyzing the Federal Aviation Administration National Airport Pavement Testing Facility's MFC section, the following was found:

1. The surface layer moduli obtained from Falling Weight Deflectometer (FWD) data was significantly different between failed and unfailed sections at early loading times, for all loads and temperatures.
2. A difference in calculated layer moduli between different sections may indicate the presence of interlayer bonding failure.
3. In pavements where slip occurs between two asphalt layers of similar properties, a Tack Coat Failure Ratio (TFR) can be defined as the ratio of the modulus of the top layer to the modulus of the lower layer:

$$\text{TFR} = \frac{E_{top-asphalt-layer}}{E_{bottom-asphalt-layer}}$$

4. The effect of slip at the interface can be measured by the difference in radial stresses at points just above and just below the interface.
5. Given enough material data, a TFR and Effect of Slip correlation may be established for a pavement structure.

6.2. Conclusion

It can be concluded that:

1. Surface layer moduli calculated from FWD data can be used to identify a lack of interlayer bonding in pavements.
2. The effect of slip between two asphalt layers of similar properties will be reflected by the moduli of the top layer being lower than the moduli of the bottom layer ($E_{top\text{-}asphalt\text{-}layer} < E_{bottom\text{-}asphalt\text{-}layer}$).

6.3. Recommendations

Based on the findings and conclusions, the following recommendations are made:

1. The procedure outlined in this study should be evaluated for a pool of pavement sections to determine the extent of its validity.
2. The outlined procedure should be tested on a different pavement section that also has detailed material data available, for two reasons:
    a. To ensure that the methods used are accurate for various pavement systems.
    b. To verify whether or not the TFR / Effect of Slip correlation obtained in this study is unique for different pavements.
3. Effect of slip should be correlated to physical results of slippage. That is, the results of slippage should be measured in some way and related to the effect of slippage, so that when one calculates the effect of slippage, one knows what failures may be expected, if any.

4. Modifications should be made to the procedure so that slip can be evaluated between layers other than layers of similar materials, such as slip between asphalt concrete and a base course.

REFERENCES

Briggs, R., Lukanen, E., and Stubstad, R., *Temperature Predictions and Adjustment Factors for Asphalt Pavement*. Report No. FHWA-RD-98-085. Federal Highway Administration, 2000.

Federal Aviation Administration, BAKFAA Pavment Backcalculation Program. July 2000.

Federal Aviation Administration, National Airport Pavement Testing Facility, FAA NAPTF website: http://www.airporttech.tc.faa.gov/NAPTF/database%20intro.asp

Garg, N., *Posttraffic Testing at the National Airport Pavement Test Facility: Test Item MFC*. Report DOT/FAA/AR-TN01/49. U.S. Department of Transportation, Federal Aviation Administration, September 2001.

Hachiya, Y., and Sato, K., *Effect of Tack Coat on Bonding Characteristics at Interface between Asphalt Concrete Layers*. Proceedings, Eighth International Conference on Asphalt Pavements, University of Washington, Seattle, 1997.

Huang, Y. H., *Pavement Analysis and Design*. Prentice Hall, Inc. Englewood Cliffs, New Jersey, 1993.

Mohammad, L.N., Raqib, M.A., and Huang, B., *Influence of Asphalt Tack Coat Materials on Interface Shear Strength*. Transportation Research Record, 2002.

Shahin M., Kirchner, K., and Blackmon, E. W., *Analysis of Asphalt Concrete Layer Slippage and its Effect on Pavement Performance and Rehabilitation Design*. Proceedings, Sixth International Conference on the Structural Design of Asphalt Pavements. University of Michigan, Ann Arbor, Michigan, 1987.

Shahin M, Van Dam T., Kirchner, K., and Blackmon, E. W., *Consequence of Layer Separation on Pavement Performance*. Report DOT/FAAPM-86/48, Federal Aviation Administration, Washington, D.C., 1987.

Sholar, G.A., Page, G.C., Musselman, J.A., Upshaw, P.B., and Mosely, H.L., *Preliminary Investigation of a Test Method to Evaluate Bond Strength of Bituminous Tack Coats*. Report FL/DOT/SMO/02-459, 2002.

Uzan, J., Liveneh, M., and Eshed, Y., *Investigation of Adhesion Properties Between Asphaltic-Concrete Layers*. Proceedings, Asphalt Paving Technology, Vol.46, Lake Buena Vista, Florida, 1978.

Appendix A

Material Data

Table A.1. P-401 HMA Layer Material Data

Test Date	Lift No.	Gmm	Gmb (field)	Gmb (lab)	% Compaction	% Air Voids
3/17/1999	1	2.580	2.497	2.512	99.4	3.2
3/17/1999	1	2.580	2.482	2.512	98.8	3.8
3/17/1999	1	2.580	2.483	2.512	98.8	3.8
3/17/1999	1	2.580	2.477	2.512	98.6	4.0
3/17/1999	1	2.580	2.388	2.512	95.1	7.4
3/17/1999	1	2.580	2.373	2.512	94.5	8.0
3/17/1999	1	2.580	2.439	2.512	97.1	5.5
3/17/1999	1	2.580	2.446	2.512	97.4	5.2
3/19/1999	2	2.586	2.498	2.518	99.2	3.4
3/19/1999	2	2.586	2.471	2.518	98.1	4.4
3/19/1999	2	2.586	2.487	2.518	98.8	3.8
3/19/1999	2	2.586	2.485	2.518	98.7	3.9
3/19/1999	2	2.586	2.359	2.518	93.7	8.8
3/19/1999	2	2.586	2.360	2.518	93.7	8.7
3/19/1999	2	2.586	2.466	2.518	97.9	4.6
3/19/1999	2	2.586	2.376	2.518	94.4	8.1

Table A.2. P-209 Base Layer Material Data

Sample ID.	Moisture Content, %	Dry Density, pcf	Confining Stress, psi	Deviator Stress, psi	Resilient Strain	Resilient Modulus, psi
A	4.5	154.2	3.00	2.67	0.000150	17643.6
A	4.5	154.2	3.00	5.39	0.000270	19844.1
A	4.5	154.2	3.00	8.10	0.000360	22691.1
A	4.5	154.2	5.00	4.49	0.000190	24277.0
A	4.5	154.2	5.00	9.00	0.000320	27962.1
A	4.5	154.2	5.00	13.51	0.000440	30748.0
A	4.5	154.2	10.00	8.98	0.000230	38455.0
A	4.5	154.2	10.00	17.98	0.000440	40720.3
A	4.5	154.2	10.00	27.05	0.000610	44335.2
A	4.5	154.2	15.10	9.02	0.000200	44811.5
A	4.5	154.2	15.00	13.50	0.000290	46465.1
A	4.5	154.2	15.00	27.00	0.000510	53013.5
A	4.5	154.2	20.00	13.50	0.000250	53876.9
A	4.5	154.2	20.00	18.00	0.000320	56232.9
A	4.5	154.2	20.00	36.03	0.000570	63571.8
B	4.6	151.9	3.00	2.67	0.000190	14382.6
B	4.6	151.9	3.00	5.41	0.000330	16251.2
B	4.6	151.9	3.00	8.12	0.000440	18455.6
B	4.6	151.9	5.00	4.50	0.000220	20134.5
B	4.6	151.9	5.00	9.02	0.000390	23189.7
B	4.6	151.9	5.00	13.55	0.000530	25632.6
B	4.6	151.9	10.00	8.98	0.000270	33037.6
B	4.6	151.9	10.00	18.07	0.000480	37303.6
B	4.6	151.9	10.00	27.15	0.000660	41061.0
B	4.6	151.9	15.00	9.02	0.000230	39952.5
B	4.6	151.9	15.00	13.54	0.000320	42354.4
B	4.6	151.9	15.00	27.05	0.000550	49239.3
B	4.6	151.9	20.00	13.56	0.000270	49815.2
B	4.6	151.9	20.00	18.05	0.000350	52325.2
B	4.6	151.9	20.00	36.17	0.000600	60390.8

Table A.3. P-154 Subbase Layer Material Data

Sample ID.	Moisture Content, %	Dry Density, pcf	Confining Stress, psi	Deviator Stress, psi	Resilient Strain	Resilient Modulus, psi
A	6.1	131.8	3.00	2.65	0.000210	12768.4
A	6.1	131.8	3.00	5.30	0.000380	13837.6
A	6.1	131.8	3.00	8.07	0.000510	15696.6
A	6.1	131.8	5.00	4.47	0.000250	17702.0
A	6.1	131.8	5.00	8.98	0.000450	19971.5
A	6.1	131.8	5.00	13.52	0.000620	21923.7
A	6.1	131.8	10.10	9.00	0.000310	29258.2
A	6.1	131.8	10.00	17.72	0.000570	31238.3
A	6.1	131.8	10.00	27.06	0.000810	33529.5
A	6.1	131.8	15.00	8.97	0.000260	33893.3
A	6.1	131.8	15.00	13.50	0.000380	35357.1
A	6.1	131.8	15.00	26.99	0.000670	40428.8
A	6.1	131.8	20.10	13.46	0.000320	41743.4
A	6.1	131.8	20.00	18.00	0.000410	43398.6
A	6.1	131.8	20.00	36.04	0.000740	48885.2
B	5.7	132.5	3.00	2.65	0.000170	15403.6
B	5.7	132.5	3.00	5.37	0.000330	16184.2
B	5.7	132.5	3.00	8.10	0.000450	17855.2
B	5.7	132.5	5.00	4.41	0.000230	19556.5
B	5.7	132.5	5.00	8.99	0.000410	21964.0
B	5.7	132.5	5.00	13.49	0.000560	24152.4
B	5.7	132.5	10.00	9.00	0.000300	30385.6
B	5.7	132.5	10.00	17.99	0.000540	33556.9
B	5.7	132.5	10.00	26.63	0.000770	34683.6
B	5.7	132.5	15.10	8.97	0.000260	34696.7
B	5.7	132.5	15.00	13.49	0.000380	35843.4
B	5.7	132.5	15.00	26.99	0.000660	40877.5
B	5.7	132.5	20.00	13.47	0.000330	40987.2
B	5.7	132.5	20.00	18.00	0.000420	42910.2
B	5.7	132.5	19.90	35.99	0.000730	49001.9

Table A.4(a). Subgrade Material Data

Moisture Content, %	Dry Density, pcf	Confining Stress, psi	Deviator Stress, psi	Resilient Strain	Resilient Modulus, psi
29.8	94.8	6.00	1.80	0.000150	12000.4
29.8	94.8	6.00	3.63	0.000320	11446.4
29.8	94.8	6.00	5.39	0.000520	10423.0
29.8	94.8	6.00	7.17	0.000770	9283.4
29.8	94.8	6.00	8.99	0.001110	8087.9
29.8	94.8	4.00	1.79	0.000150	11565.4
29.8	94.8	4.00	3.58	0.000320	11015.9
29.8	94.8	4.00	5.41	0.000530	10213.8
29.8	94.8	4.00	7.17	0.000780	9174.0
29.8	94.8	4.00	8.98	0.001120	8032.4
29.8	94.8	2.00	1.81	0.000170	10464.7
29.8	94.8	2.00	3.59	0.000360	9995.1
29.8	94.8	2.00	5.39	0.000570	9385.7
29.8	94.8	2.00	7.17	0.000840	8581.2
29.8	94.8	2.00	8.97	0.001170	7685.1
29.1	92.5	6.00	1.79	0.000140	12684.1
29.1	92.5	6.00	3.62	0.000290	12567.2
29.1	92.5	6.00	5.39	0.000460	11698.7
29.1	92.5	6.00	7.12	0.000670	10673.5
29.1	92.5	6.00	8.85	0.000910	9687.3
29.1	92.5	4.00	1.79	0.000140	12435.9
29.1	92.5	4.00	3.60	0.000310	11756.0
29.1	92.5	4.00	5.39	0.000490	11120.8
29.1	92.5	4.00	7.13	0.000690	10269.4
29.1	92.5	4.00	8.86	0.000950	9307.4
29.1	92.5	2.00	1.80	0.000170	10855.6
29.1	92.5	2.00	3.61	0.000350	10251.6
29.1	92.5	2.00	5.36	0.000550	9671.8
29.1	92.5	2.00	7.12	0.000780	9138.5
29.1	92.5	2.00	8.85	0.001040	8534.2

Table A.4(b). Subgrade Material Data

Moisture Content, %	Dry Density, pcf	Confining Stress, psi	Deviator Stress, psi	Resilient Strain	Resilient Modulus, psi
32.4	91.5	6.00	1.78	0.000190	9275.9
32.4	91.5	6.00	3.63	0.000420	8602.5
32.4	91.5	6.00	5.45	0.000750	7273.4
32.4	91.5	6.00	7.29	0.001190	6132.4
32.4	91.5	6.00	9.05	0.001780	5091.1
32.4	91.5	4.00	1.81	0.000200	8855.3
32.4	91.5	4.00	3.64	0.000450	8108.8
32.4	91.5	4.00	5.47	0.000800	6817.0
32.4	91.5	4.00	7.27	0.001290	5630.1
32.4	91.5	4.00	8.85	0.001830	4840.3
32.4	91.5	2.00	1.80	0.000230	7711.6
32.4	91.5	2.00	3.62	0.000520	6986.5
32.4	91.5	2.00	5.46	0.000920	5937.0
32.4	91.5	2.00	7.10	0.001420	5014.2
32.4	91.5	2.00	8.85	0.002010	4413.6

Appendix B

Raw Falling Weight Deflectometer Data

Table B.1(a). Raw FWD Data

FWD #	Load (lb)	Defl0 (mils)	Defl2 (mils)	Defl3 (mils)	Defl4 (mils)	Defl5 (mils)	Defl6 (mils)	Air Temp (F)	Pave Temp (F)
24881	35139	37.3	25.34	16.63	10.66	7.37	5.42	44	48
24882	11779	11.72	7.95	5.32	3.51	2.49	1.86	44	48
24883	23697	23.55	16.09	10.73	6.98	4.94	3.7	44	48
24884	35641	35.78	24.51	16.46	10.79	7.52	5.64	44	48
24885	35128	35.4	25.88	16.93	10.74	7.4	5.39	44	48
24886	11840	10.97	8.14	5.41	3.51	2.49	1.88	44	48
24887	23544	21.99	16.25	10.81	6.9	4.87	3.63	44	48
24888	35642	33.99	24.81	16.66	10.84	7.52	5.57	44	48
24889	35073	35.62	25.96	16.88	10.62	7.24	5.35	44	48
24890	11872	10.97	8.14	5.38	3.48	2.46	1.85	44	48
24891	23730	22.09	16.25	10.87	6.89	4.81	3.62	44	48
24892	35676	34.21	24.91	16.57	10.68	7.36	5.49	44	48
24893	35187	35.24	24.97	16.57	10.59	7.19	5.25	43	48
24894	11932	10.91	7.87	5.27	3.45	2.42	1.78	43	48
24895	23669	21.77	15.79	10.68	6.89	4.79	3.55	43	48
24896	35586	33.5	23.89	16.22	10.56	7.3	5.39	43	48
24855	34617	39.59	30.81	19.8	12.49	8.22	5.81	48	46
24856	11613	11.72	9.05	5.93	3.88	2.72	1.94	48	46
24857	23221	23.65	18.41	12.15	7.83	5.35	3.86	48	46
24858	35117	36.27	28.36	18.78	12.13	8.22	5.92	48	46
24859	34833	40.24	32.18	20.35	12.67	8.37	5.88	48	46
24860	11685	12.1	9.56	6.17	3.93	2.72	1.98	48	46
24861	23374	24.08	19.34	12.53	7.92	5.44	3.92	48	46
24862	35250	36.92	29.54	19.22	12.26	8.26	5.98	48	46
24863	34750	43.82	35.22	21.07	12.71	8.21	5.74	48	46
24864	11726	12.91	10.25	6.31	3.96	2.72	1.98	48	46
24865	23367	25.86	20.7	12.8	7.88	5.34	3.8	48	46
24866	35190	39.86	31.94	19.83	12.26	8.14	5.82	48	46
24867	34874	42.68	33.39	20.96	12.62	8.12	5.68	49	46
24916	11726	12.7	9.82	6.28	3.95	2.67	1.96	49	46
24917	23424	25.21	19.74	12.7	7.84	5.25	3.8	49	46
24918	35153	38.77	30.4	19.64	12.15	8.07	5.74	49	46
24919	34519	37.85	28.95	18.7	11.71	7.66	5.45	59	52
24920	11347	11.29	8.65	5.57	3.6	2.52	1.82	59	52

Table B.1(b). Raw FWD Data

FWD #	Load (lb)	Defl0 (mils)	Defl2 (mils)	Defl3 (mils)	Defl4 (mils)	Defl5 (mils)	Defl6 (mils)	Air Temp (F)	Pave Temp (F)
24921	23162	22.52	17.23	11.28	7.25	4.97	3.62	59	52
24922	35055	34.7	26.58	17.51	11.33	7.62	5.52	59	52
24923	34629	38.28	31.02	19.86	12.38	8	5.49	58	52
24924	11649	11.24	9.02	5.82	3.72	2.57	1.85	58	52
24925	23302	22.36	18.03	11.74	7.46	5.08	3.64	58	52
24926	35141	35.02	28.22	18.42	11.77	7.8	5.53	58	52
24927	34471	41.81	32.96	20.77	12.49	7.93	5.53	58	52
24928	11592	11.89	9.34	5.93	3.75	2.56	1.89	58	52
24929	23244	23.87	18.75	12.18	7.46	5.05	3.67	58	52
24930	35055	38.12	29.84	19.14	11.86	7.8	5.61	58	52
24931	34254	44.47	34.33	20.82	12.14	7.65	5.34	59	53
24932	11492	12.26	9.42	5.74	3.57	2.49	1.81	59	53
24933	23315	25.27	19.42	12.09	7.34	4.93	3.55	59	53
24934	34869	40.13	30.89	19.19	11.58	7.55	5.43	59	53
25303	33596	64.4	41.99	23.67	13.31	7.78	5.43	71	73
25304	11294	16.69	11.06	6.5	3.97	2.54	1.88	71	73
25305	23101	34.67	23.18	13.61	8.33	5.13	3.79	71	73
25306	34386	53.75	35.9	21.19	12.67	7.79	5.59	71	73
25307	33610	64.84	41.97	23.75	13.46	7.81	5.42	71	73
25308	11475	16.36	10.85	6.36	3.9	2.55	1.88	71	73
25309	23111	34.34	22.54	13.39	8.15	5.07	3.71	71	73
25310	34193	54.03	35.66	21.05	12.67	7.76	5.55	71	73
25311	33596	64.19	41.65	23.39	13.35	7.86	5.6	71	73
25312	11427	16.14	10.71	6.33	3.86	2.54	1.88	71	73
25313	23006	33.8	22.41	13.17	8.1	5.07	3.77	71	73
25314	34295	53.81	35.6	20.97	12.58	7.82	5.69	71	73
25315	33570	65.44	41.97	22.98	12.87	7.64	5.5	70	73
25316	11423	16.31	10.71	6.11	3.76	2.44	1.83	70	73
25317	22946	34.18	22.52	12.87	7.81	4.93	3.65	70	73
25318	34257	54.46	35.77	20.44	12.21	7.57	5.58	70	73
25319	28822	179.12	108.02	52.13	20.77	7.75	3.73	71	74
25320	11281	30.6	19.58	9.98	5.19	2.93	2.09	71	74
25321	21532	67.65	44.42	22.56	11.07	5.65	3.74	71	74
25322	31710	108.87	73.84	37.85	17.84	8.49	5.12	71	74
25323	29463	165.41	105.87	50.25	21.67	8.7	4.44	72	74
25324	10919	29.46	19.21	9.73	5.08	2.92	2.08	72	74
25325	21713	68.63	45.38	23.27	11.82	5.99	3.99	72	74

Table B.1(c). Raw FWD Data

FWD #	Load (lb)	Defl0 (mils)	Defl2 (mils)	Defl3 (mils)	Defl4 (mils)	Defl5 (mils)	Defl6 (mils)	Air Temp (F)	Pave Temp (F)
25326	31773	108	73.03	37.99	18.54	8.9	5.42	72	74
25327	29716	152.08	99.27	48.46	20.78	8.44	4.43	71	74
25328	10587	27.29	17.93	9.18	4.76	2.76	1.96	71	74
25329	21754	64.95	43.44	22.77	11.35	5.83	3.93	71	74
25330	31925	102.92	70.13	37.19	17.94	8.75	5.36	71	74
25331	29602	158.8	101.55	48.46	19.55	8.04	4.23	71	75
25332	10705	27.29	17.69	8.96	4.52	2.69	1.95	71	75
25333	21765	64.46	42.51	21.77	10.53	5.54	3.81	71	75
25334	32009	103.3	69.6	35.87	16.7	8.26	5.23	71	75

Appendix C

Backcalculation Analysis Results

Table C.1. Backcalculation Round 1 Results (BAKFAA) *

FWD #	E_{P-401} (psi)	E_{P-209} (psi)	E_{P-154} (psi)	$E_{subgrade}$ (psi)	E_{stiff} (psi)
24919	334,405	**57,484**	**41,612**	11,185	1,000,000
24920	575,886	**32,723**	**106,709**	10,271	1,000,000
24921	459579	**48,461**	**71,503**	11,090	1,000,000
24922	319,330	**64,327**	**57,880**	11,229	1,000,000
24923	1,460,862	**6,974**	**594,558**	9,639	1,000,000
24924	1,480,247	**9,325**	**827,023**	9302	1,000,000
24925	1617,132	**8,547**	**876,249**	9521	1,000,000
24926	1,499,482	**9,731**	**524,317**	9,633	1,000,000
24927	1,137,501	**7,205**	**444,183**	9,644	1,000,000
24928	1,198,919	**9,740**	**713,632**	9209	1,000,000
24929	1,365,196	**8,353**	**794,312**	9576	1,000,000
24930	1,075,314	**11,664**	**305,644**	9,652	1,000,000
24931	858,285	**8,194**	**278,430**	10,021	1,000,000
24932	923,276	**10537**	**630,028**	9,586	1,000,000
24933	657,910	20993	**108,457**	10,779	1,000,000
24934	923,968	**10,334**	**337,530**	9,985	1,000,000
24959	572,663	**91,647**	**25,762**	11,033	1,000,000
24960	597,551	**67,412**	**51,987**	10,607	1,000,000
24961	1,201,093	28,869	**91,419**	10,134	1,000,000
24962	593,520	**90,175**	**38,941**	10,965	1,000,000
24963	310,602	**117,025**	17,012	11,630	1,000,000
24964	414,212	**80,705**	**47,851**	10,920	1,000,000
24965	1,166,635	**34,163**	**61,473**	10,784	1,000,000
24966	557,522	**88,715**	**30,014**	11,490	1,000,000
24967	1,225,732	**9,554**	**436,865**	9,466	1,000,000
24968	1,277,746	**11,861**	**625,429**	9,005	1,000,000
24969	1,518,398	**11,553**	**734,613**	10,203	1,000,000
24970	1,081,294	18,959	**163,896**	9,703	1,000,000
24971	819,873	19,193	**85,076**	10,449	1,000,000
24972	920,831	**14,874**	**458,667**	9,567	1,000,000
24973	1,211,087	**11,203**	**565,669**	9,783	1,000,000
24974	768,850	25,505	**90,410**	10,534	1,000,000

* Values in bold indicate they were outside the expected range

Table C.2. Backcalculation Round 1 Results (EVERCALC) *

FWD #	E_{P-401} (psi)	E_{P-209} (psi)	E_{P-154} (psi)	$E_{subgrade}$ (psi)	E_{stiff} (psi)
24919	1,330,300	**7,100**	**868,300**	9,800	1,000,000
24920	1,156,200	**11,200**	**697,000**	9,400	1,000,000
24921	1,380,100	**9,600**	**903,000**	9,700	1,000,000
24922	1,419,600	**9,300**	**818,000**	9,700	1,000,000
24923	1,530,600	**5,800**	**903,000**	9,800	1,000,000
24924	1,535,500	**8,300**	**1,057,000**	9,400	1,000,000
24925	1,695,100	**7,300**	**1,223,000**	9,600	1,000,000
24926	1,719,200	**6,700**	**1,120,000**	9,700	1,000,000
24927	1,342,200	**4,700**	**1,310,000**	9,400	1,000,000
24928	1,396,400	**7,200**	**1,362,000**	9,000	1,000,000
24929	1,572,200	**6,000**	**1,746,000**	9,100	1,000,000
24930	1,457,200	**5,900**	**1,352,000**	9,300	1,000,000
24931	1,080,900	**4,800**	**1,123,000**	9,700	1,000,000
24932	1,034,200	**8,700**	**942,000**	9,600	1,000,000
24933	1,214,900	**7,000**	**1,134,000**	9,900	1,000,000
24934	1,229,900	**5,800**	**1,279,000**	9,600	1,000,000
24960	1,804,800	**8,800**	**836,400**	9,200	1,000,000
24968	1,580,900	**7,800**	**1,411,100**	8,800	1,000,000
24972	1,199,600	**9,800**	**1,009,900**	9,500	1,000,000
24964	1,941,200	**6,700**	**1,426,300**	9,000	1,000,000
24961	1,995,500	**7,200**	**1,204,200**	9,300	1,000,000
24973	1,455,000	**7,700**	**1,224,200**	9,600	1,000,000
24965	2,127,400	**5,800**	**1,656,300**	9,400	1,000,000
24969	1,637,600	**7,500**	**1,368,500**	9,200	1,000,000
24963	1,966,300	**3,900**	**1,518,400**	10,100	1,000,000
24971	1,341,500	**5,800**	**1,176,400**	9,700	1,000,000
24959	2,161,700	**4,700**	**1,555,900**	9,400	1,000,000
24967	1,500,800	**5,900**	**1,259,500**	9,300	1,000,000
24974	1,467,100	**6,500**	**1,411,000**	9,300	1,000,000
24970	1,642,600	**7,000**	**1,253,900**	9,200	1,000,000
24962	2,244,600	**6,200**	**1,372,200**	9,200	1,000,000
24966	2,147,800	**5,100**	**1,690,700**	9,600	1,000,000

* Values in bold indicate they were outside the expected range

Table C.3(a). Backcalculation Round 2 Results (BAKFAA) *

FWD #	$E_{P\text{-}401}$ (psi)	$E_{base/subbase}$ (psi)	$E_{subgrade}$ (psi)	E_{stiff} (psi)
24919	439,310	**46,338**	10,980	1,000,000
24920	276,488	**62,402**	11,232	1,000,000
24921	331,374	**61,412**	11,412	1,000,000
24922	360,516	**59,649**	11,140	1,000,000
24923	895,933	**35,061**	10,924	1,000,000
24924	690,075	**51,367**	11,261	1,000,000
24925	815,440	**48,721**	11,389	1,000,000
24926	852,698	**44,974**	11,137	1,000,000
24927	681,557	**32,064**	10,856	1,000,000
24928	496,476	**50,222**	11,183	1,000,000
24929	648,748	**45,606**	11,405	1,000,000
24930	597,204	**42,428**	11,063	1,000,000
24931	516,538	**29,865**	11,189	1,000,000
24932	321,955	**49,988**	11,750	1,000,000
24933	370,701	**45,668**	11,800	1,000,000
24934	478,290	**39,203**	11,446	1,000,000
24959	1,123,712	**39,285**	10,479	1,000,000
24960	710,170	**56,841**	10,452	1,000,000
24961	888,865	**52,558**	10,781	1,000,000
24962	1,006,431	**51,061**	10,541	1,000,000
24963	1,114,602	**30,720**	10,763	1,000,000
24964	657,618	**55,924**	10,590	1,000,000
24965	998,058	**47,412**	11,081	1,000,000
24966	1,033,836	**43,010**	10,971	1,000,000
24967	675,704	**41,235**	10,895	1,000,000
24968	520,486	**57,434**	10,966	1,000,000
24969	687,944	**58,192**	12,245	1,000,000
24970	665,048	**49,665**	10,919	1,000,000
24971	571,428	**39,004**	11,206	1,000,000
24972	297,047	**60,908**	11,716	1,000,000
24973	540,522	**51,443**	11,635	1,000,000
24974	496,025	**48,373**	11,300	1,000,000
25304	**20,546**	**69,333**	11,027	1,000,000
25316	**17,698**	**81,930**	11,628	1,000,000
25312	**20,242**	**77,733**	11,259	1,000,000
25308	**19,820**	**77,038**	11,255	1,000,000
25317	**20,042**	**66,215**	11,522	1,000,000
25313	**21,377**	**67,804**	11,136	1,000,000
25305	**24,929**	**58,580**	11,021	1,000,000

* Values in bold indicate they were outside the expected range

Table C.3(b). Backcalculation Round 2 Results (BAKFAA) *

FWD #	E_{P-401} (psi)	$E_{base/subbase}$ (psi)	$E_{subgrade}$ (psi)	E_{stiff} (psi)
25309	**21,684**	**65,289**	11,181	1,000,000
25315	**23,009**	**34,245**	10,614	1,000,000
25303	**31,675**	**32,015**	10,289	1,000,000
25311	**25,522**	**35,114**	10,260	1,000,000
25307	**27,597**	**33,438**	10,231	1,000,000
25310	**24,702**	**53,089**	10,802	1,000,000
25318	**21,156**	**55,625**	11,136	1,000,000
25314	**24,054**	**54,730**	10,809	1,000,000
25306	**29,827**	**49,182**	10,845	1,000,000

* Values in bold indicate they were outside the expected range

Table C.4(a). Backcalculation Round 2 Results (EVERCALC) *

FWD #	$E_{P\text{-}401}$ (psi)	$E_{base/subbase}$ (psi)	$E_{subgrade}$ (psi)	E_{stiff} (psi)
24919	445,700	**46,100**	11,200	1,000,000
24920	319,100	**62,100**	11,300	1,000,000
24921	384,800	**60,800**	11,600	1,000,000
24922	427,800	**57,600**	11,400	1,000,000
24923	685,400	**38,600**	11,000	1,000,000
24924	487,600	**57,100**	11,300	1,000,000
24925	585,000	**54,100**	11,400	1,000,000
24926	661,600	**48,700**	11,200	1,000,000
24927	520,900	**35,200**	10,900	1,000,000
24928	375,200	**55,000**	11,200	1,000,000
24929	483,200	**50,200**	11,400	1,000,000
24930	475,900	**45,500**	11,200	1,000,000
24931	386,000	**32,900**	11,200	1,000,000
24932	261,800	**54,600**	11,700	1,000,000
24933	349,100	**48,000**	11,900	1,000,000
24934	374,900	**42,300**	11,500	1,000,000
24960	688,600	**56,800**	10,700	1,000,000
24968	416,000	**61,800**	11,000	1,000,000
24972	307,200	**63,000**	11,700	1,000,000
24964	657,300	**55,600**	10,800	1,000,000
24961	767,900	**54,700**	11,000	1,000,000
24973	427,400	**55,500**	11,700	1,000,000
24965	864,600	**49,400**	11,300	1,000,000
24969	487,100	**58,300**	11,300	1,000,000
24963	1,072,800	**30,500**	11,100	1,000,000
24971	465,700	**41,600**	11,300	1,000,000
24959	1,043,800	**39,800**	10,700	1,000,000
24967	527,000	**44,600**	11,000	1,000,000
24974	432,100	**50,700**	11,400	1,000,000
24970	538,400	**52,900**	11,000	1,000,000
24962	953,100	**51,300**	10,800	1,000,000
24966	957,200	**43,600**	11,200	1,000,000
25312	**116,300**	**42,300**	11,200	1,000,000
25304	**113,900**	**39,900**	11,200	1,000,000
25316	**20,400**	**81,000**	11,800	1,000,000
25308	**24,800**	**72,400**	11,400	1,000,000
25317	**30,000**	**57,100**	11,700	1,000,000
25313	**116,300**	**39,600**	11,300	1,000,000
25305	**120,700**	**37,300**	11,200	1,000,000

* Values in bold indicate they were outside the expected range

Table C.4(b). Backcalculation Round 2 Results (EVERCALC)

FWD #	$E_{P\text{-}401}$ (psi)	$E_{base/subbase}$ (psi)	$E_{subgrade}$ (psi)	E_{stiff} (psi)
25309	**120,300**	**38,300**	11,400	1,000,000
25303	**122,200**	23,800	10,600	1,000,000
25311	**105,200**	25,100	10,500	1,000,000
25307	**121,900**	23,700	10,600	1,000,000
25310	**121,400**	**34,100**	11,000	1,000,000
25318	**106,400**	**34,600**	11,300	1,000,000
25314	**117,700**	**35,200**	11,000	1,000,000
25306	**129,700**	**34,000**	11,000	1,000,000
25315	**99,400**	26,100	11,500	1,000,000

* Values in bold indicate they were outside the expected range

Appendix D

Trafficking Data

Table D.1(a). Dates of Traffic Repetitions and FWD Tests

Date	FWD Test	Daily Traffic Repetitions	Traffic Repetition to Date
6/14/1999	**X**	0	**0**
11/17/1999	**X**	0	**0**
1/11/2000	**X**	0	**0**
2/11/2000	**X**	0	**0**
2/14/2000		28	28
2/16/2000	**X**	0	**28**
2/25/2000	**X**	0	**28**
3/20/2000	**X**	105	**133**
3/31/2000		166	299
4/3/2000		64	363
4/4/2000		168	531
4/5/2000		130	661
4/6/2000		212	873
4/7/2000	**X**	58	**931**
4/10/2000		262	1193
4/12/2000		255	1448
4/13/2000		174	1622
4/14/2000	**X**	270	**1892**
4/17/2000		278	2170
4/18/2000		300	2470
4/19/2000		276	2746
4/20/2000	**X**	0	**2746**
4/21/2000		288	3034
4/24/2000		314	3348
4/25/2000		204	3552
4/26/2000	**X**	4	**3556**
4/27/2000		156	3712
4/28/2000		146	3858
5/1/2000		85	3943
5/2/2000		318	4261
5/3/2000		200	4461
5/4/2000		234	4695
5/5/2000		320	5015
5/6/2000	**X**	0	**5015**
5/8/2000		279	5294
5/10/2000		78	5372
5/11/2000		240	5612
5/12/2000		300	5912
5/15/2000		310	6222
5/16/2000		342	6564
5/17/2000		344	6908

Table D.1(b). Dates of Traffic Repetitions and FWD Tests

Date	FWD Test	Daily Traffic Repetitions	Traffic Repetition to Date
5/18/2000		294	7202
5/19/2000		310	7512
5/22/2000		278	7790
5/23/2000	**X**	250	**8040**
5/24/2000		42	8082
6/1/2000		22	8104
6/2/2000		336	8440
6/5/2000		282	8722
6/6/2000		308	9030
6/7/2000		278	9308
6/8/2000		256	9564
6/9/2000		4	9568
6/12/2000		314	9882
6/13/2000		320	10202
6/14/2000		326	10528
6/15/2000		212	10740
6/16/2000		296	11036
6/19/2000		316	11352
6/20/2000		178	11530
6/21/2000		346	11876
6/22/2000	**X**	72	**11948**
6/23/2000		159	12107
6/26/2000		332	12439
6/27/2000		322	12761
6/28/2000		191	12952
8/31/2000	**X**	0	**12952**

Appendix E

Lane 5 Forward Calculation Deflection Basins

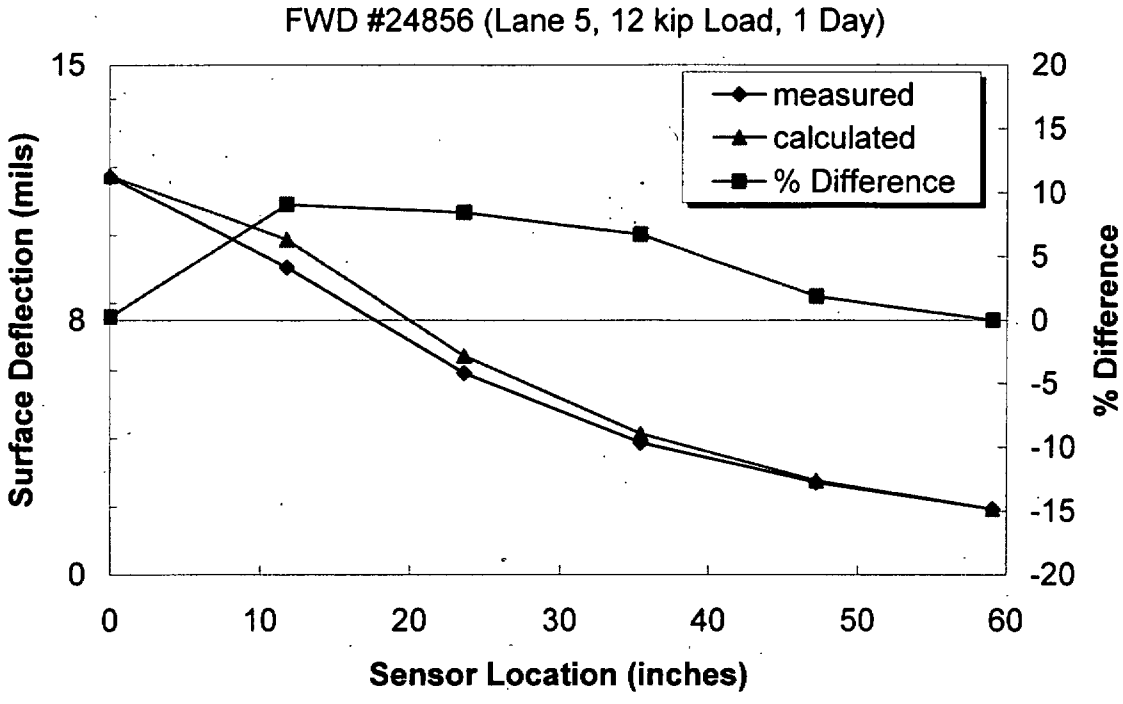

Figure E.1. FWD #24856 Deflection Basins

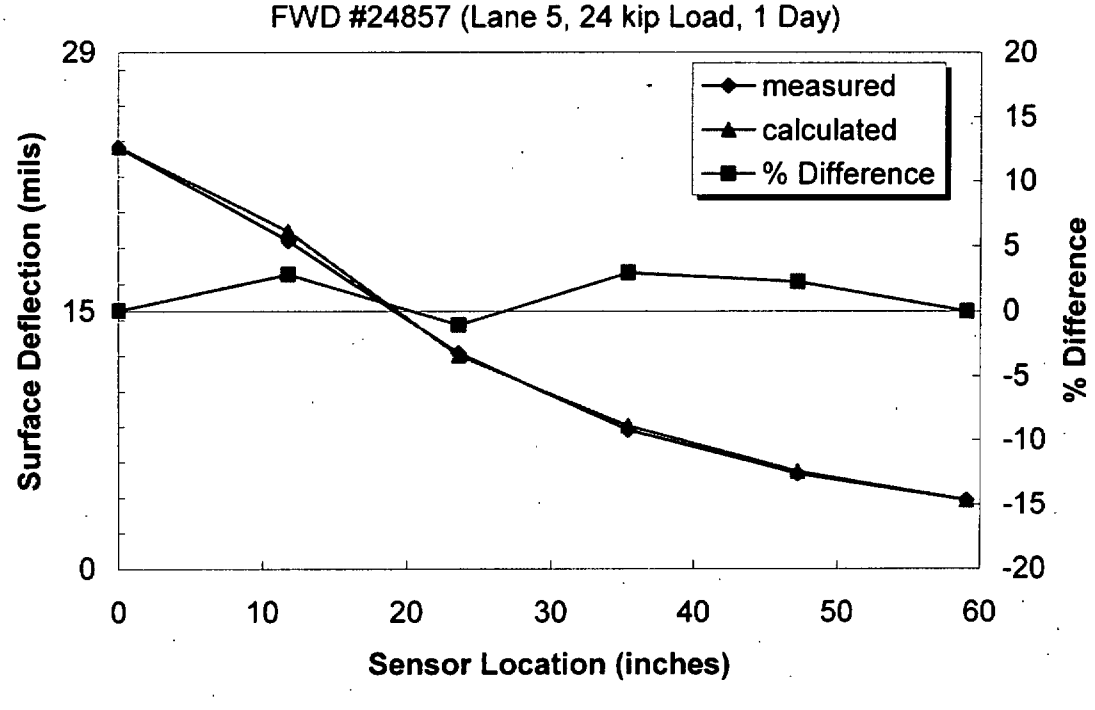

Figure E.2. FWD #24857 Deflection Basins

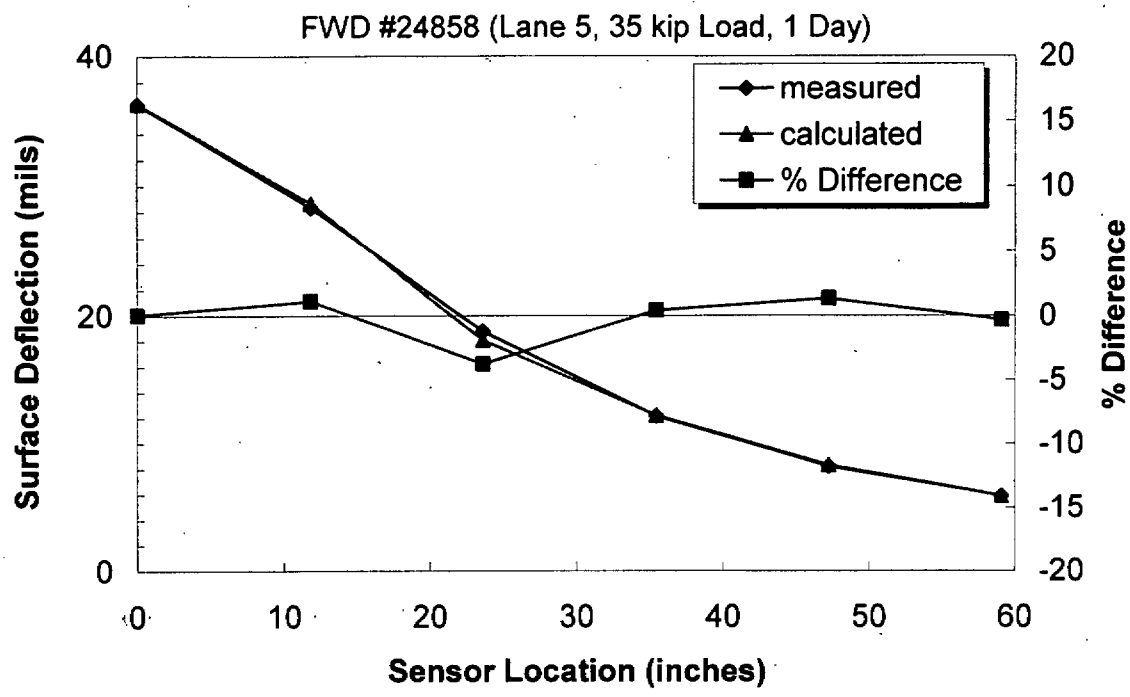

Figure E.3. FWD #24858 Deflection Basins

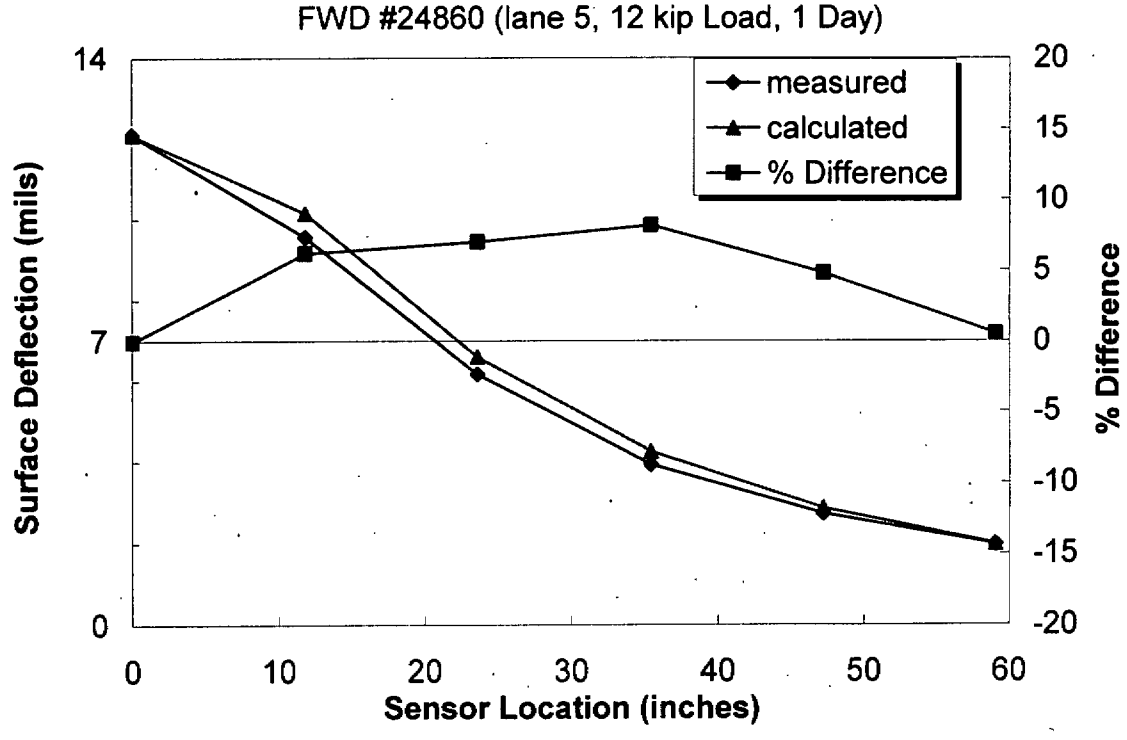

Figure E.4. FWD #24860 Deflection Basins

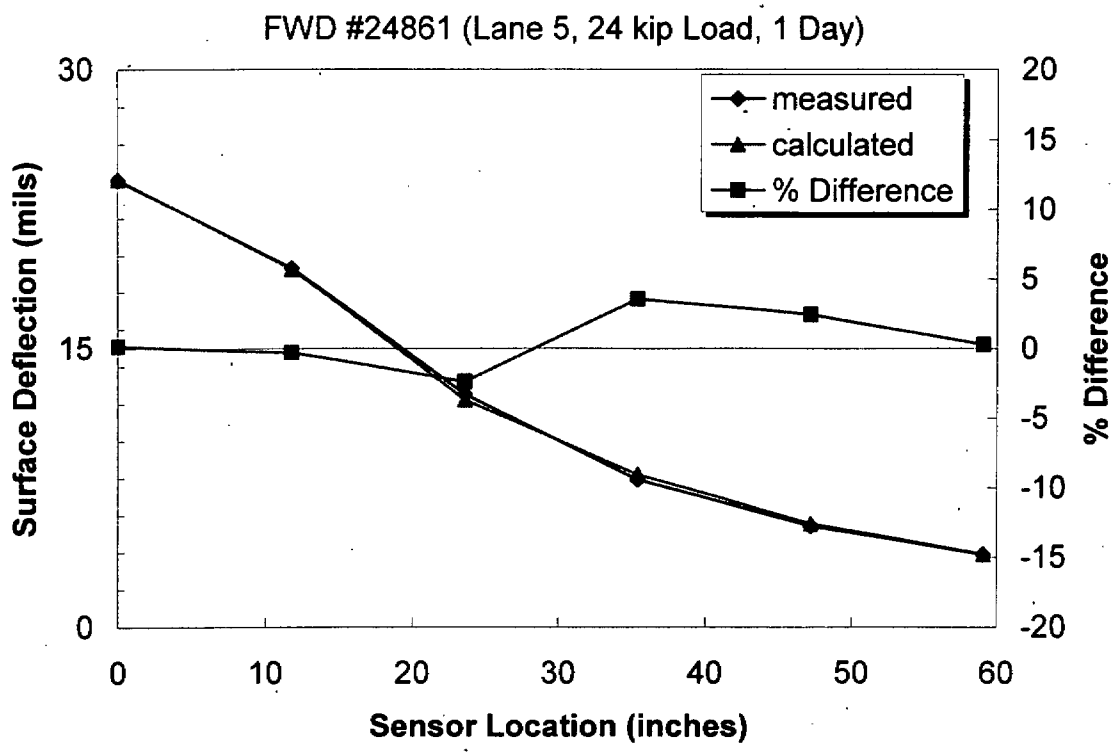

Figure E.5. FWD #24861 Deflection Basins

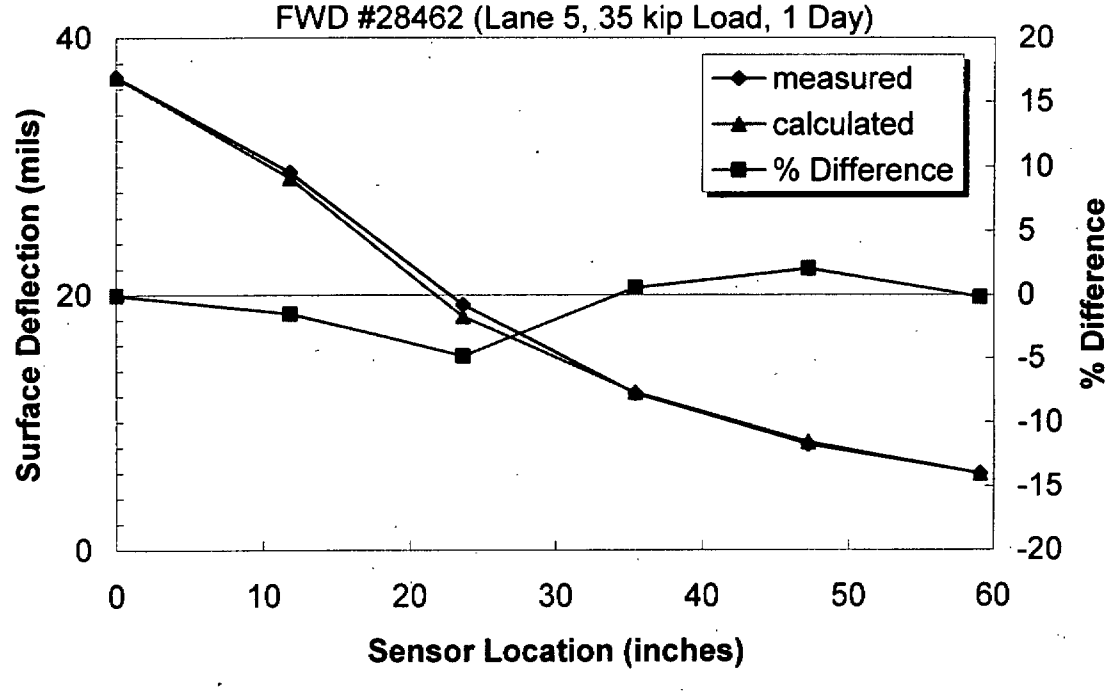

Figure E.6. FWD #24862 Deflection Basins

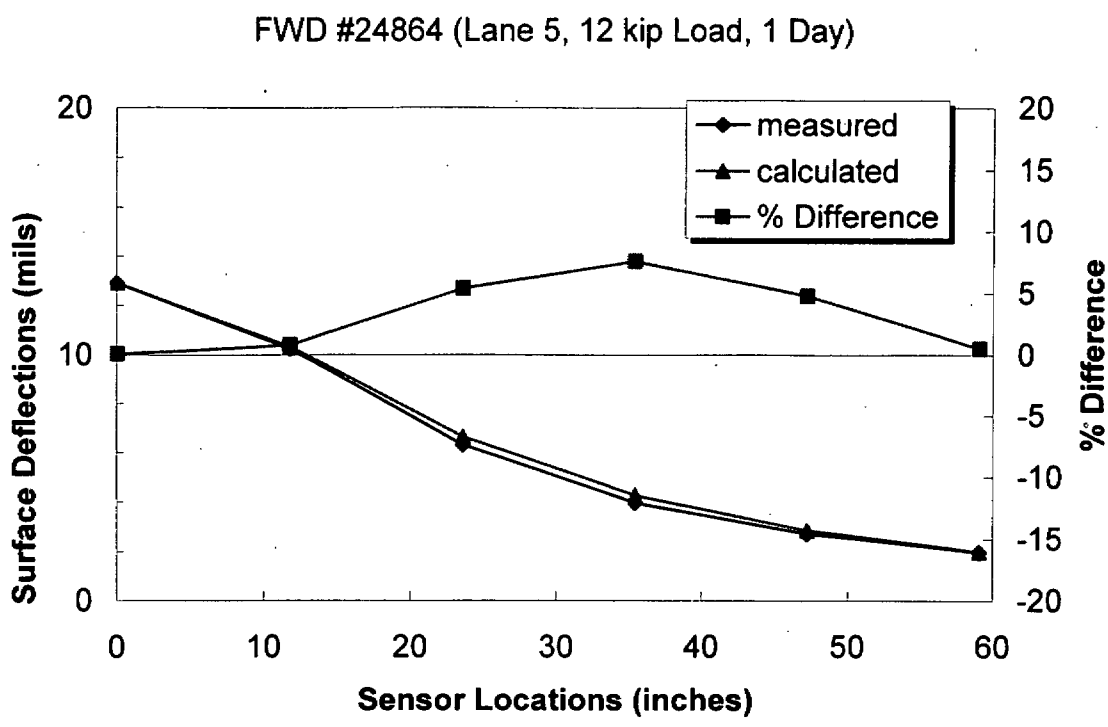

Figure E.7. FWD #24864 Deflection Basins

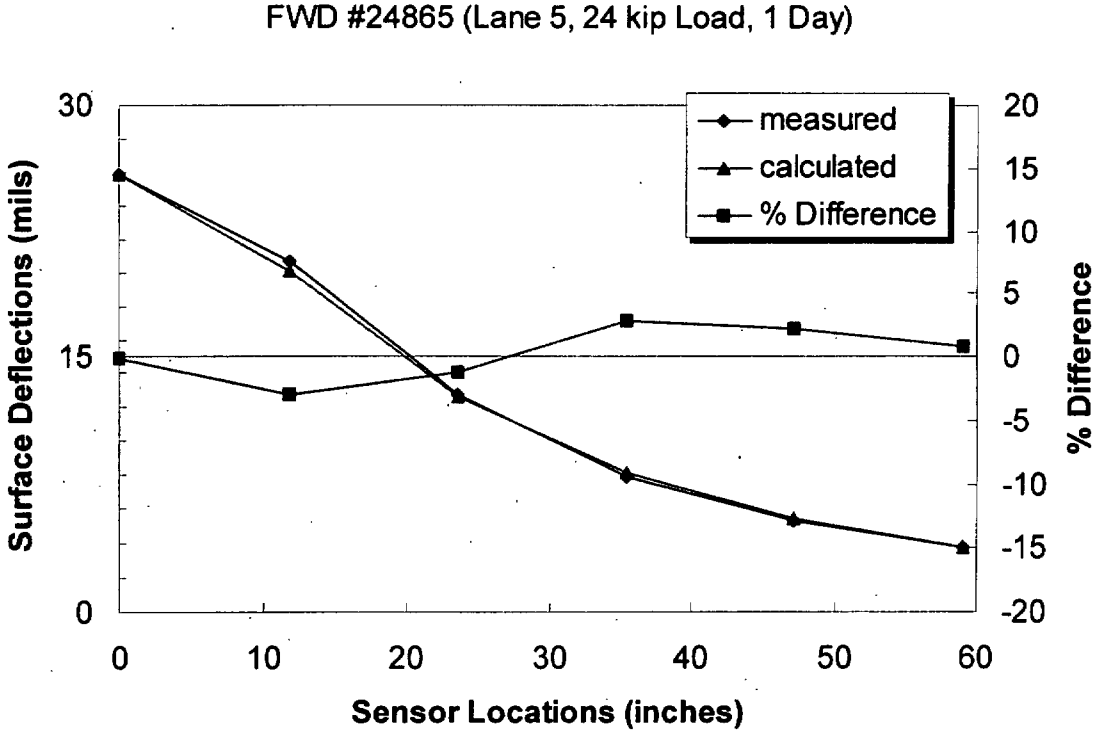

Figure E.8. FWD #24865 Deflection Basins

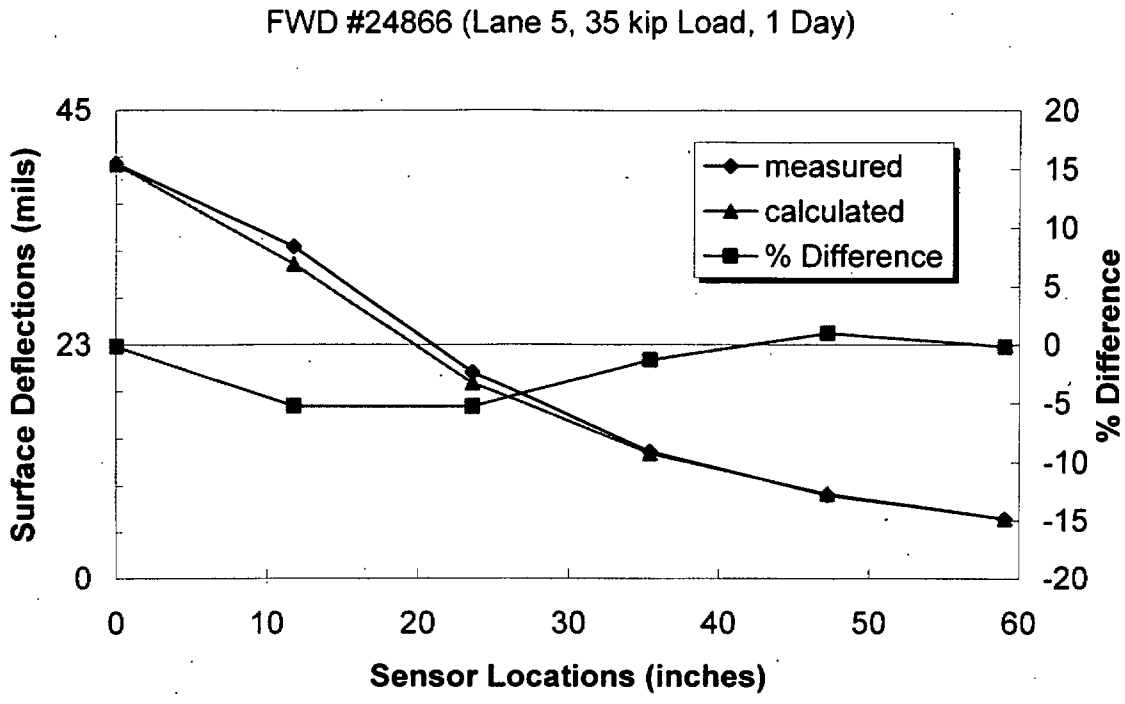

Figure E.9. FWD #24866 Deflection Basins

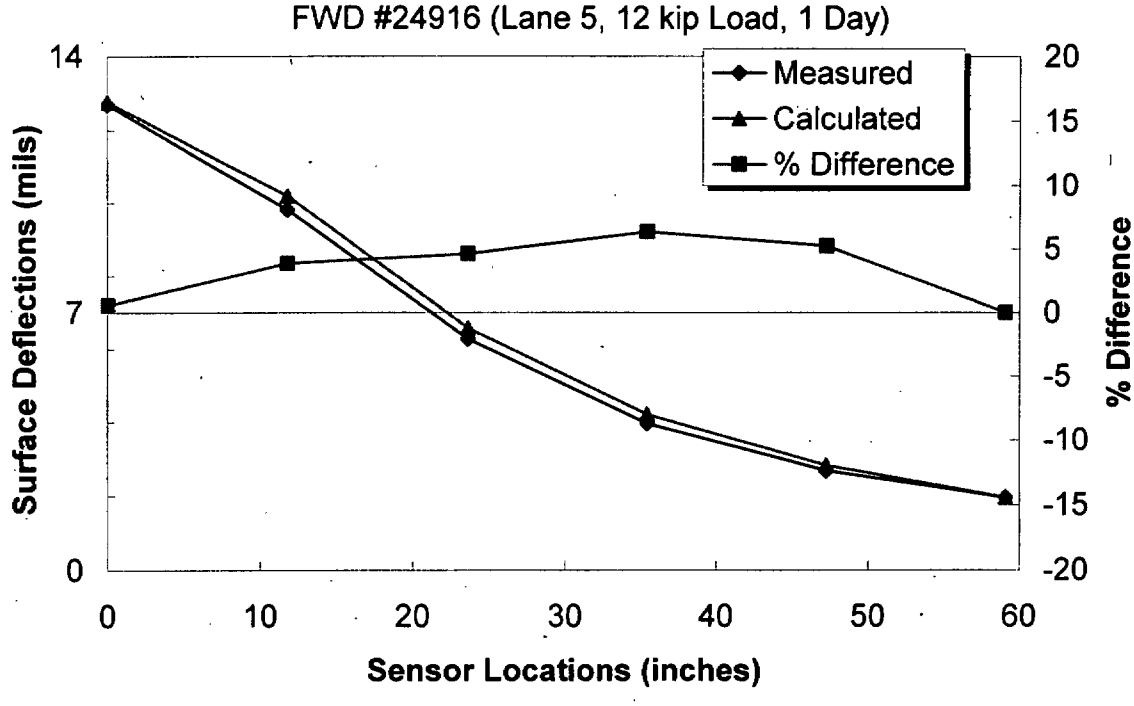

Figure E.10. FWD #24916 Deflection Basins

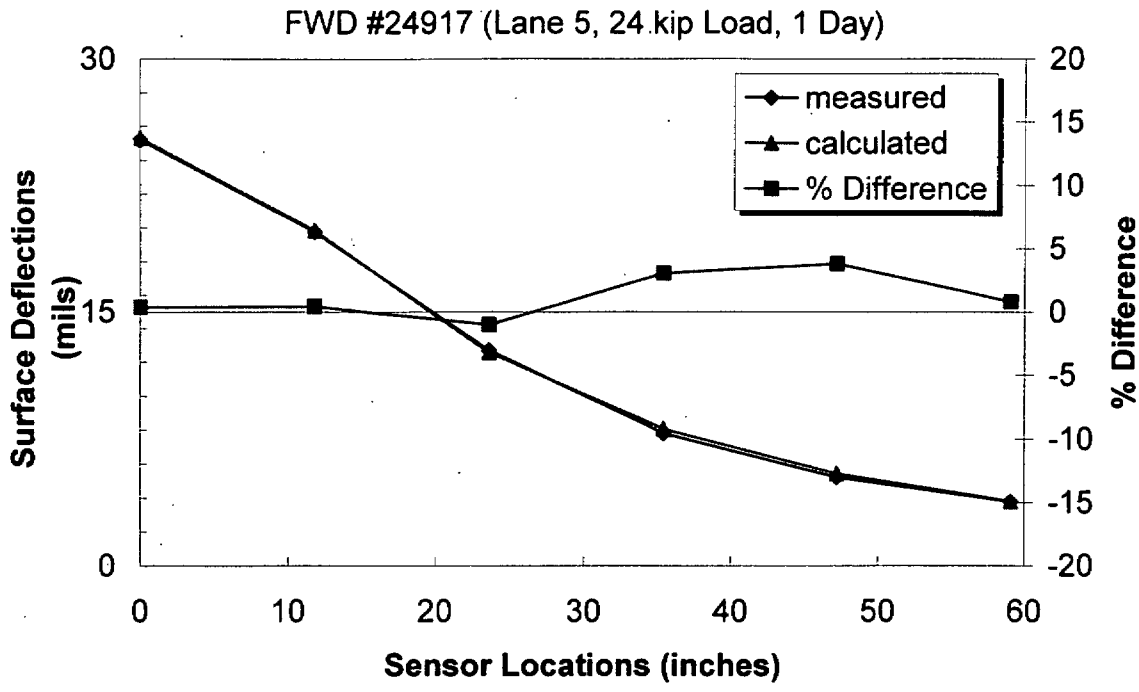

Figure E.11. FWD #24917 Deflection Basins

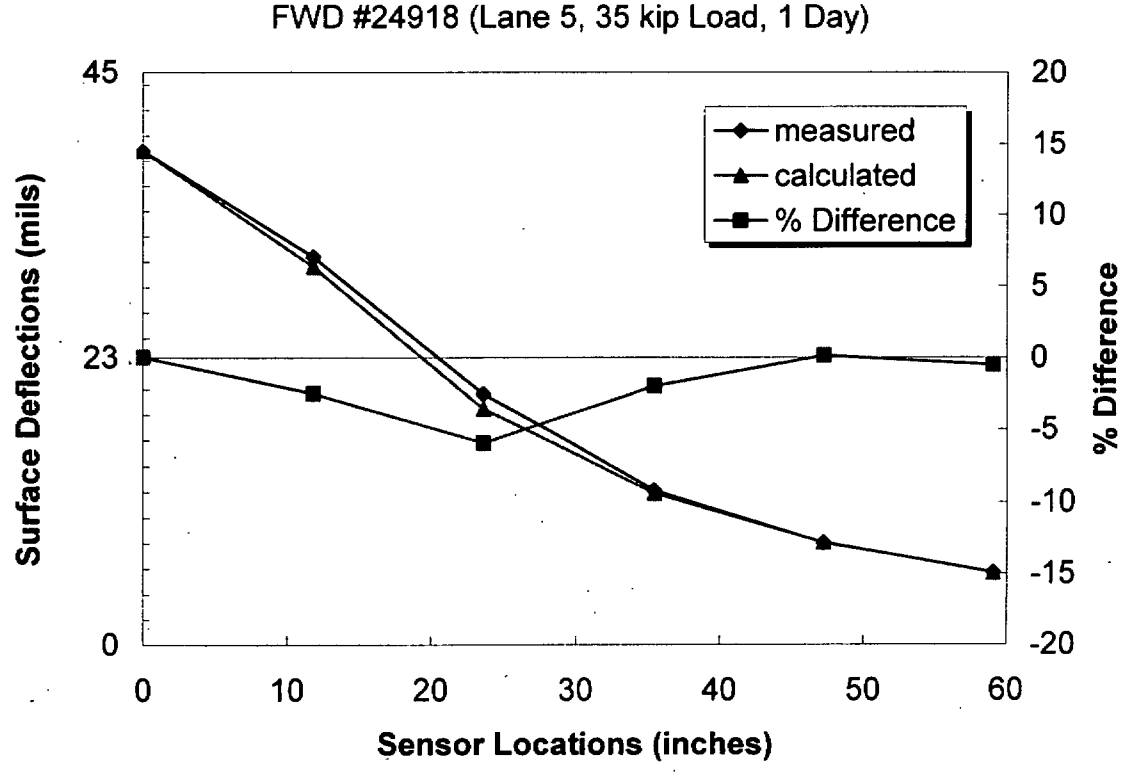

Figure E.12. FWD #24918 Deflection Basins

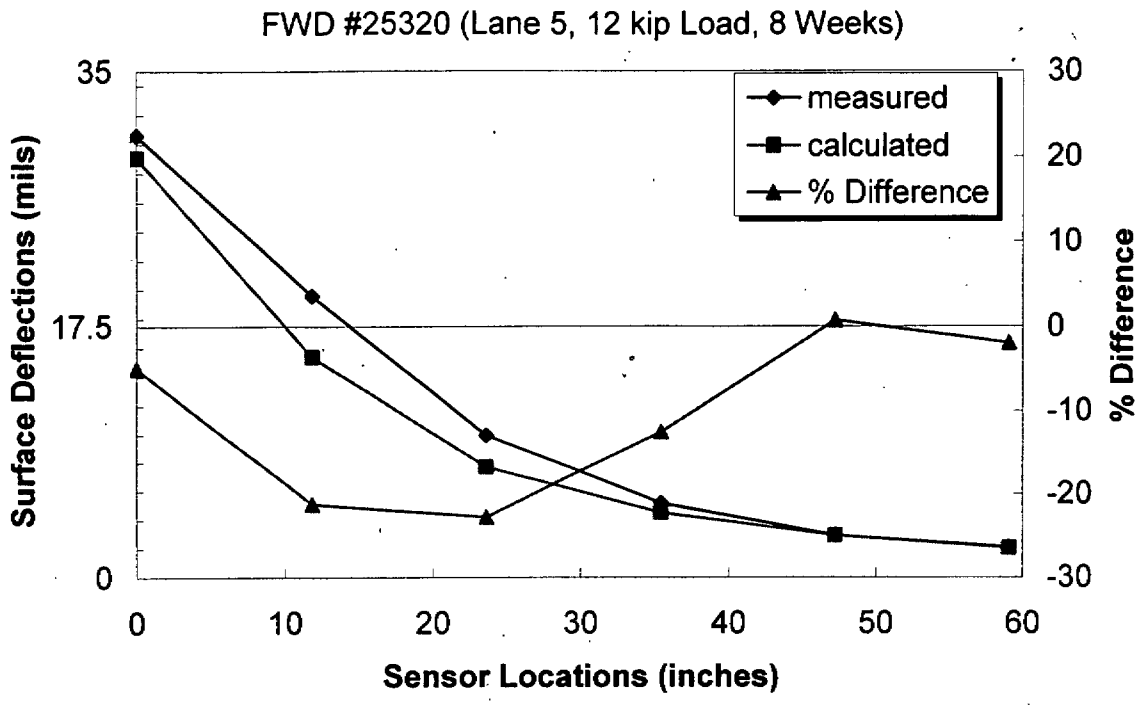

Figure E.13. FWD #25320 Deflection Basins

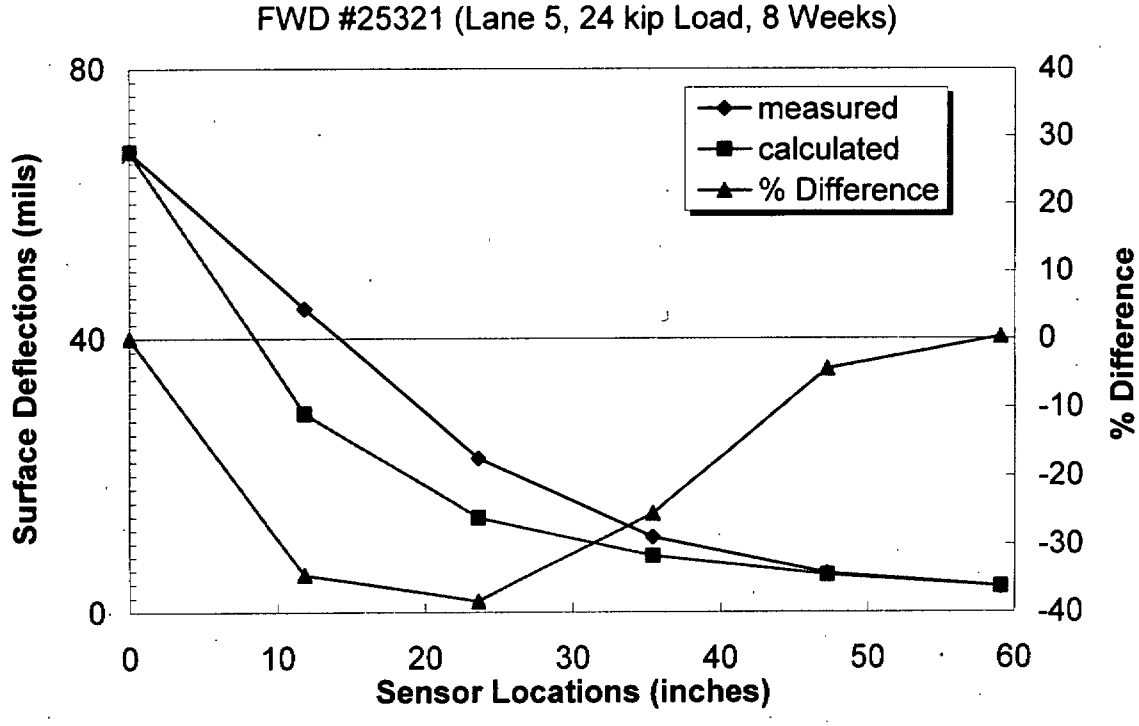

Figure E.14. FWD #25321 Deflection Basins

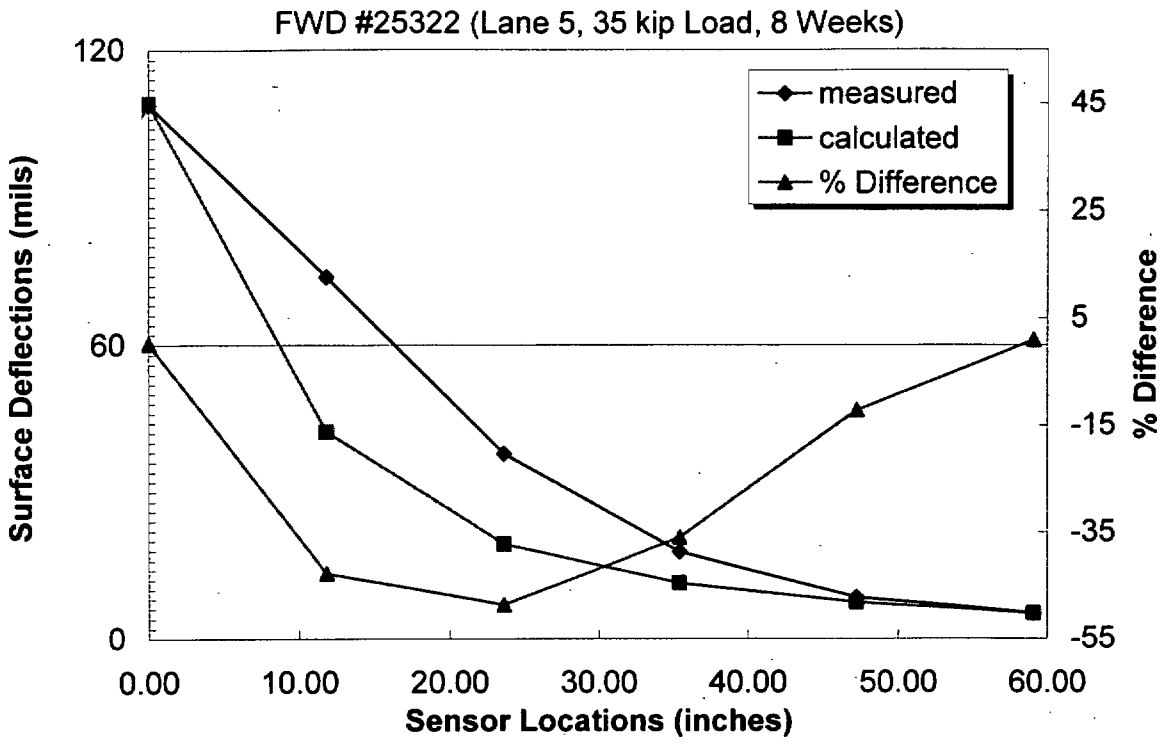

Figure E.15. FWD #25322 Deflection Basins

Appendix F

Centerline Forward Calculation Deflection Basins

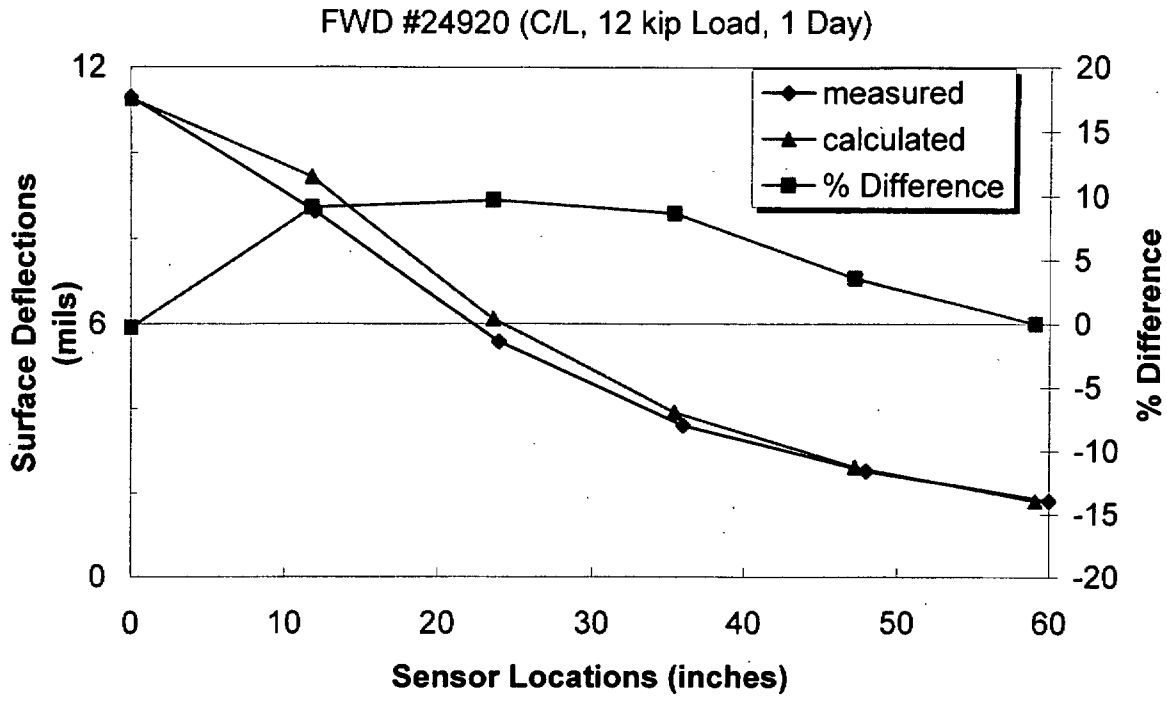

Figure F.1. FWD #24920 Deflection Basins

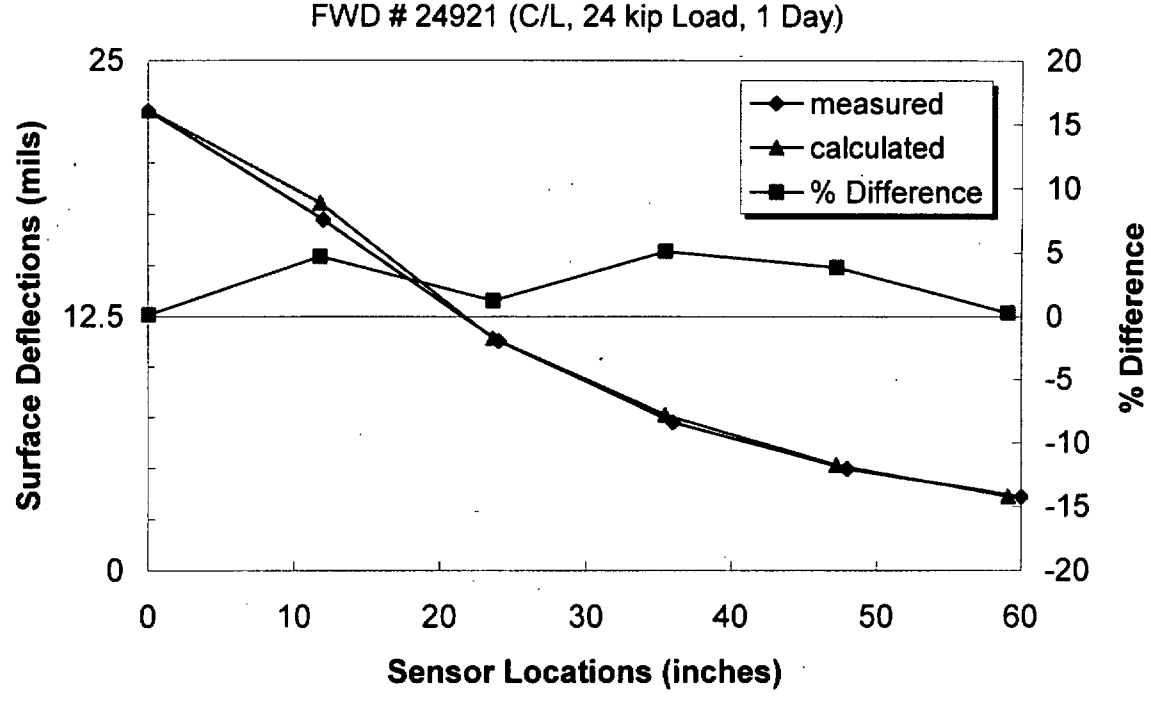

Figure F.2. FWD #24921 Deflection Basins

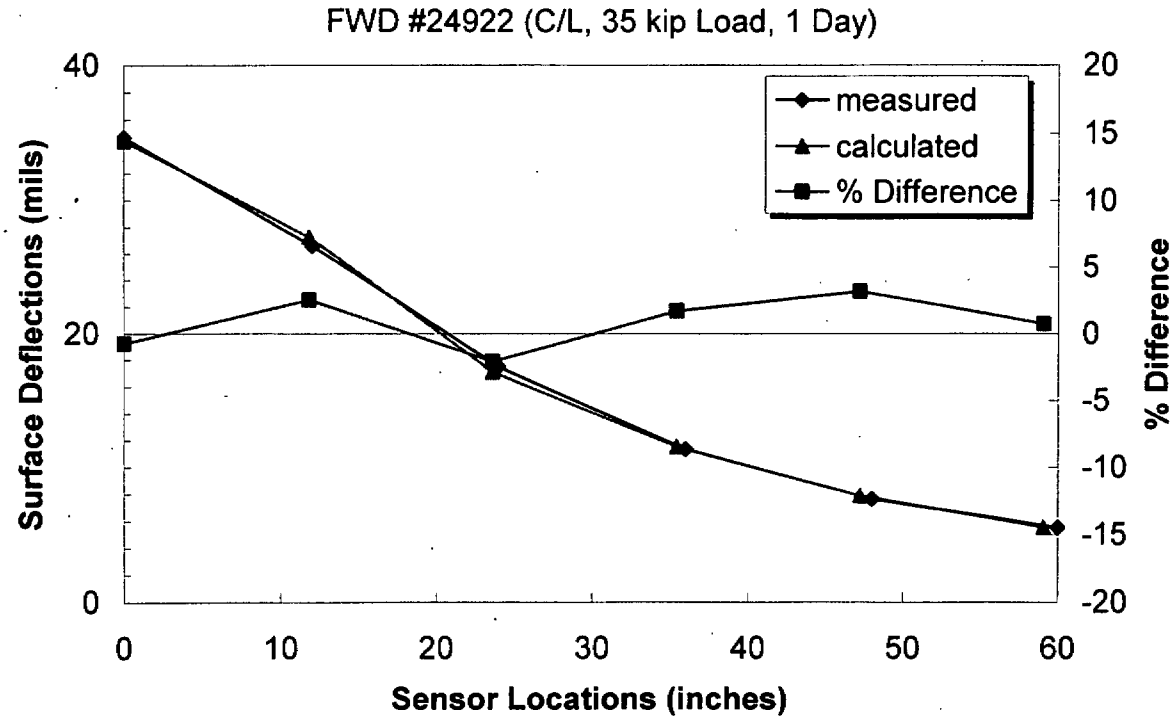

Figure F.3. FWD #24922 Deflection Basins

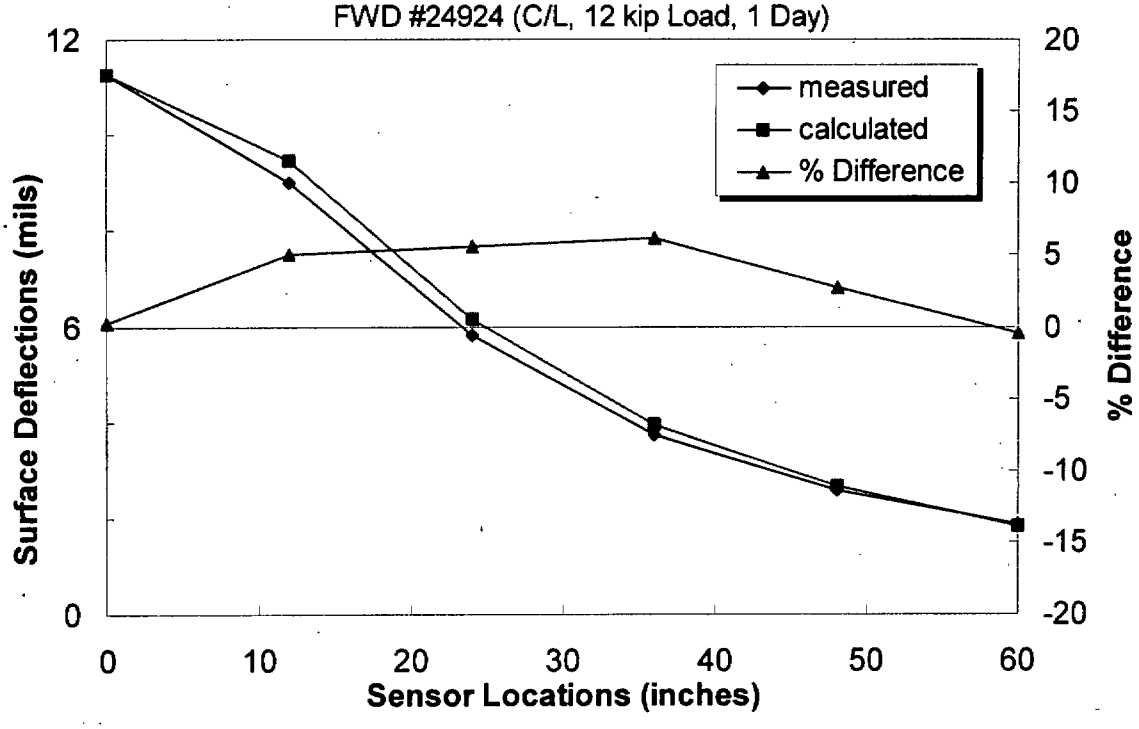

Figure F.4. FWD #24924 Deflection Basins

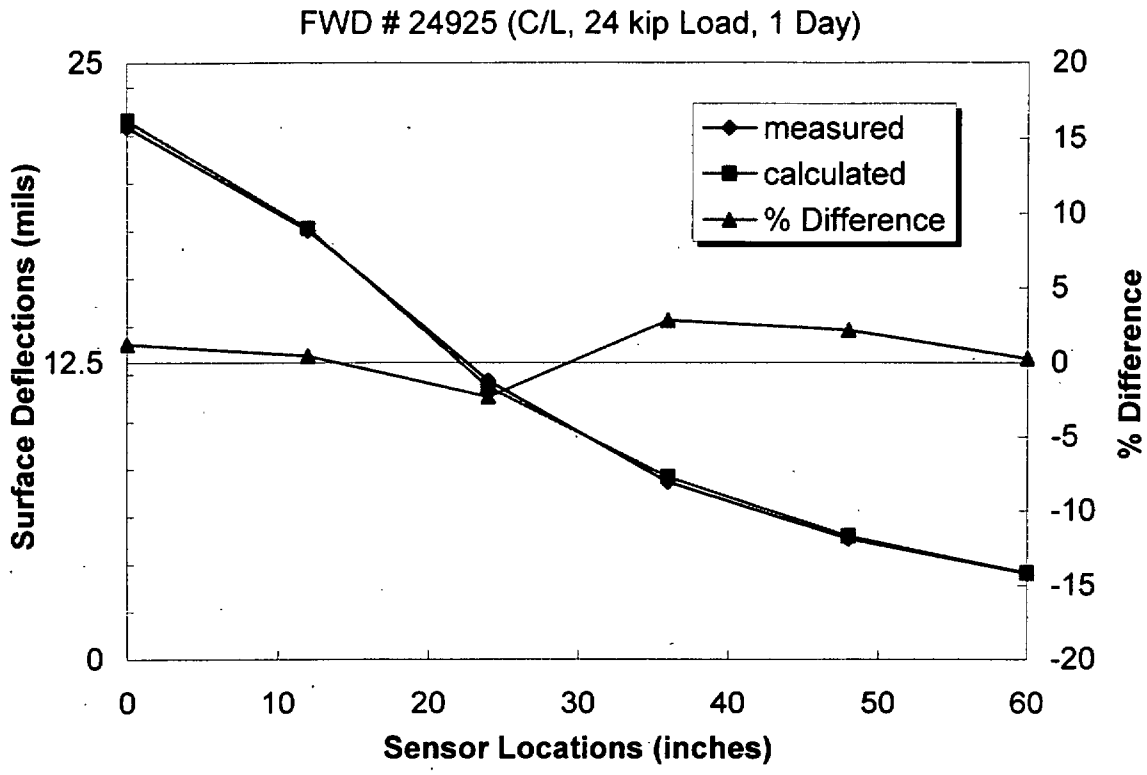

Figure F.5. FWD #24925 Deflection Basins

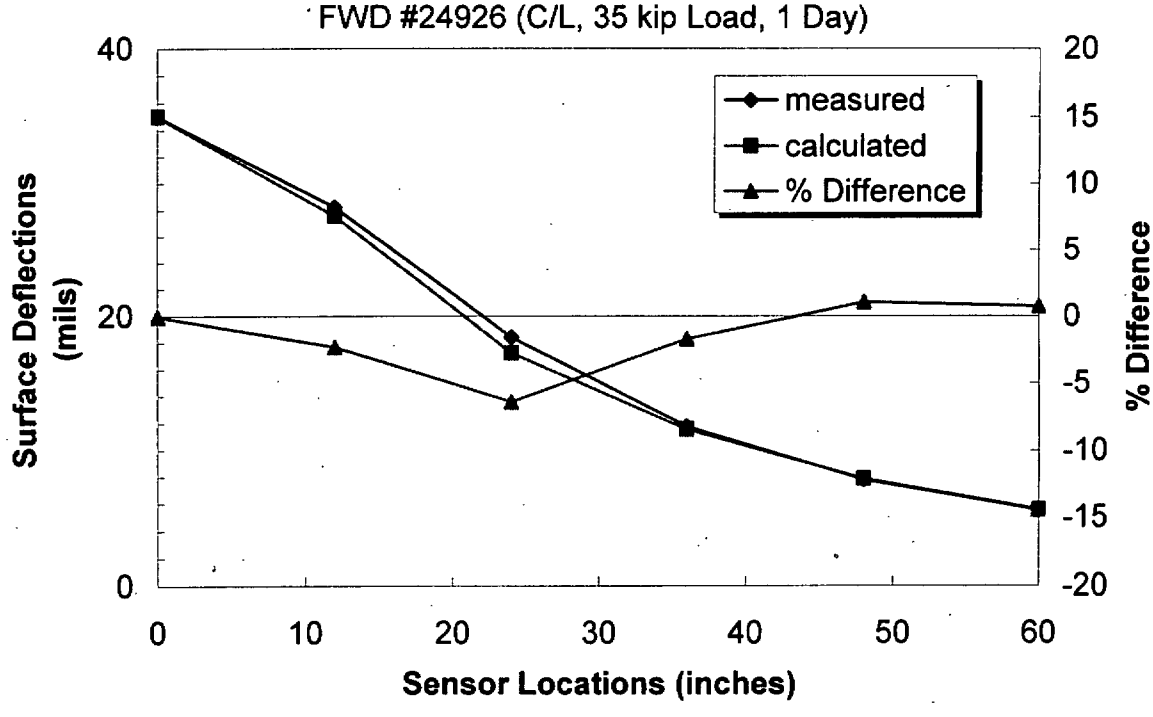

Figure F.6. FWD #24926 Deflection Basins

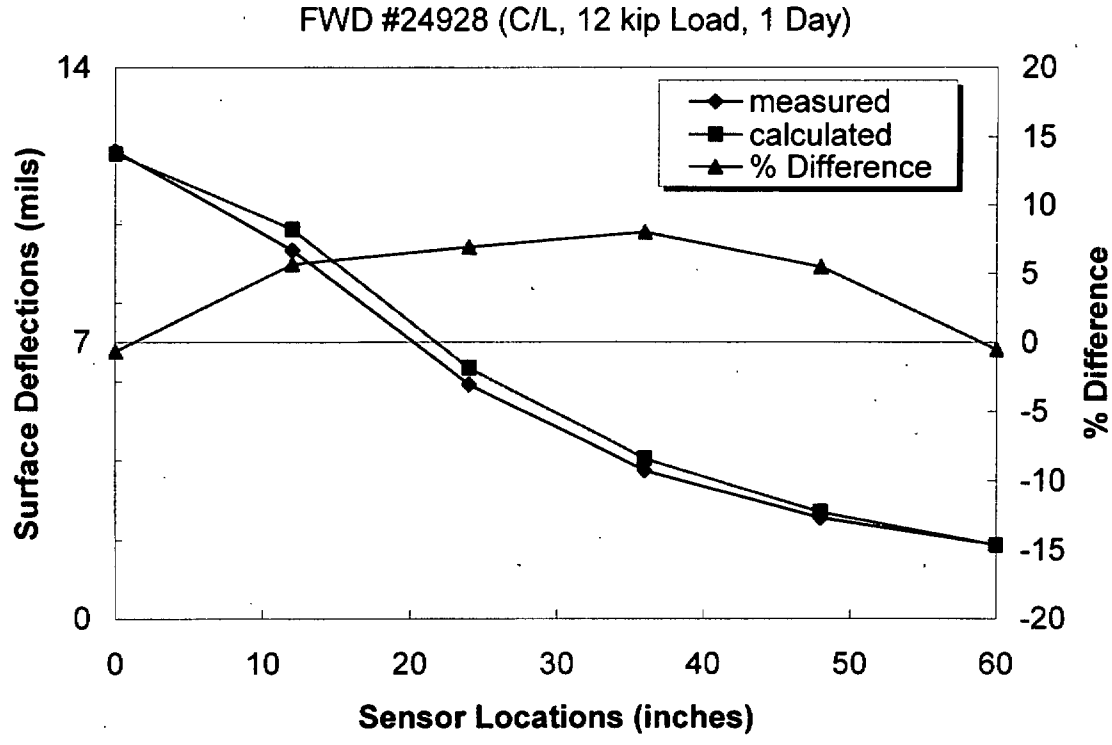

Figure F.7. FWD #24928 Deflection Basins

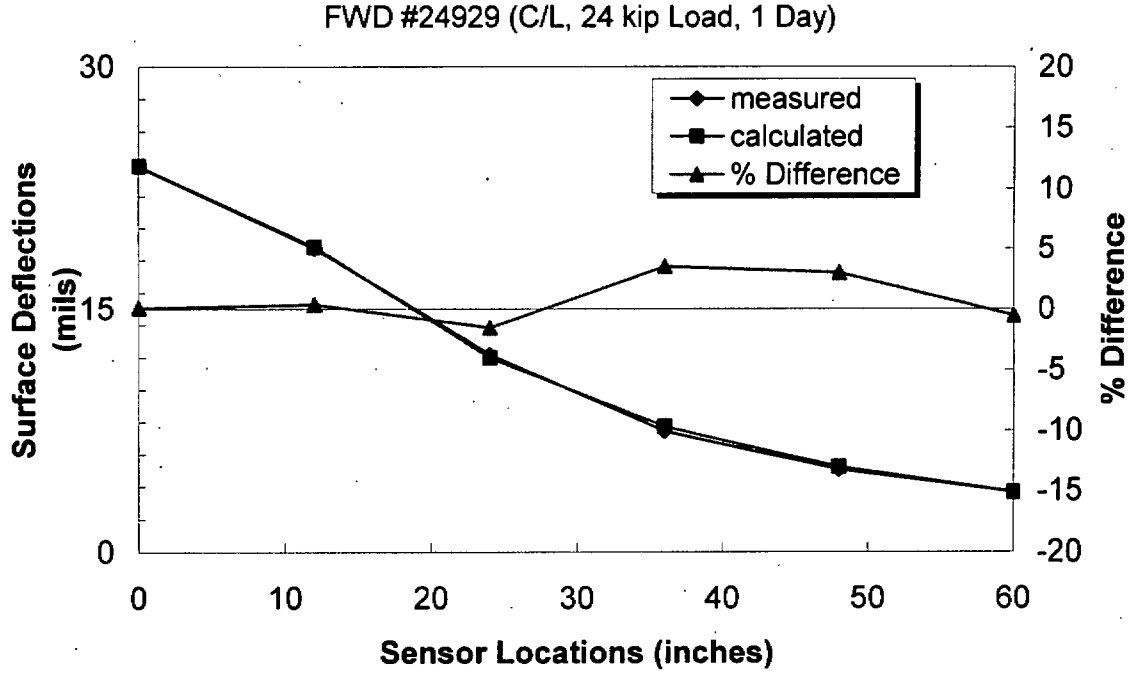

Figure F.8. FWD #24929 Deflection Basins

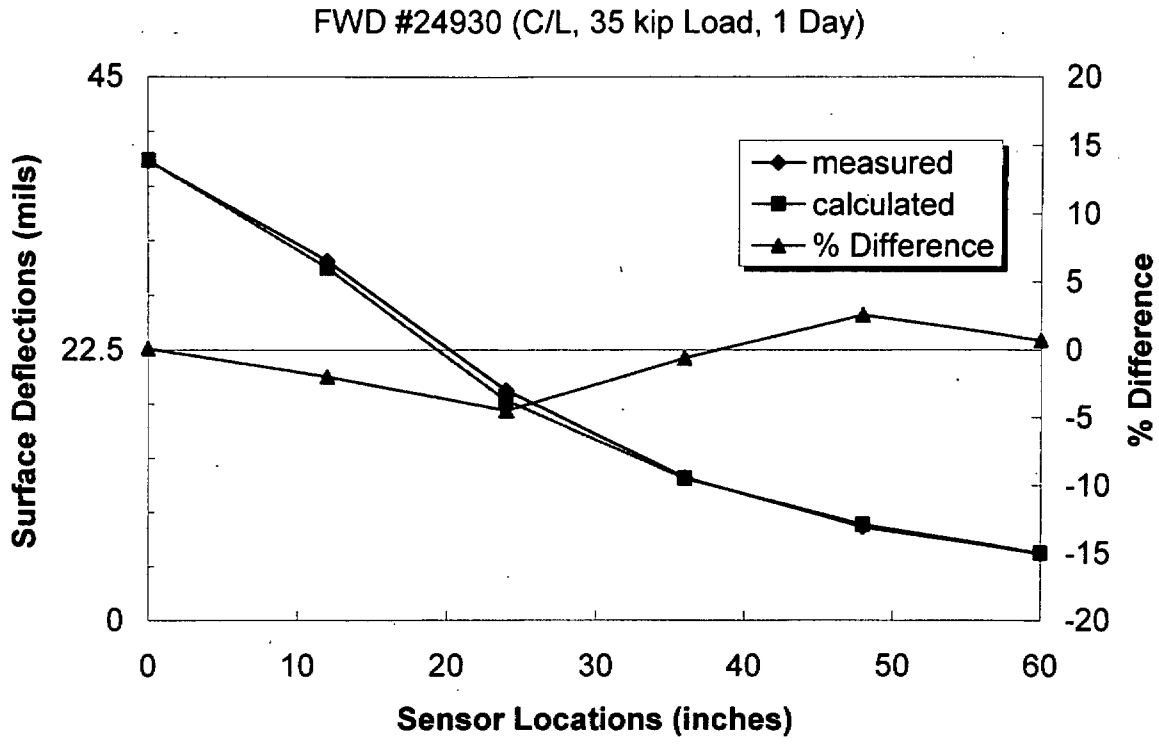

Figure F.9. FWD #24930 Deflection Basins

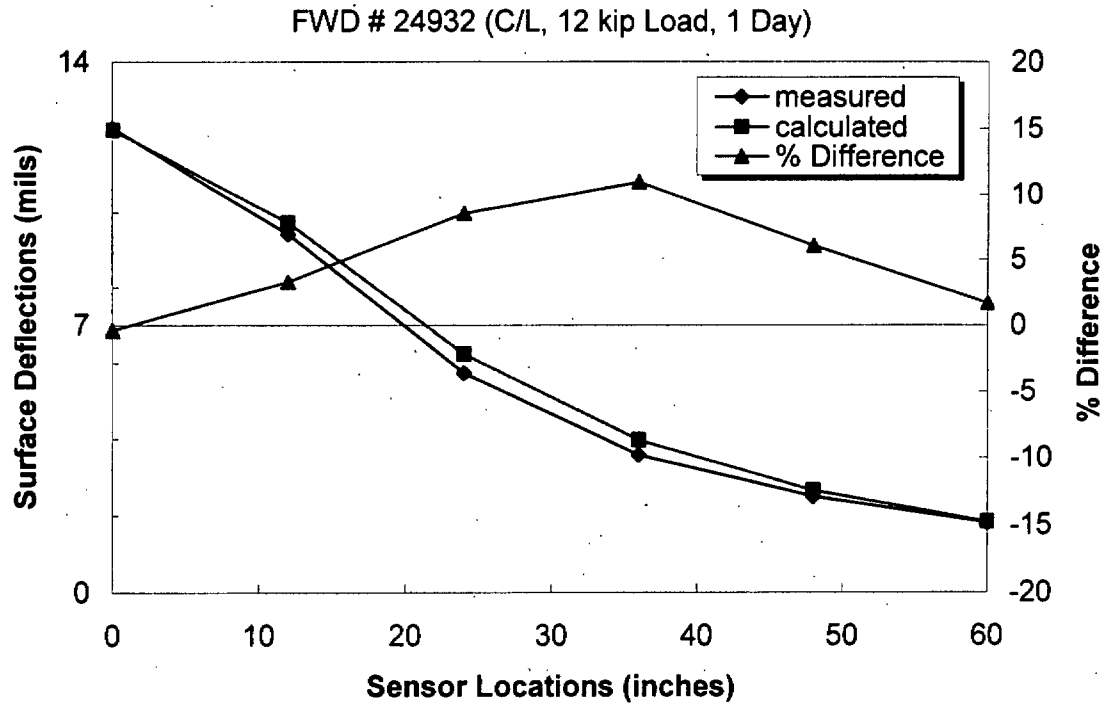

Figure F.10. FWD #24932 Deflection Basins

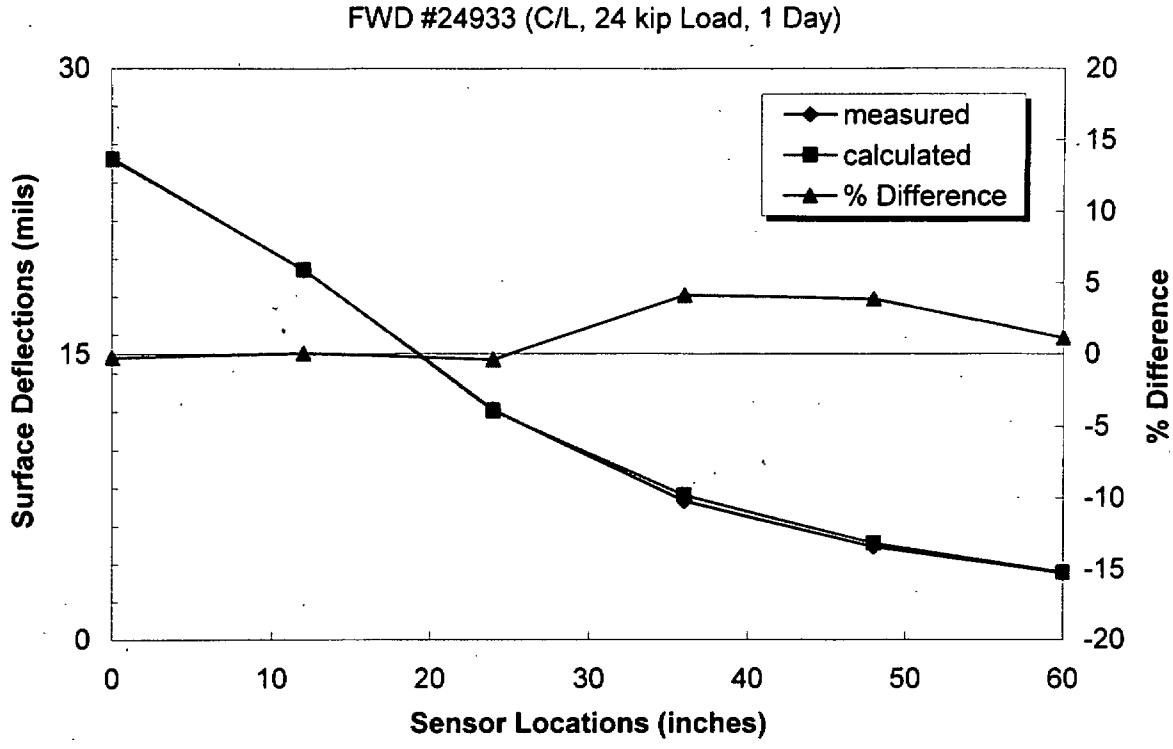

Figure F.11. FWD #24933 Deflection Basins

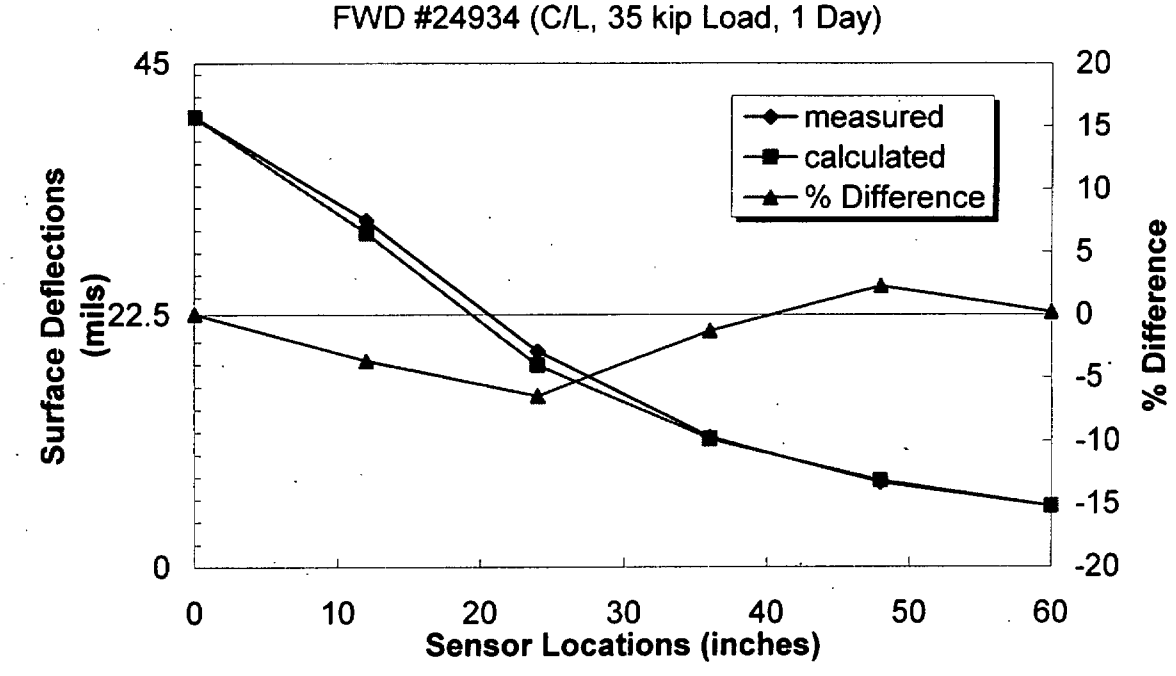

Figure F.12. FWD #24934 Deflection Basins

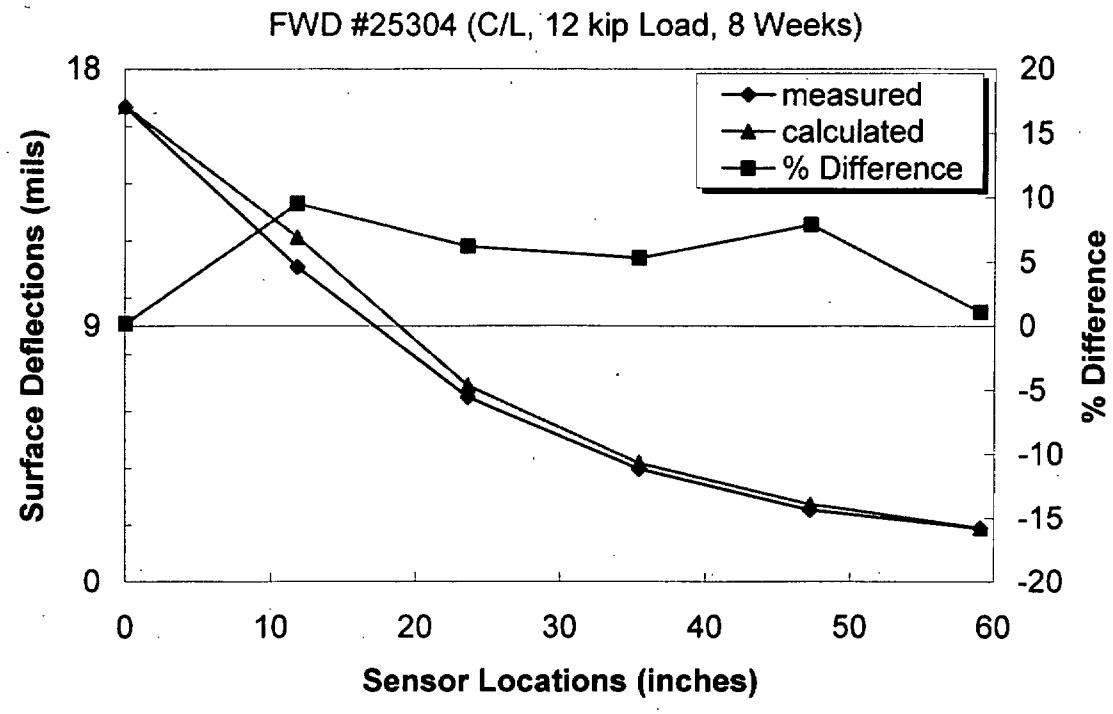

Figure F.13. FWD #25304 Deflection Basins

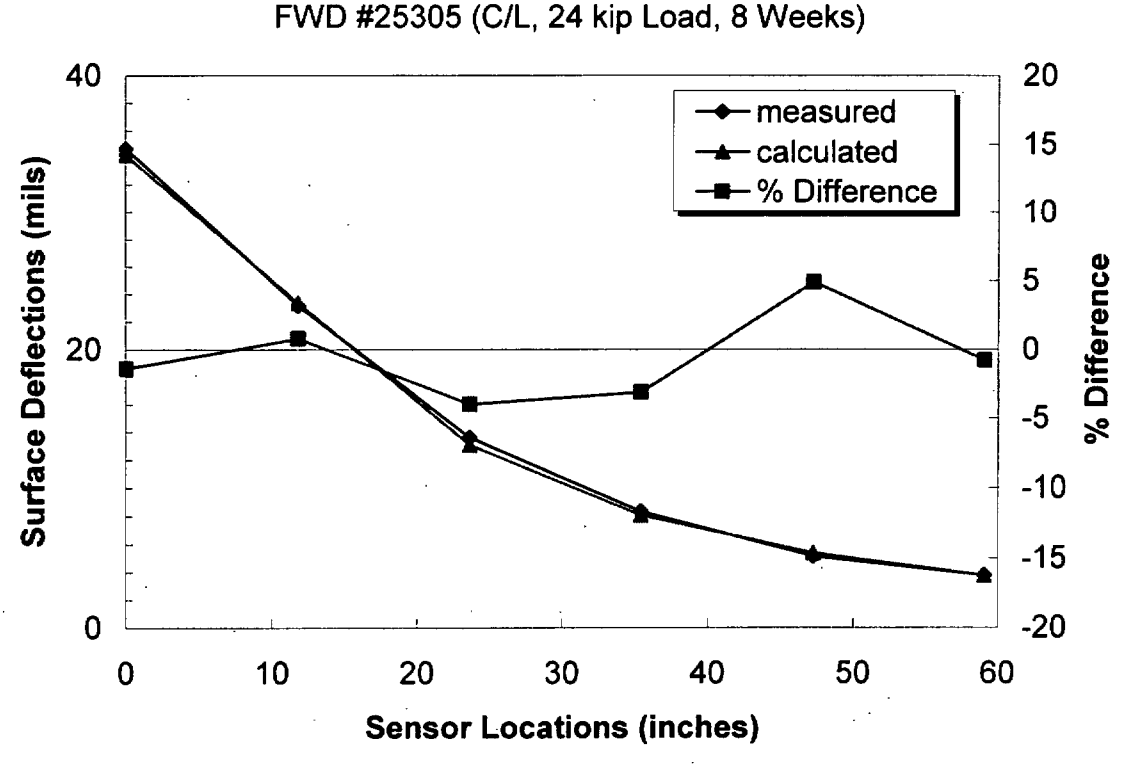

Figure F.14. FWD #25305 Deflection Basins

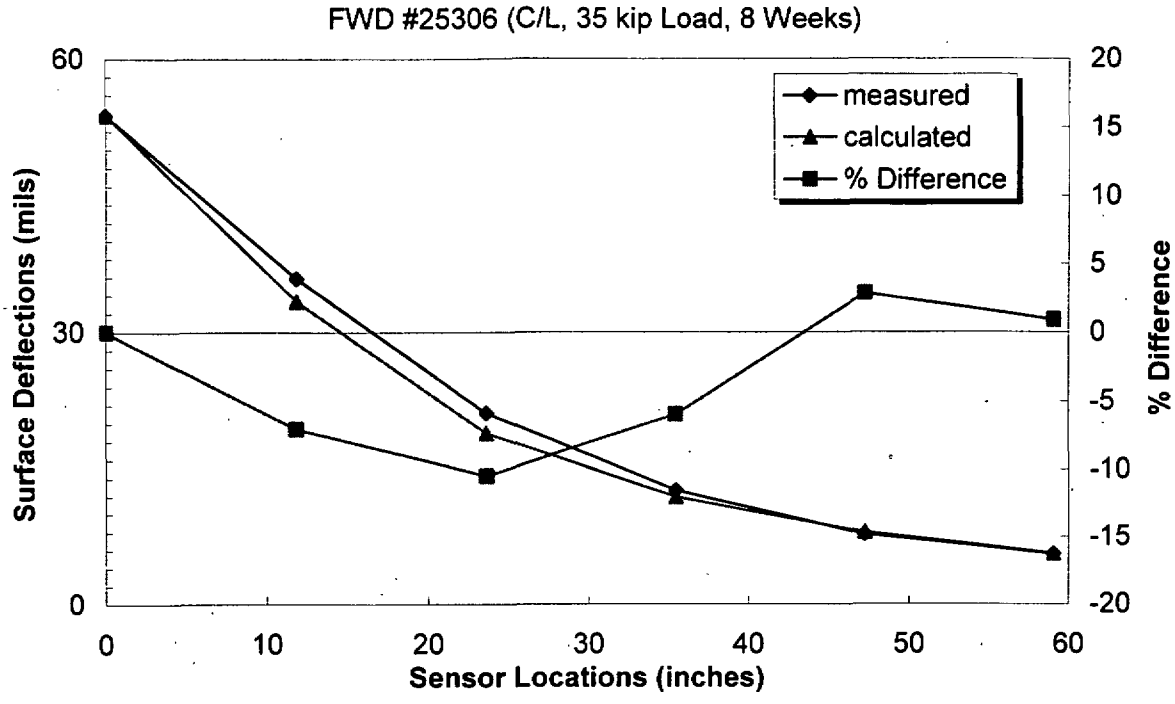

Figure F.15. FWD #25306 Deflection Basins

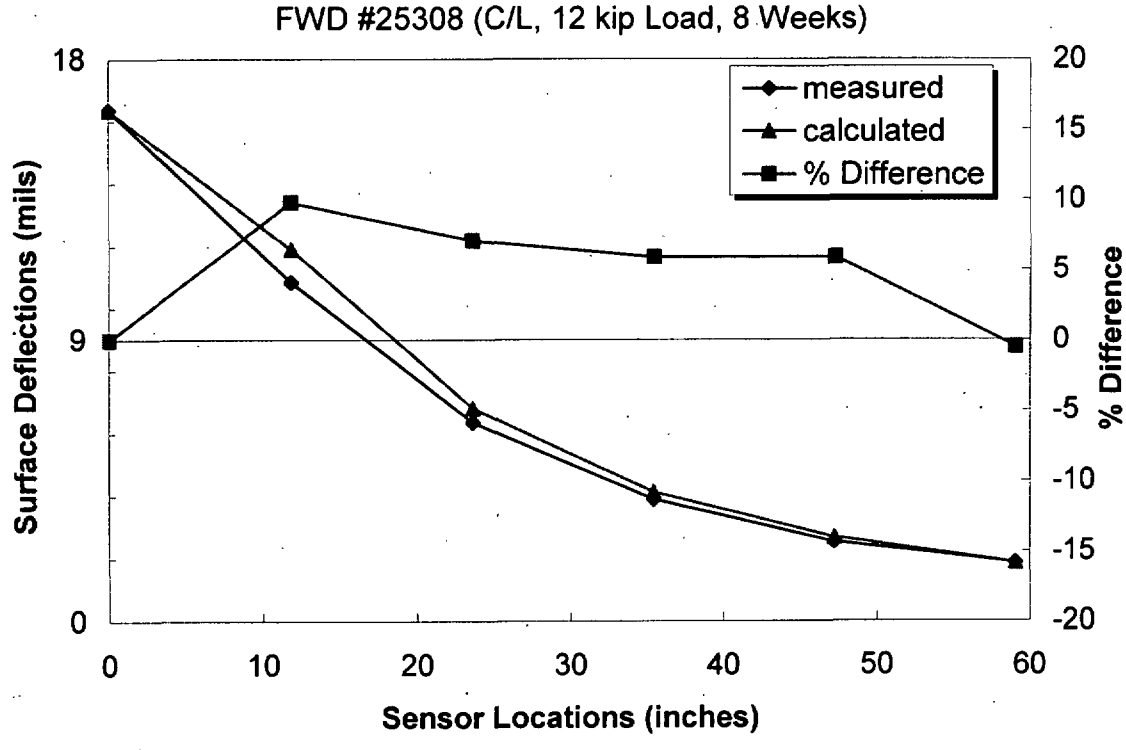

Figure F.16. FWD #25308 Deflection Basins

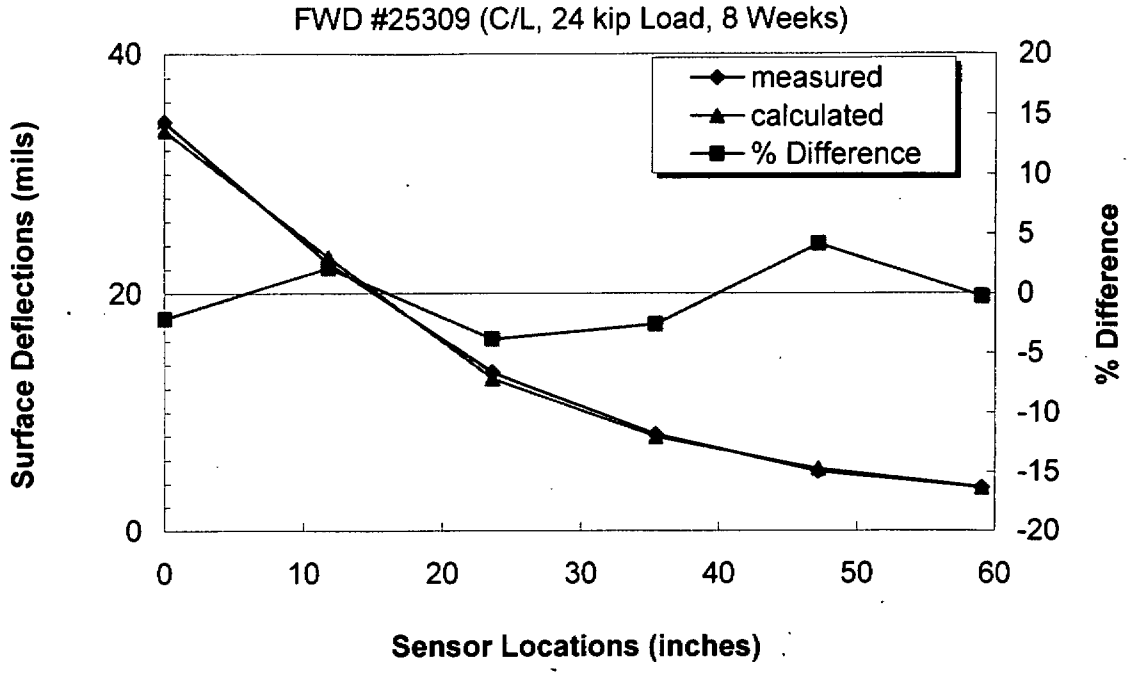

Figure F.17. FWD #25309 Deflection Basins

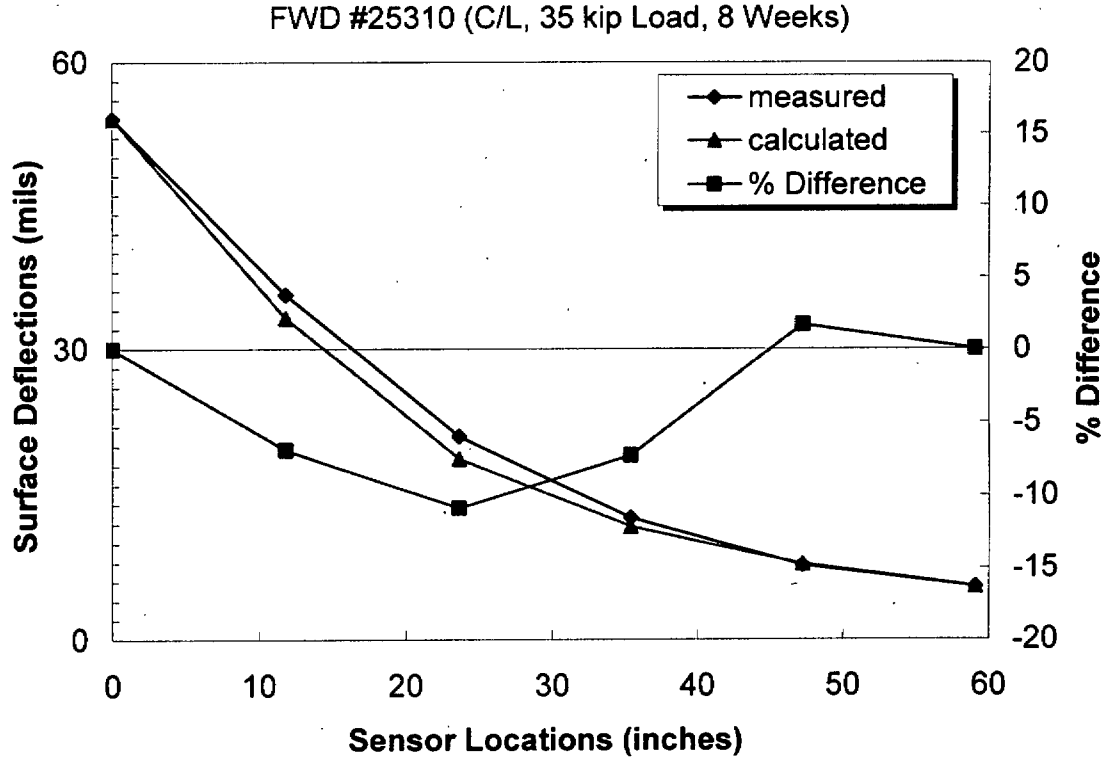

Figure F.18. FWD #25310 Deflection Basins

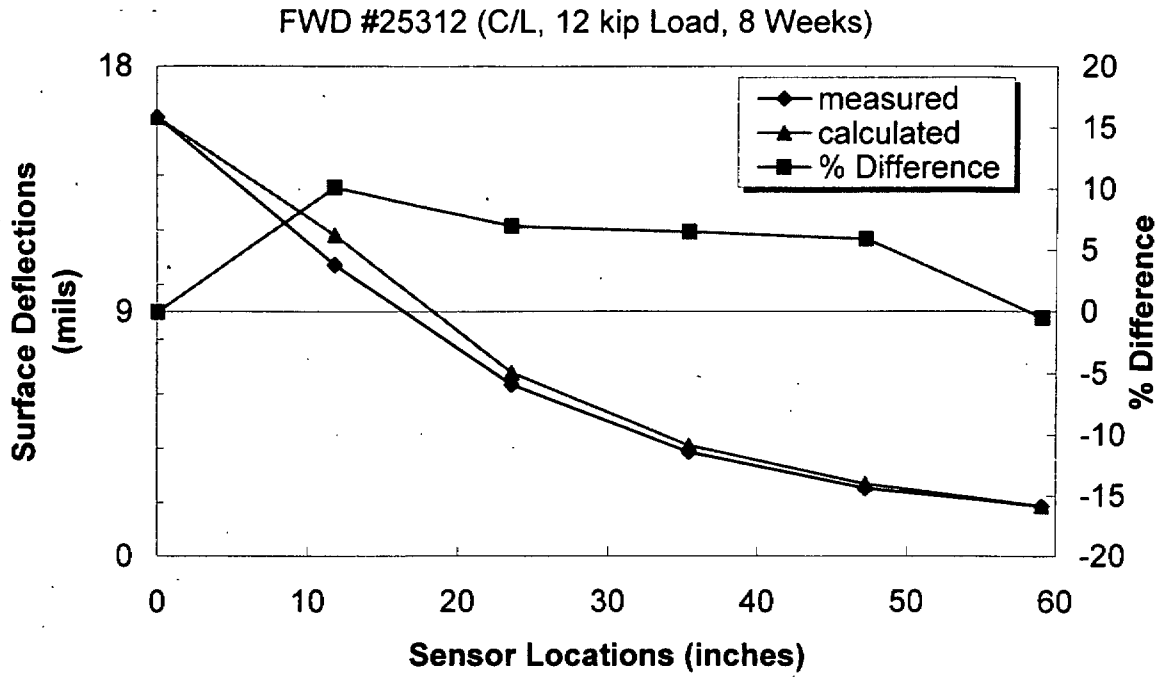

Figure F.19. FWD #25312 Deflection Basins

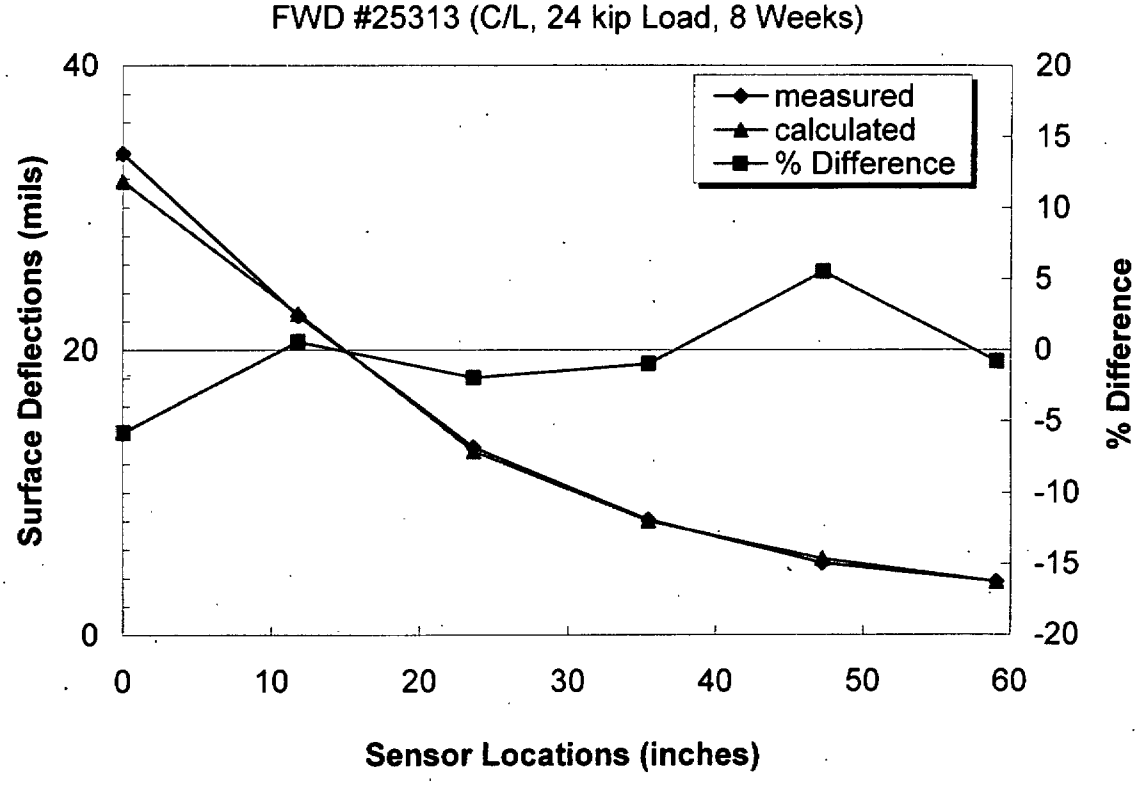

Figure F.20. FWD #25313 Deflection Basins

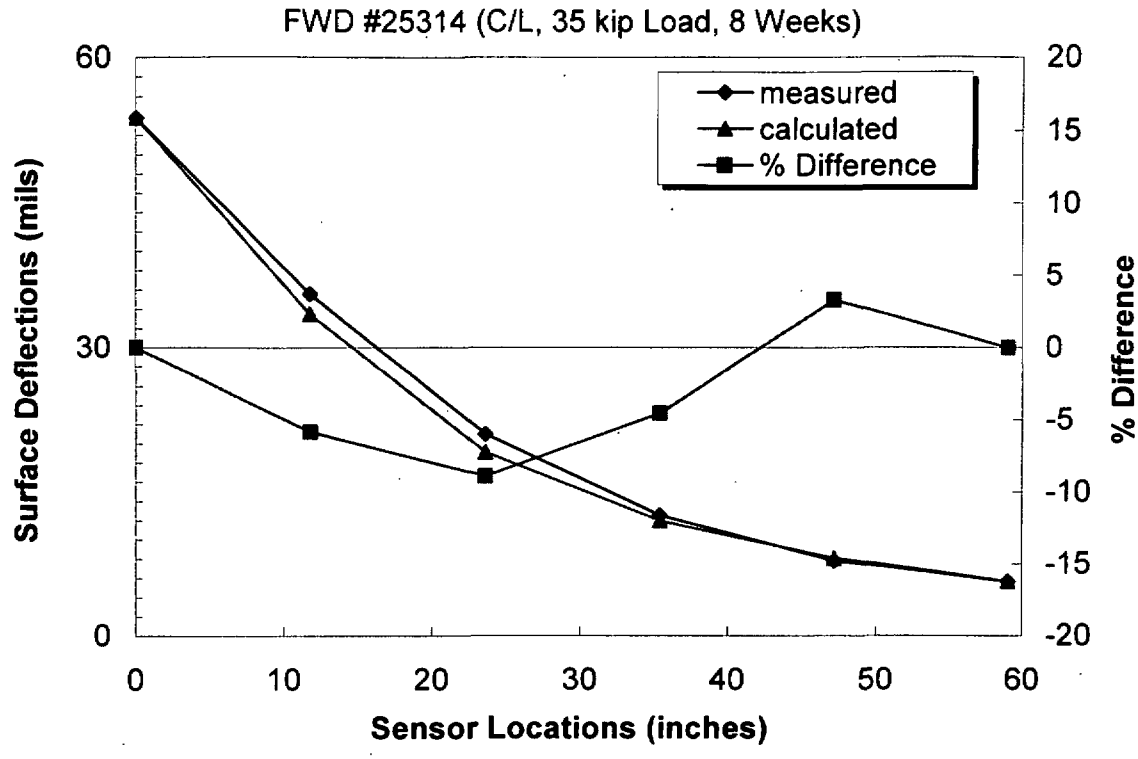

Figure F.21. FWD #25314 Deflection Basins

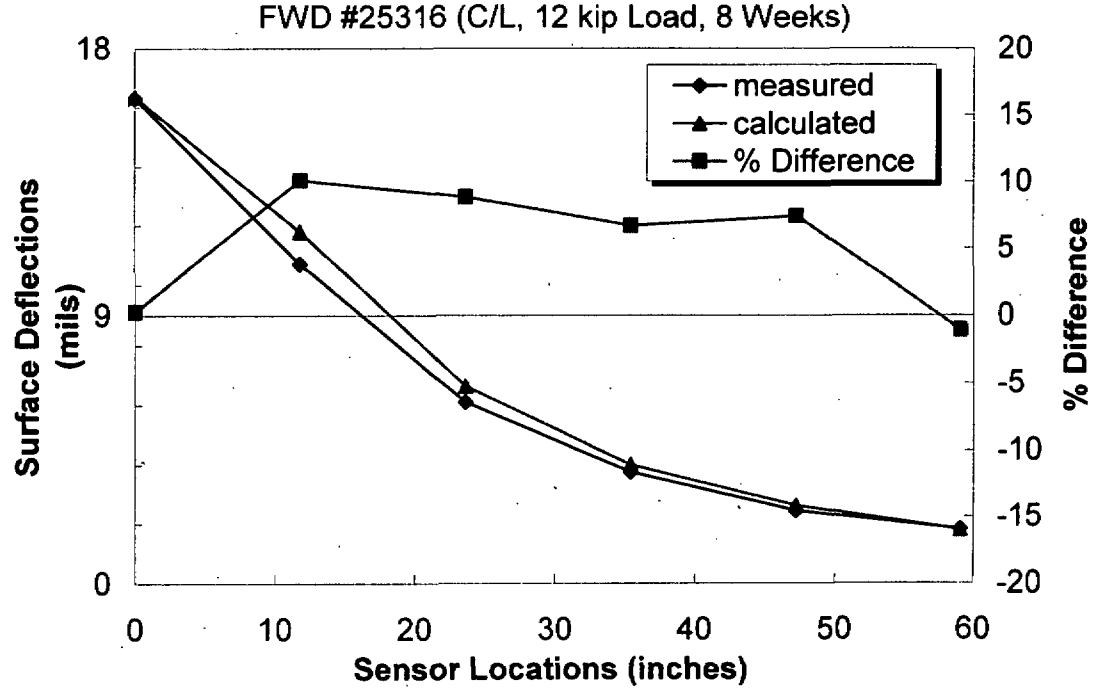

Figure F.22. FWD #25316 Deflection Basins

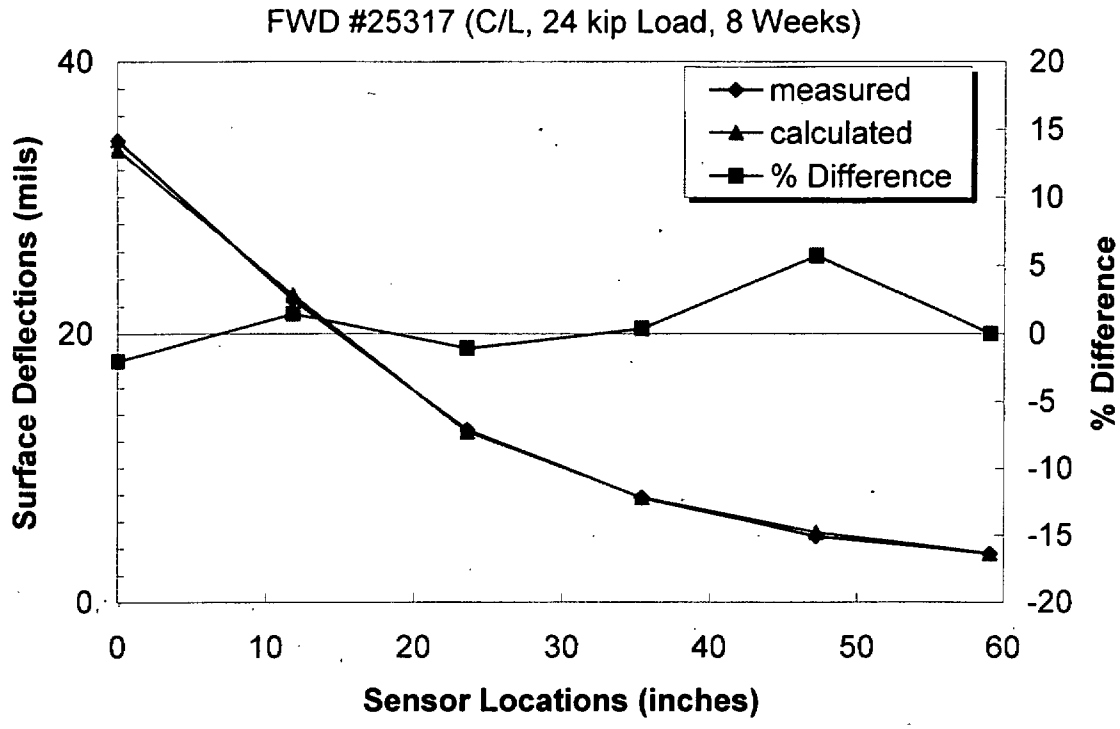

Figure F.23. FWD #25317 Deflection Basins

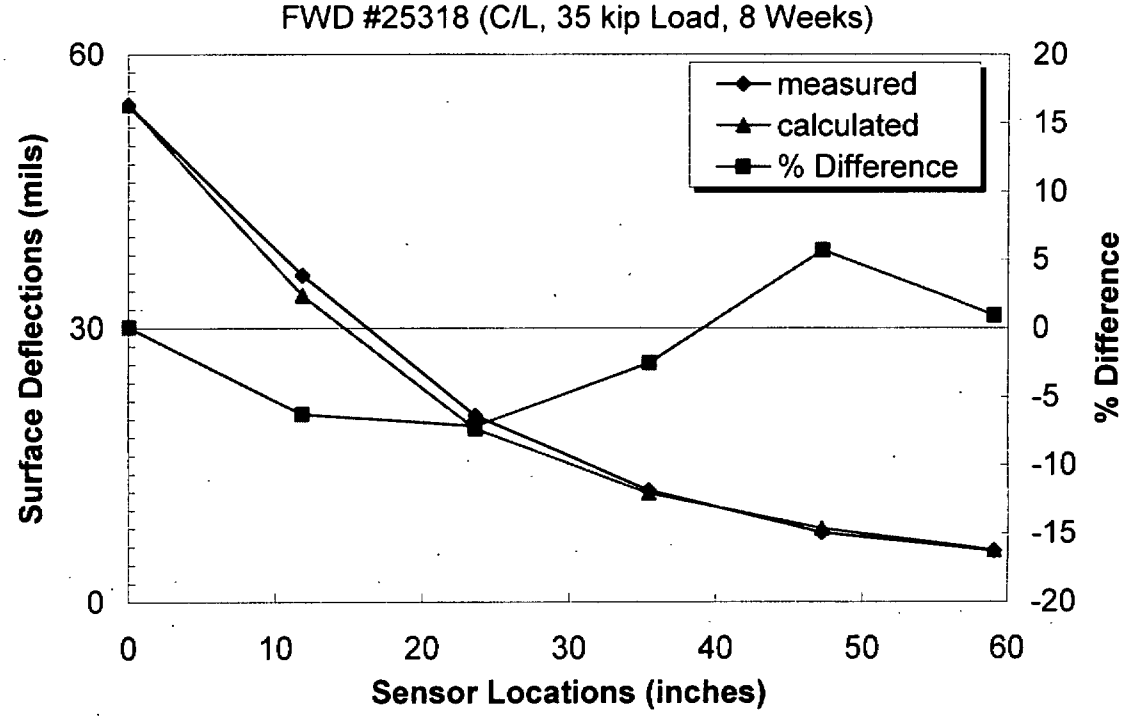

Figure F.24. FWD #25318 Deflection Basins

Appendix G

Temperature Adjusted Surface Layer Moduli

Table G.1(a). Temperature Adjusted P-401 Moduli*

FWD #	Lane	Pavement Temp, C	E_T (psi)	ATAF (Asphalt Temperature Adjustment Factor)	Temperature Adjusted E_T (psi)	Rounded Temperature Adjusted E_T (psi)
12899	5	21	480,000	1.453784	697,817	700,000
12900	5	21	440,000	1.453784	639,665	640,000
12901	5	21	335,000	1.453784	487,018	490,000
24856	5	8	1,700,000	0.798914	1,358,154	1,360,000
24857	5	8	1,510,000	0.798914	1,206,360	1,210,000
24858	5	8	1,200,000	0.798914	958,697	960,000
24860	5	8	1,625,000	0.798914	1,298,235	1,300,000
24861	5	8	1,470,000	0.798914	1,174,403	1,170,000
24862	5	8	1,150,000	0.798914	918,751	920,000
24864	5	8	1,500,000	0.798914	1,198,371	1,200,000
24865	5	8	1,050,000	0.798914	838,860	840,000
24866	5	8	700,000	0.798914	559,240	560,000
24882	5	9	1,620,000	0.839782	1,360,447	1,360,000
24883	5	9	1,480,000	0.839782	1,242,878	1,240,000
24884	5	9	1,170,000	0.839782	982,545	980,000
24886	5	9	2,100,000	0.839782	1,763,543	1,760,000
24887	5	9	1,645,000	0.839782	1,381,442	1,380,000
24888	5	9	1,410,000	0.839782	1,184,093	1,180,000
24890	5	9	2,050,000	0.839782	1,721,554	1,720,000
24891	5	9	1,660,000	0.839782	1,394,038	1,390,000
24892	5	9	1,330,000	0.839782	1,116,910	1,120,000
24894	5	9	2,000,000	0.839782	1,679,564	1,680,000
24895	5	9	1,680,000	0.839782	1,410,834	1,410,000
24896	5	9	1,420,000	0.839782	1,192,491	1,190,000
24916	5	8	1,525,000	0.798914	1,218,344	1,220,000
24917	5	8	1,150,000	0.798914	918,751	920,000
24918	5	8	775,000	0.798914	619,158	620,000
24920	CL	11	1,700,000	0.922571	1,568,371	1,570,000
24921	CL	11	1,600,000	0.922571	1,476,114	1,480,000
24922	CL	11	1,310,000	0.922571	1,208,569	1,210,000
24924	CL	11	1,800,000	0.922571	1,660,629	1,660,000
24925	CL	11	1,612,000	0.922571	1,487,185	1,490,000
24926	CL	11	1,230,000	0.922571	1,134,763	1,130,000
24928	CL	11	1,571,000	0.922571	1,449,360	1,450,000
24929	CL	11	1,300,000	0.922571	1,199,343	1,200,000
24930	CL	11	820,000	0.922571	756,509	760,000

* P-401 moduli from forward calculation analysis

Table G.1(b). Temperature Adjusted P-401 Moduli*

FWD #	Lane	Pavement Temp, C	E_T (psi)	ATAF (Asphalt Temperature Adjustment Factor)	Temperature Adjusted E_T (psi)	Rounded Temperature Adjusted E_T (psi)
24932	CL	12	1,550,000	0.947691	1,468,921	1,470,000
24933	CL	12	1,000,000	0.947691	947,691	950,000
24934	CL	12	515,000	0.947691	488,061	490,000
25304	CL	23	450,000	1.62181	729,815	730,000
25305	CL	23	141,400	1.62181	229,324	230,000
25306	CL	23	72,000	1.62181	116,770	120,000
25308	CL	23	500,000	1.62181	810,905	810,000
25309	CL	23	155,000	1.62181	251,381	250,000
25310	CL	23	65,000	1.62181	105,418	110,000
25312	CL	23	525,000	1.62181	851,450	850,000
25313	CL	23	275,000	1.62181	445,998	450,000
25314	CL	23	73,000	1.62181	118,392	120,000
25316	CL	23	460,000	1.62181	746,033	750,000
25317	CL	23	148,000	1.62181	240,028	240,000
25318	CL	23	64,000	1.62181	103,796	100,000
25320	5	23	21,800	1.606325	35,018	40,000
25321	5	23	12,750	1.606325	20,481	20,000
25322	5	23	9,300	1.606325	14,939	10,000
25508	5	12	1,485,000	0.951335	1,412,732	1,410,000
25509	5	12	1,150,000	0.951335	1,094,035	1,090,000
25510	5	12	775,000	0.951335	737,284	740,000
25512	5	12	1,400,000	0.975364	1,365,509	1,370,000
25513	5	12	950,000	0.975364	926,596	930,000
25514	5	12	550,000	0.975364	536,450	540,000
25516	5	13	1,440,000	1	1,440,000	1,440,000
25517	5	13	900,000	1	900,000	900,000
25518	5	13	485,000	1	485,000	490,000
25520	5	13	1,450,000	1	1,450,000	1,450,000
25521	5	13	960,000	1	960,000	960,000
25522	5	13	520,000	1	520,000	520,000

* P-401 moduli from forward calculation analysis

Appendix H

SPSS Analysis of Forward Calculated Surface Layer Moduli Results

Table H.1. SPSS Output: Univariate Analysis of Variance

Between-Subjects Factors

		#
LOAD	1	21
	2	21
	3	21
TIME	2	12
	3	12
	4	24
	5	15
SECTION	UF	33
	F	30
LANE	C/L	24
	5	39

Tests of Between-Subjects Effects, Dependent Variable: $ADJE_T$

Source	Type III Sum of Squares	df	Mean Square	F	Sig.
Corrected Model	14479676.984(a)	32	452489.90	51.4	.000
Intercept	49999964.665	1	49999964.6	5689.3	.000
CP	3667710.117	2	1833855.05	208.6	.000
TIME	7300618.300	3	2433539.43	276.9	.000
SECTION	96092.916	1	96092.91	10.9	.002
LANE	456193.939	1	456193.93	51.9	.000
CP * TIME	306771.070	6	51128.51	5.8	.000
CP * SECTION	67080.222	2	33540.11	3.8	.033
CP * LANE	140692.424	2	70346.21	8.0	.002
TIME * SECTION	453805.556	3	151268.51	17.2	.000
TIME * LANE	8003.333	1	8003.33	.91	.348
SECTION * LANE	18150.000	1	18150.00	2.0	.161
CP * TIME * SECTION	47786.111	6	7964.35	.90	.504
CP * TIME * LANE	79706.667	2	39853.33	4.5	.019
CP * SECTION * LANE	6475.000	2	3237.50	.36	.695
TIME * SECTION * LANE	.000	0	.	.	.
CP * TIME * SECTION * LANE	.000	0	.	.	.
Error	263650.000	30	8788.33		
Total	72306000.000	63			
Corrected Total	14743326.984	62			

Appendix I

Mechanical Response Analysis of Failed Section Results

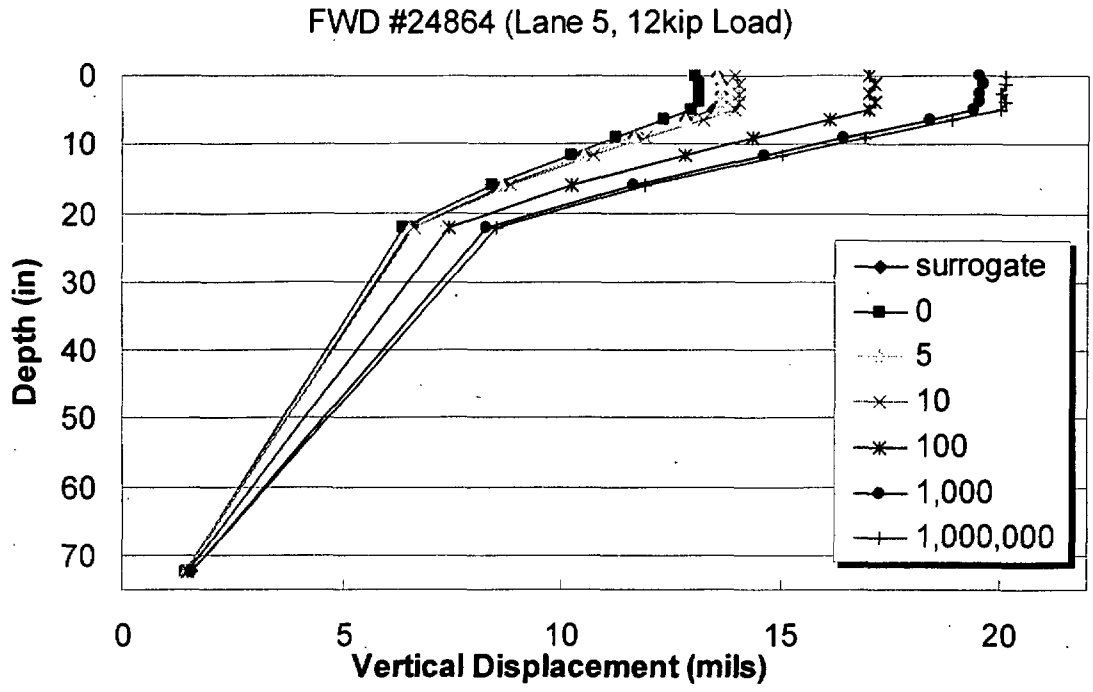

Figure I.1. FWD #24864 Vertical Displacement

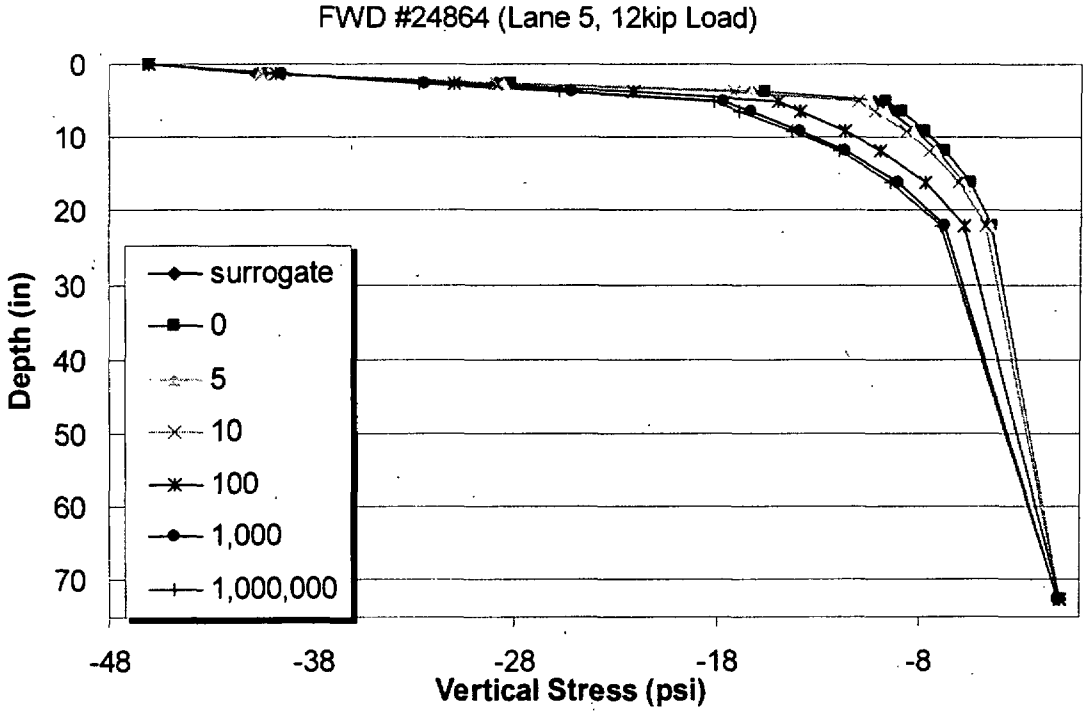

Figure I.2. FWD #24864 Vertical Stress

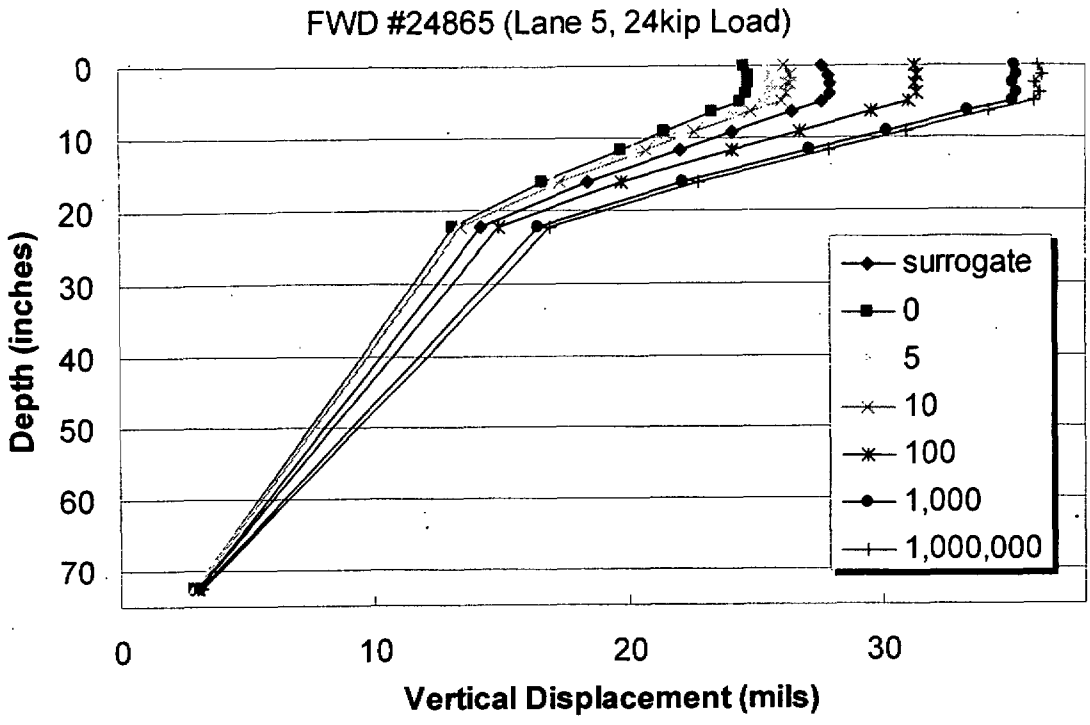

Figure I.3. FWD #24865 Vertical Displacement

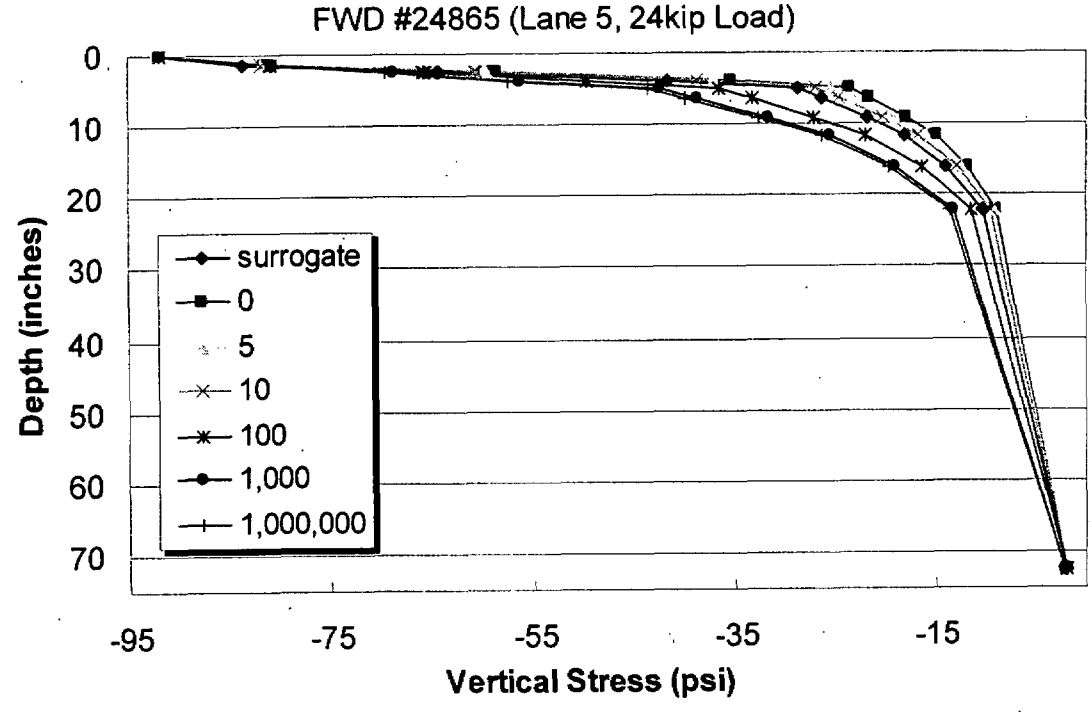

Figure I.4. FWD #24865 Vertical Stress

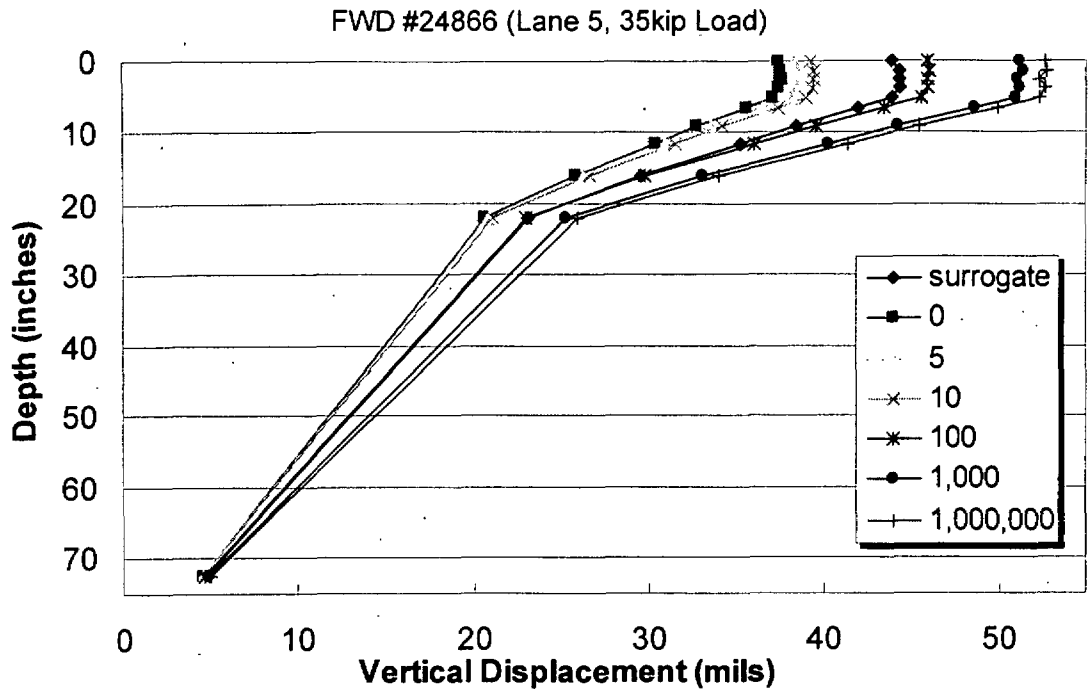

Figure I.5. FWD #24866 Vertical Displacement

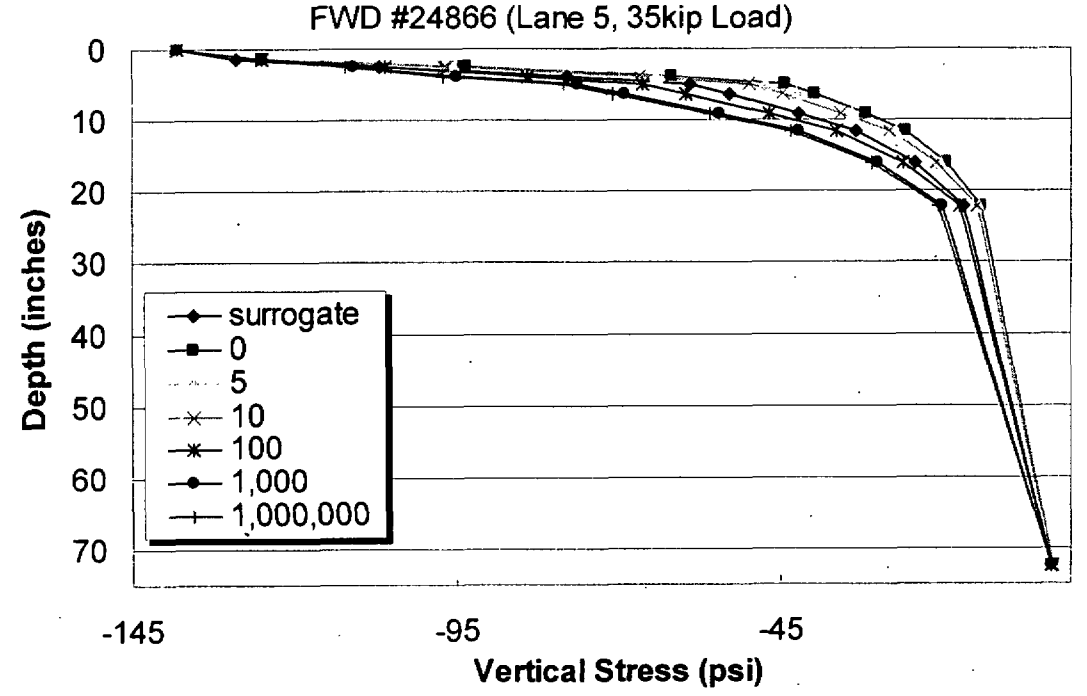

Figure I.6. FWD #24866 Vertical Stress

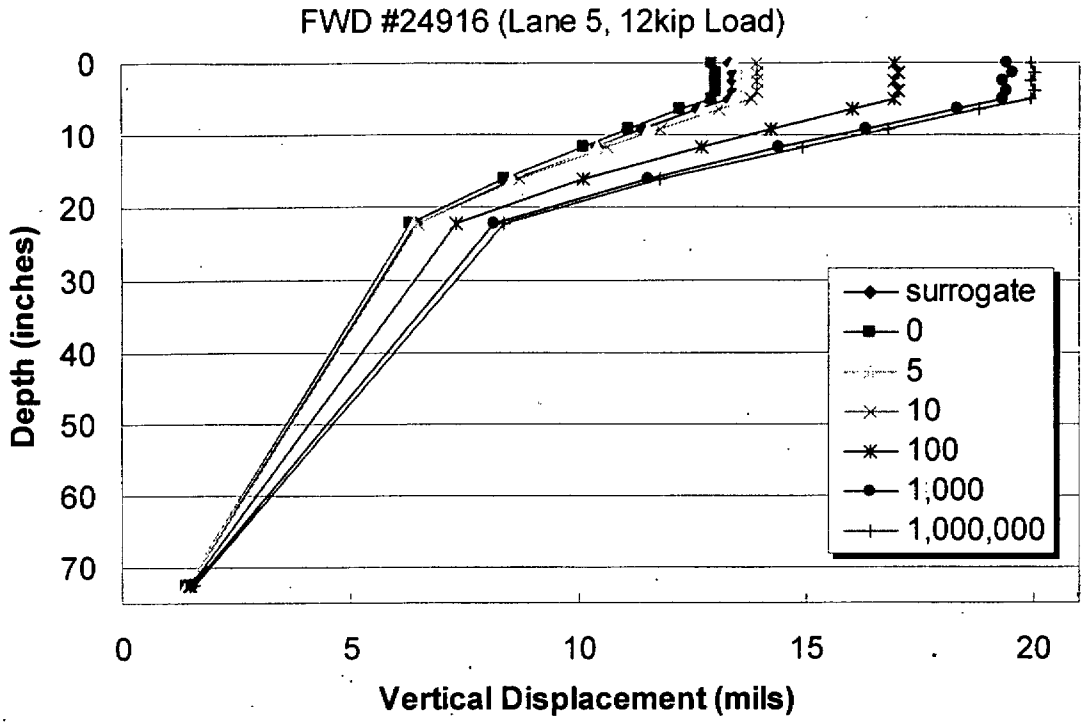

Figure I.7. FWD #24916 Vertical Displacement

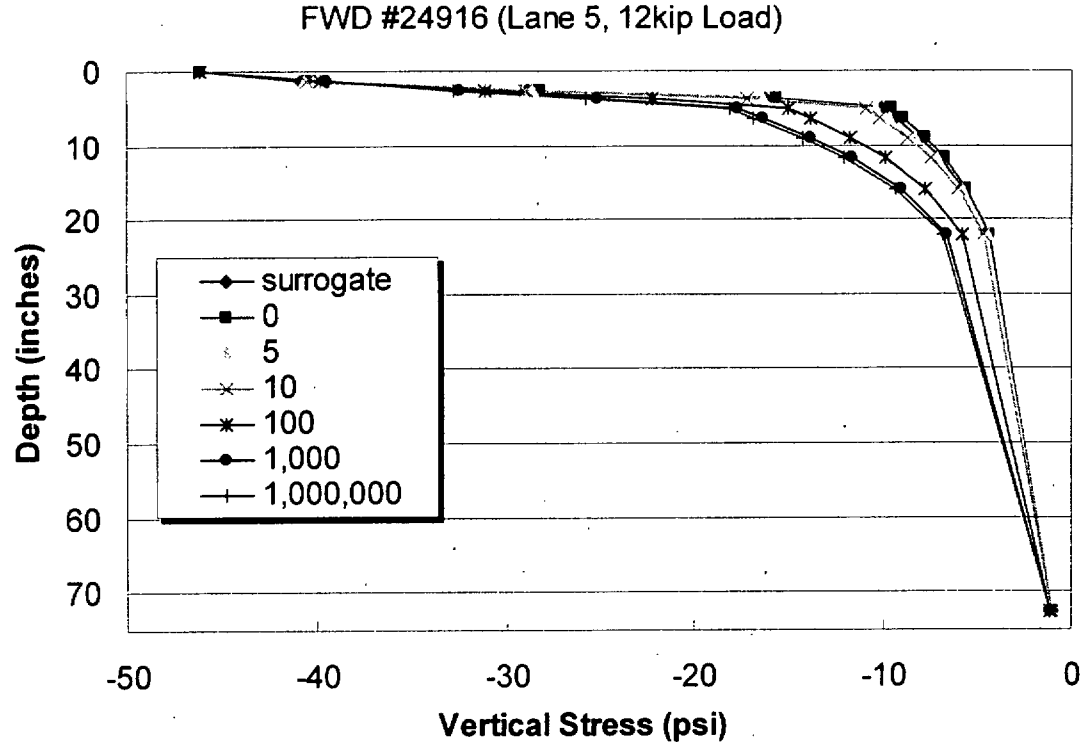

Figure I.8. FWD #24916 Vertical Stress

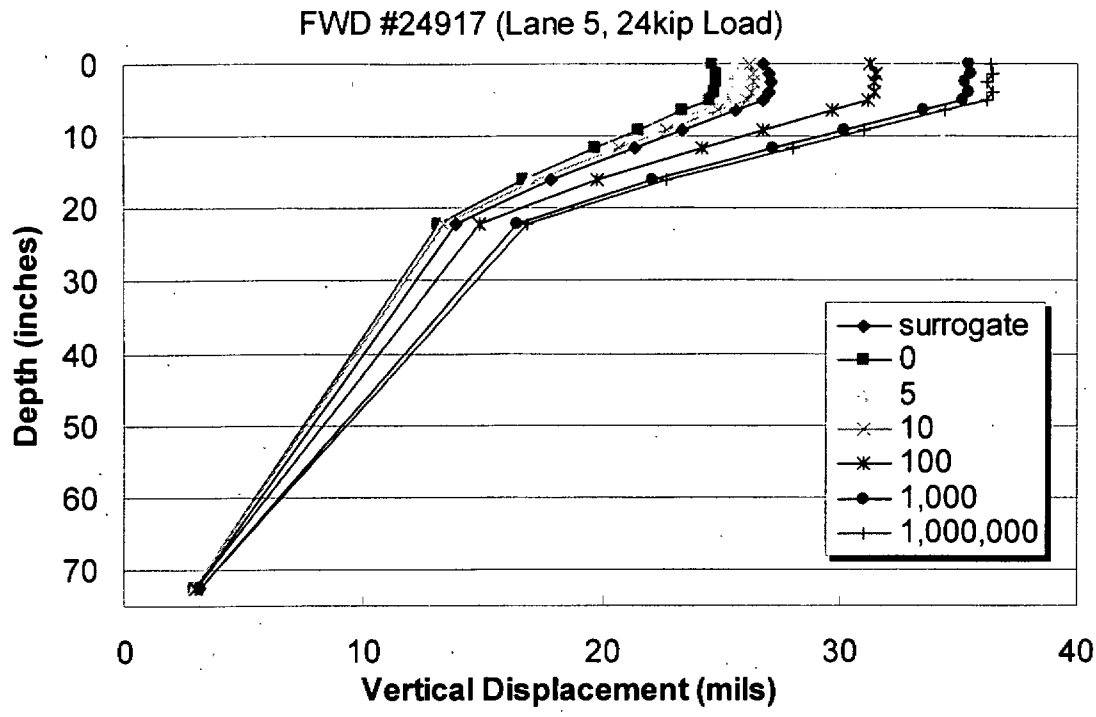

Figure I.9. FWD #24917 Vertical Displacement

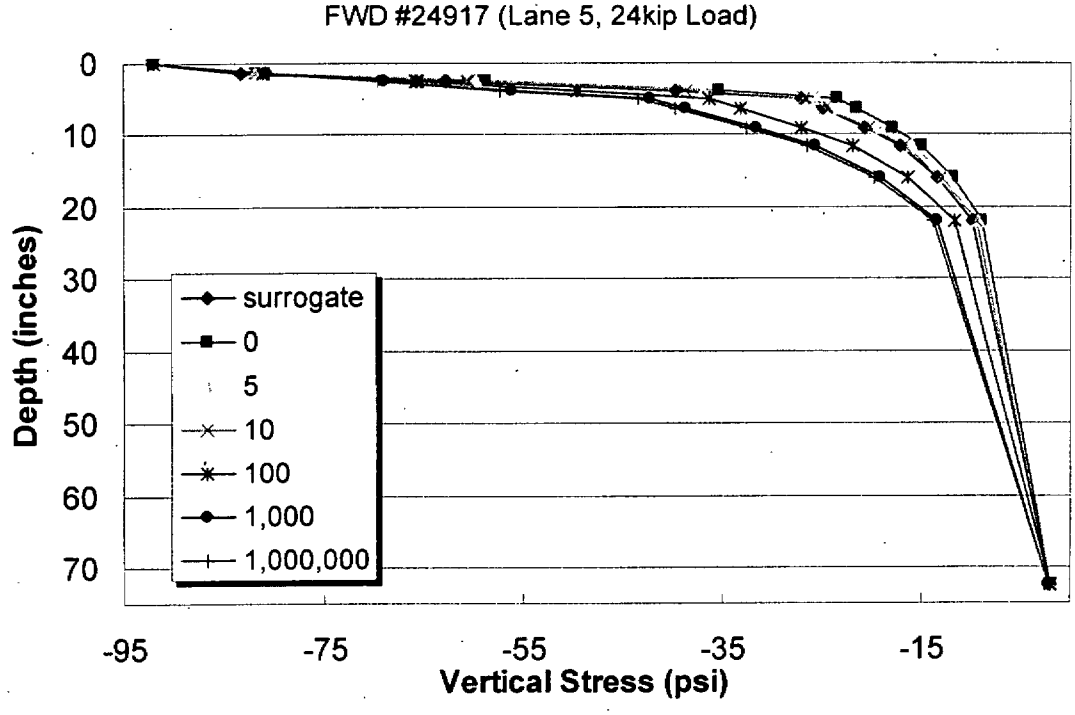

Figure I.10. FWD #24917 Vertical Stress

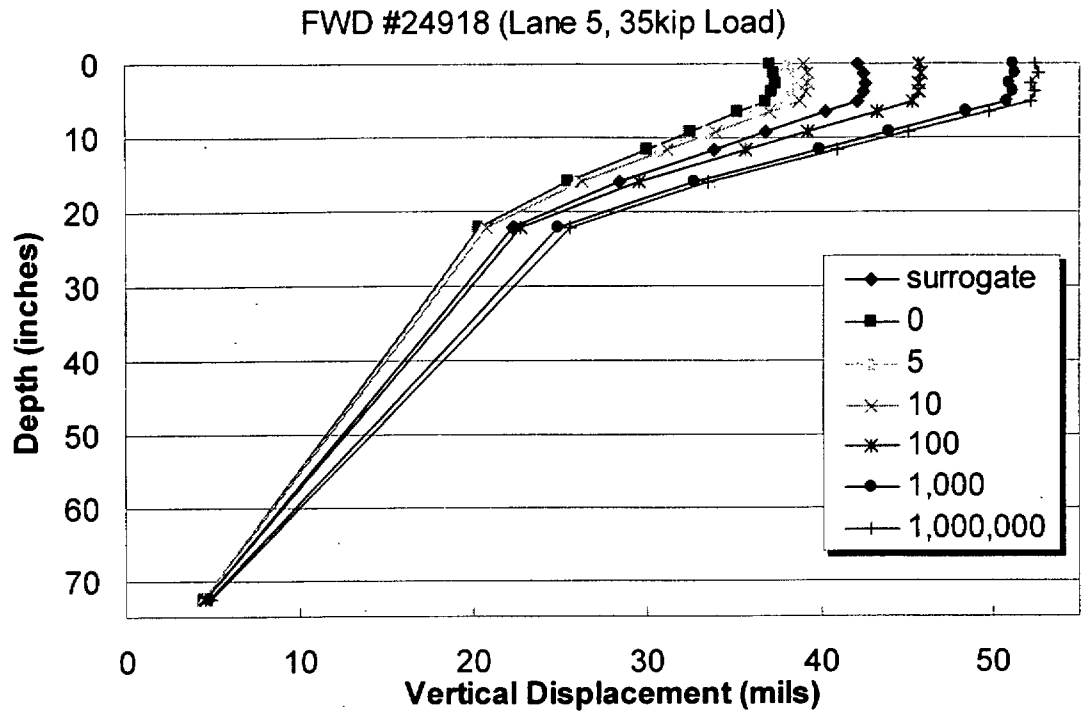

Figure I.11. FWD #24918 Vertical Displacement

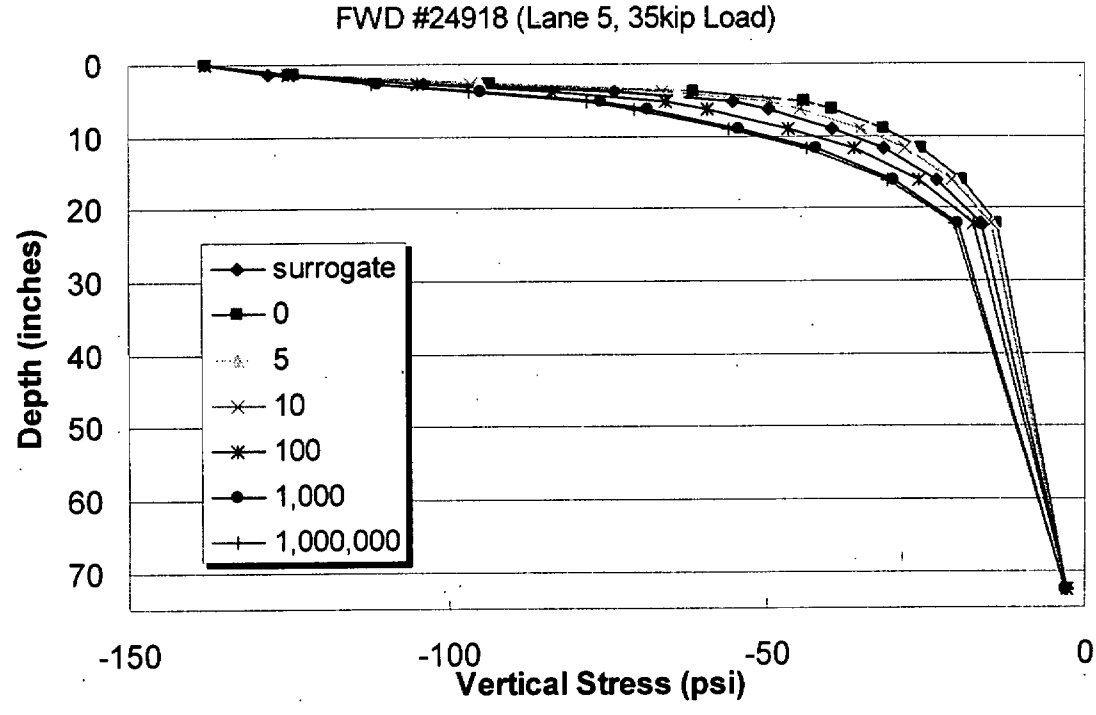

Figure I.12. FWD #24918 Vertical Stress

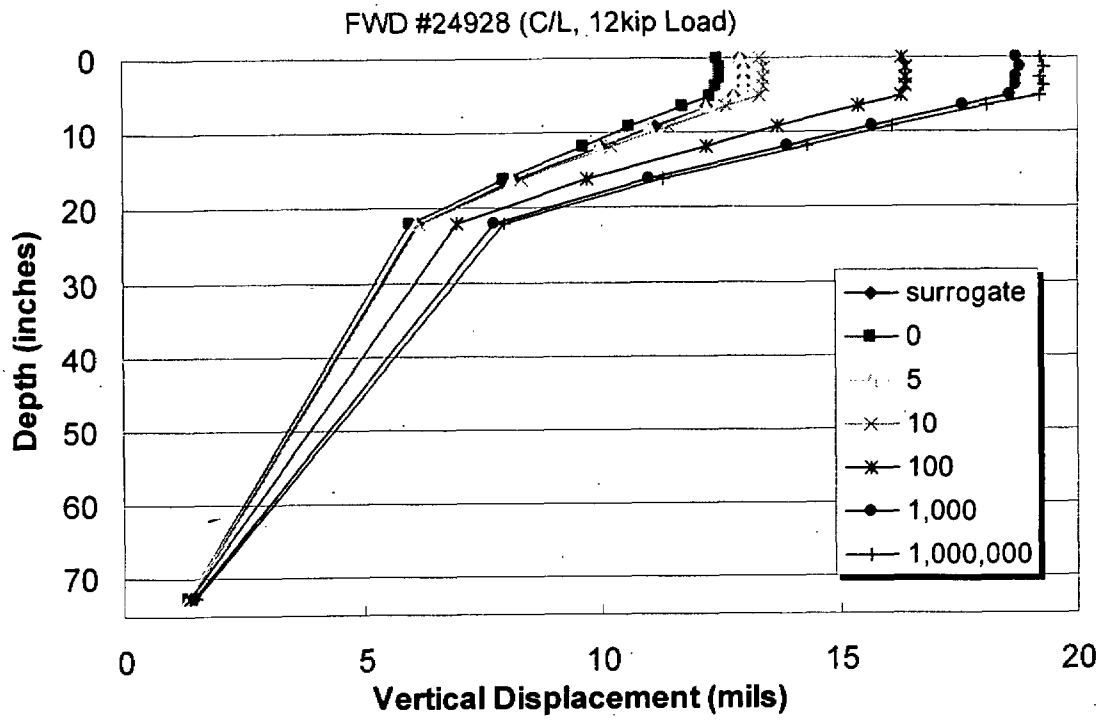

Figure I.13. FWD #24928 Vertical Displacement

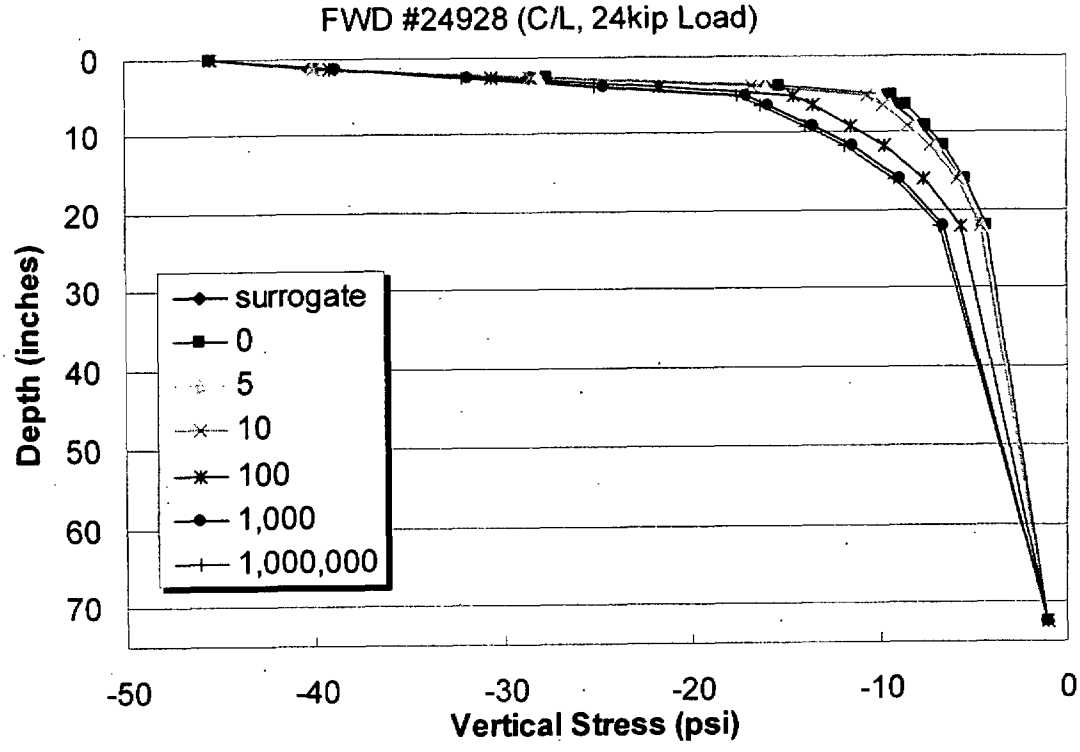

Figure I.14. FWD #24928 Vertical Stress

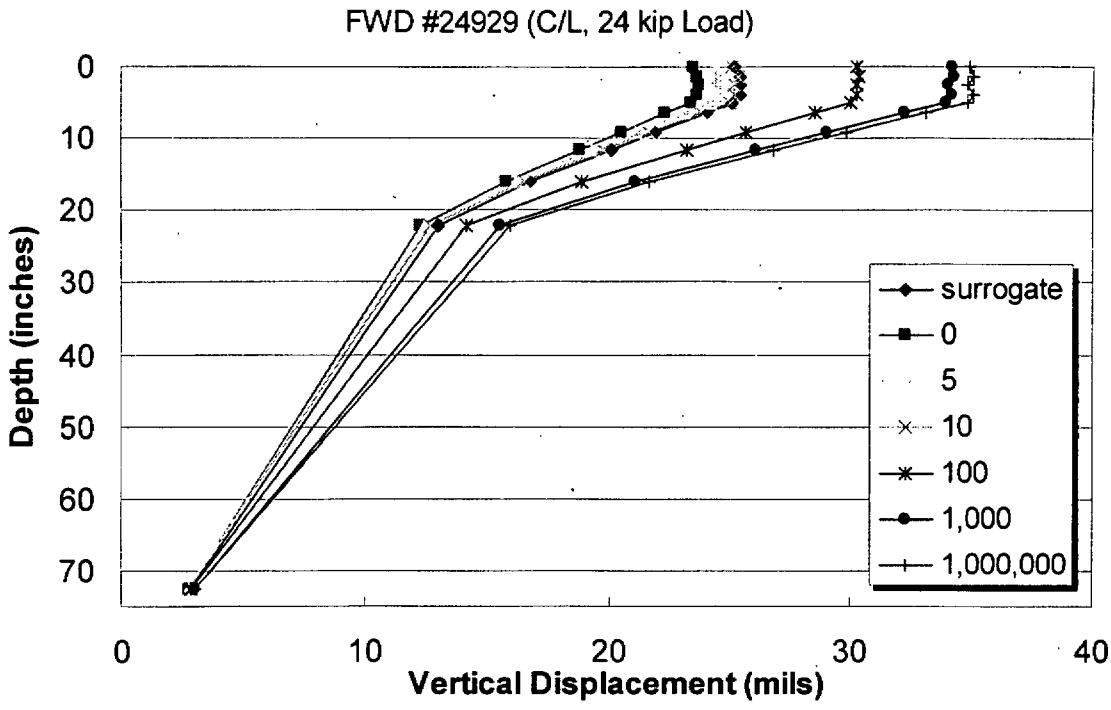

Figure I.15. FWD #24929 Vertical Displacement

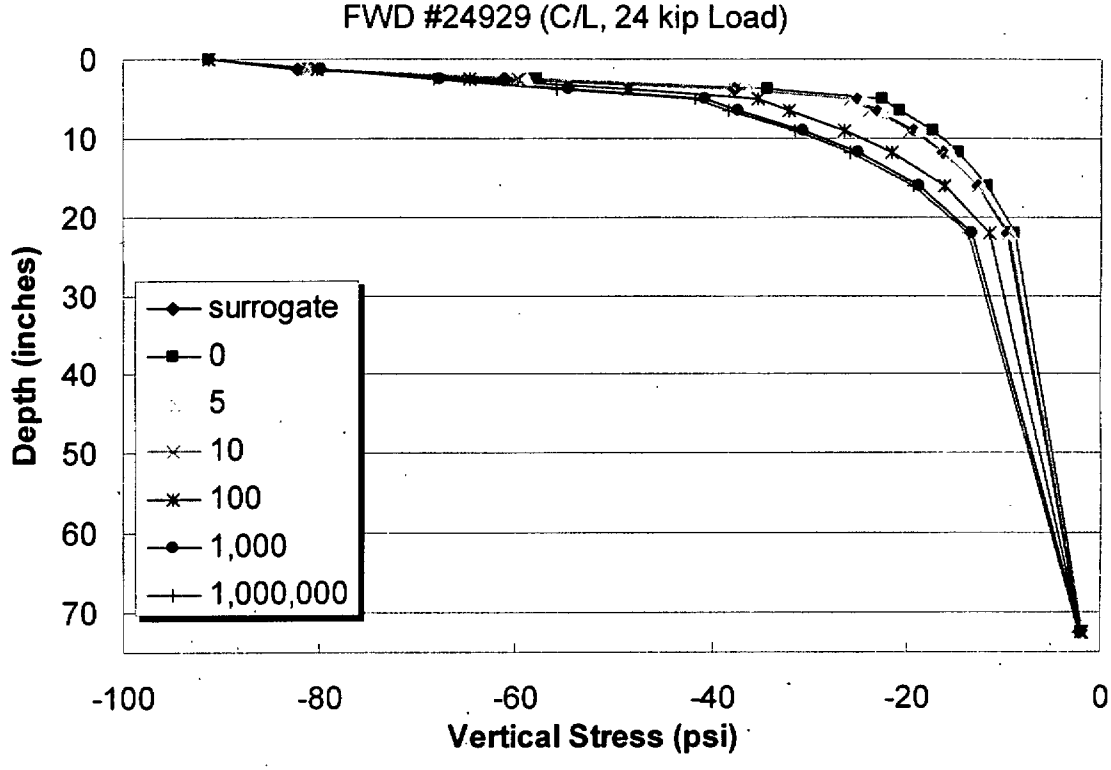

Figure I.16. FWD #24929 Vertical Stress

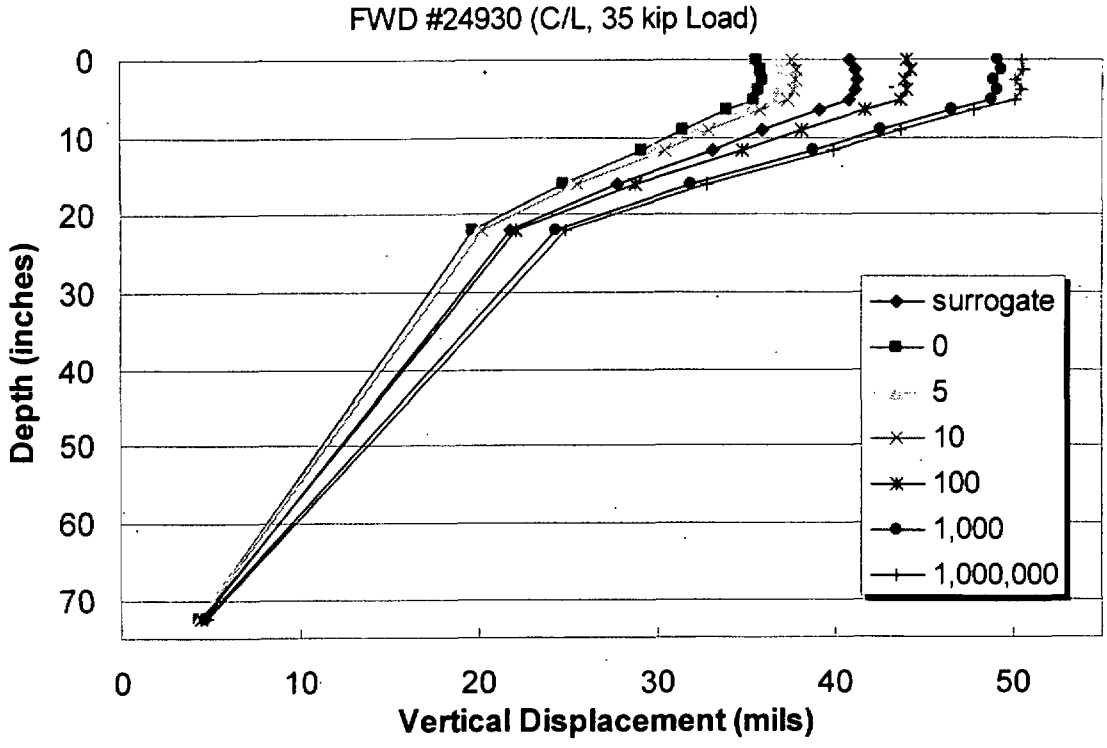

Figure I.17. FWD #24930 Vertical Displacement

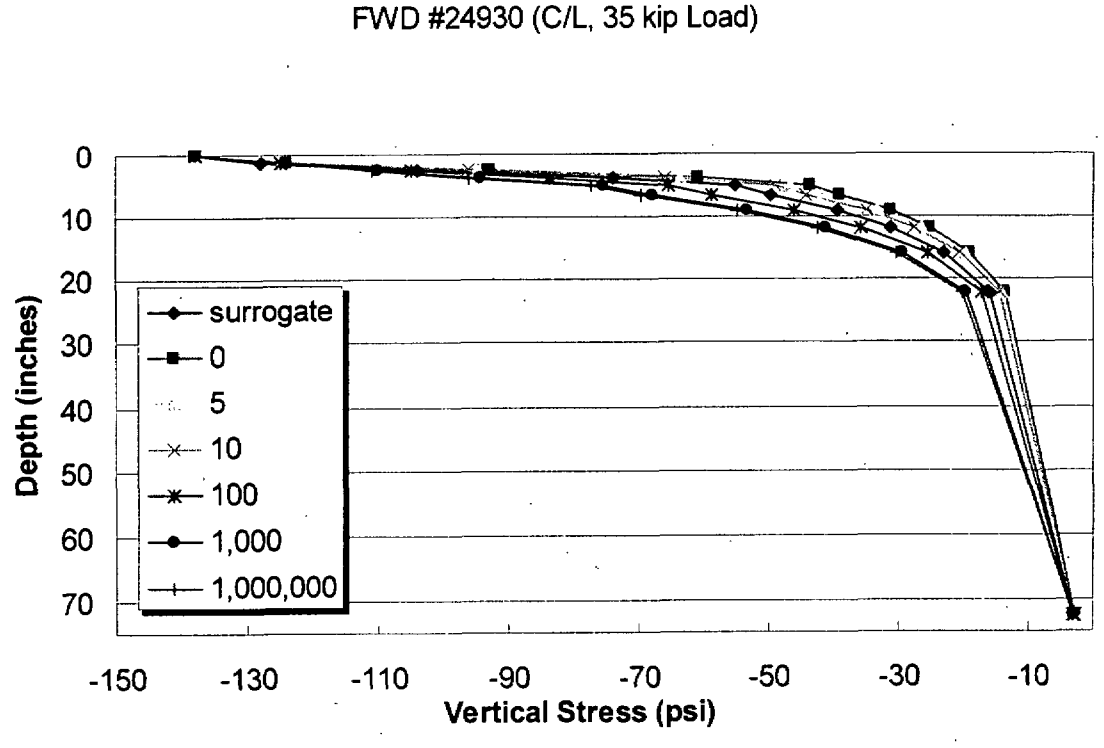

Figure I.18. FWD #24930 Vertical Stress

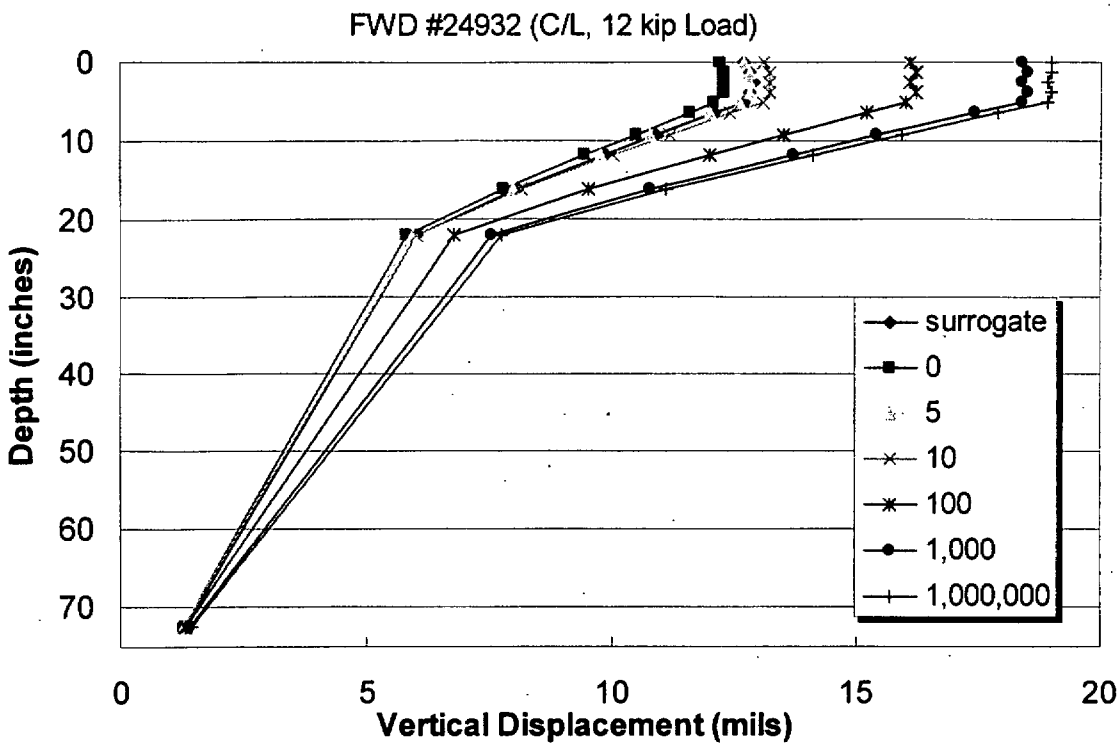

Figure I.19. FWD #24932 Vertical Displacement

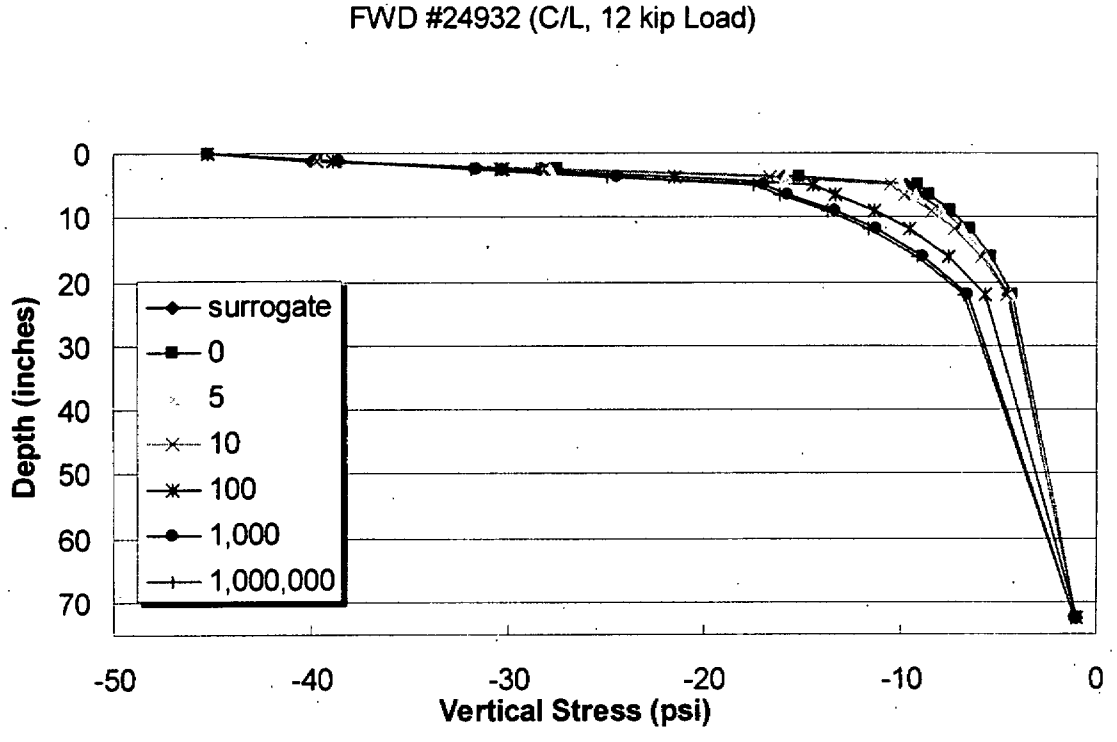

Figure I.20. FWD #24932 Vertical Stress

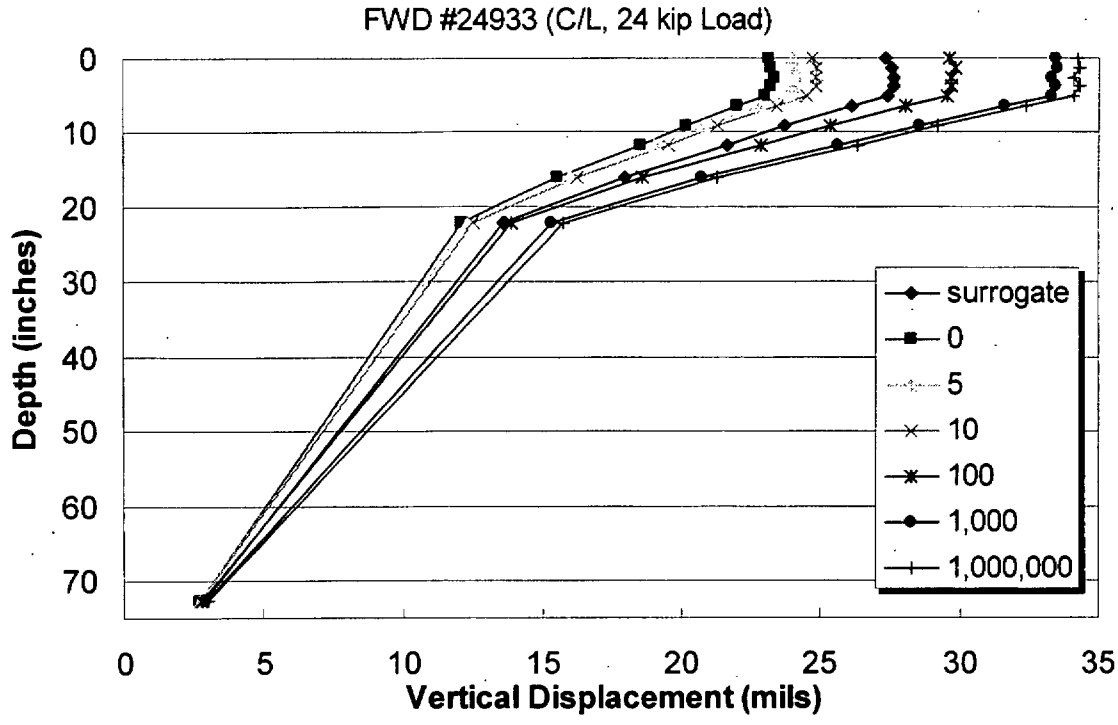

Figure I.21. FWD #24933 Vertical Displacement

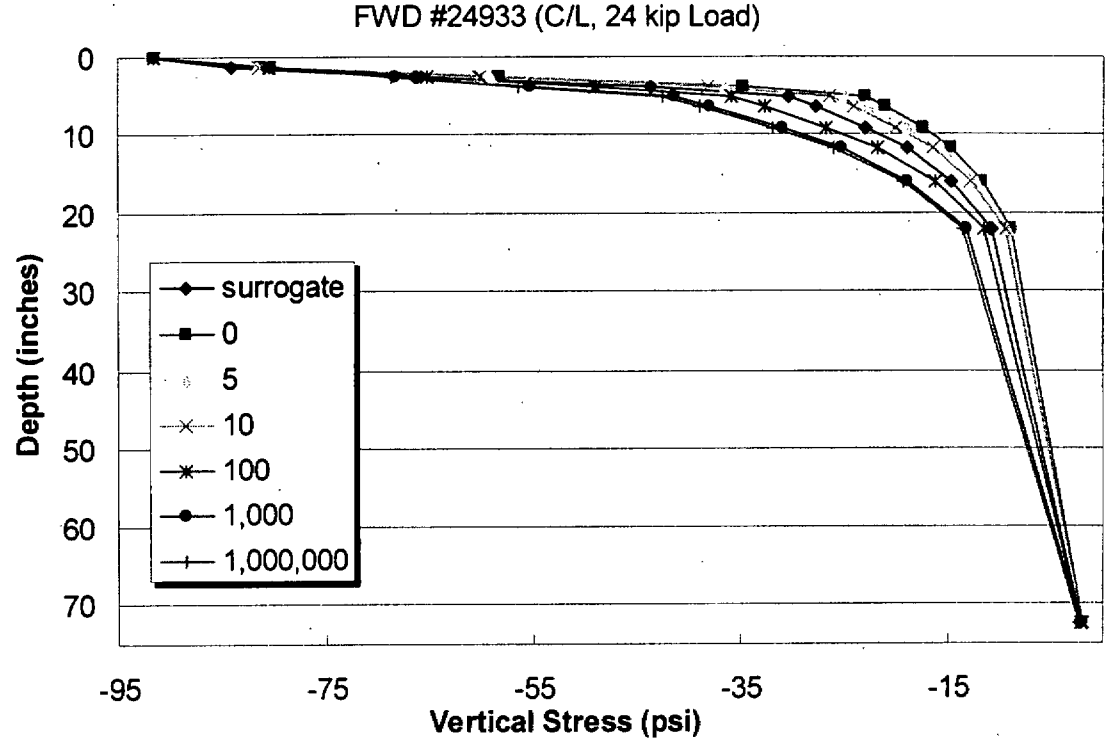

Figure I.22. FWD #24933 Vertical Stress

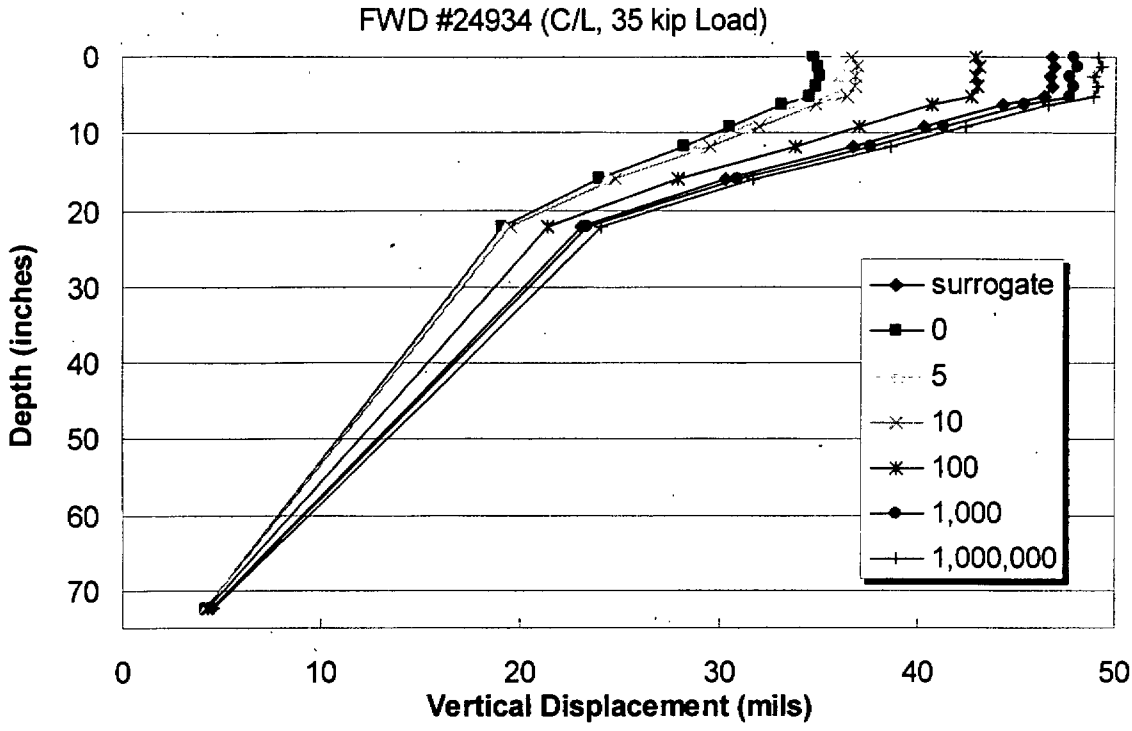

Figure I.23. FWD #24934 Vertical Displacement

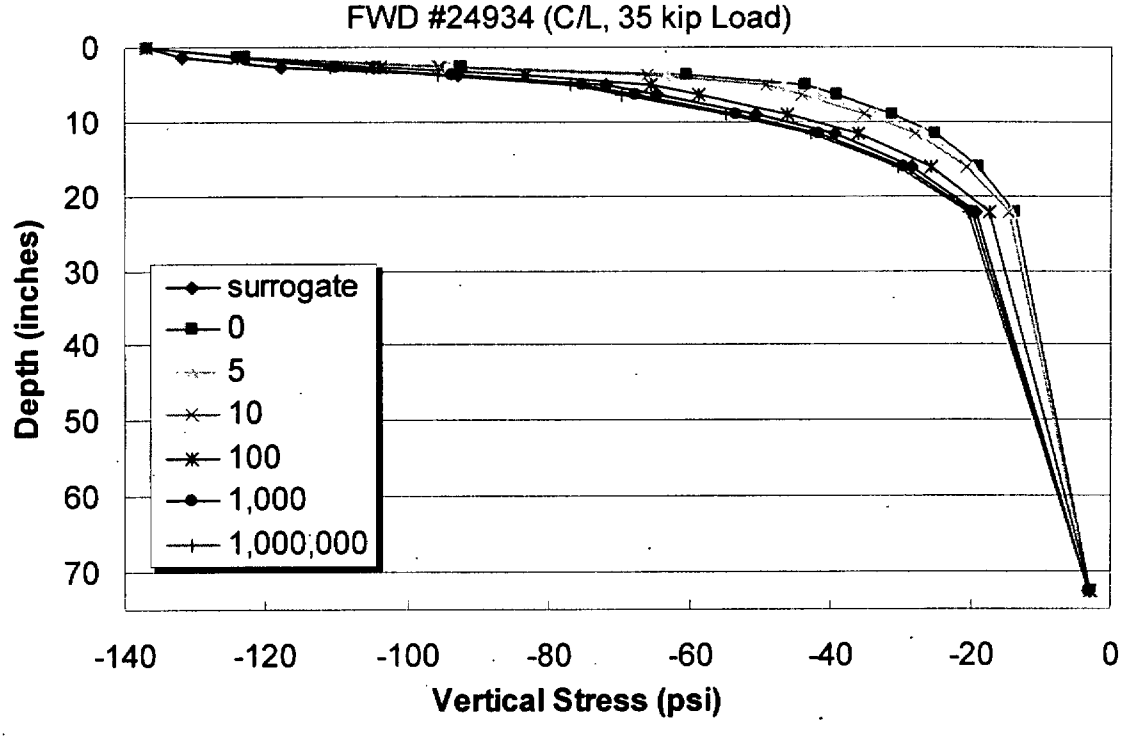

Figure I.24. FWD #24934 Vertical Stress

Appendix J

Radial Stress Difference at Interface Analysis Results

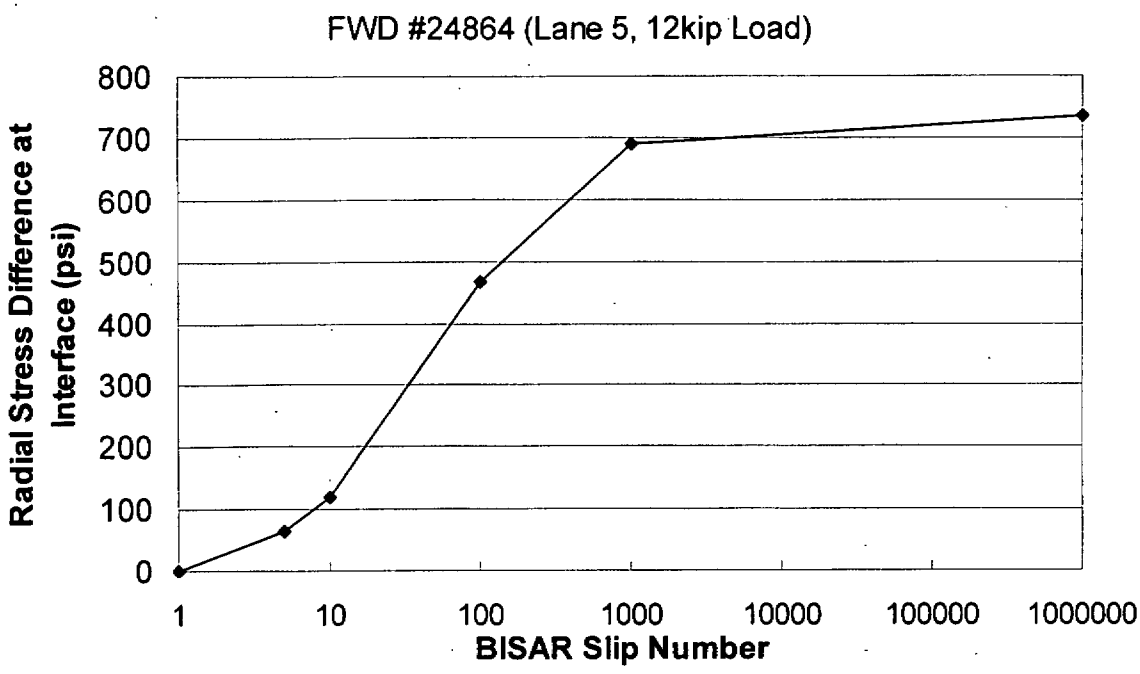

Figure J.1. FWD #24864 Radial Stress Difference vs. BISAR Slip Number

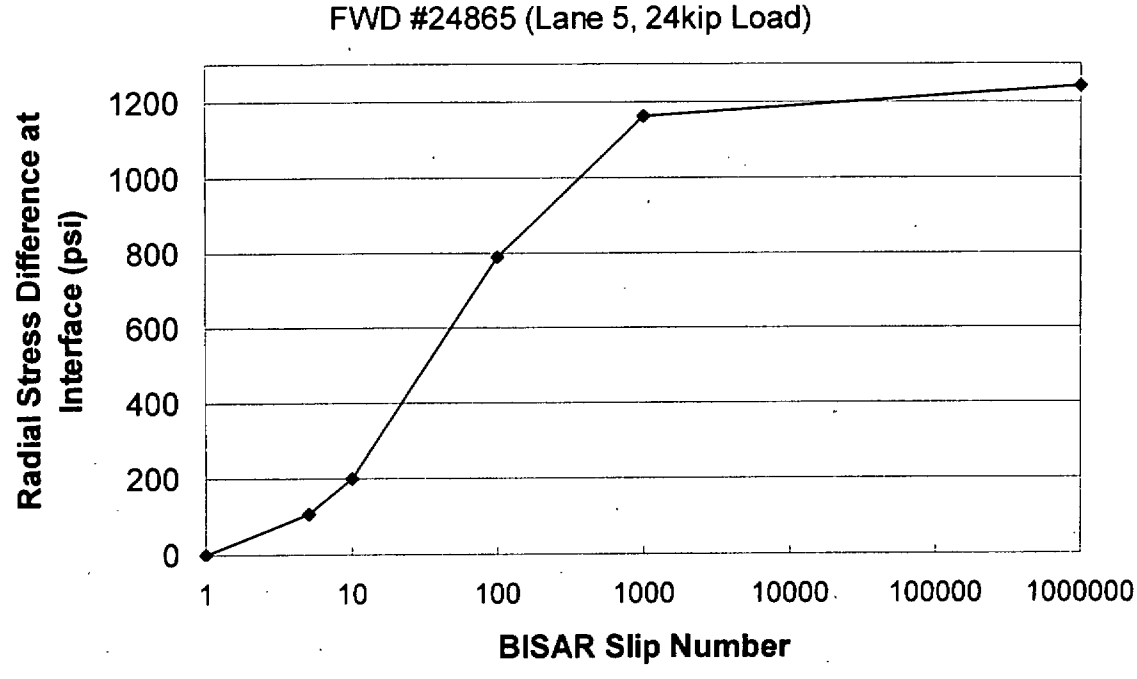

Figure J.2. FWD #24865 Radial Stress Difference vs. BISAR Slip Number

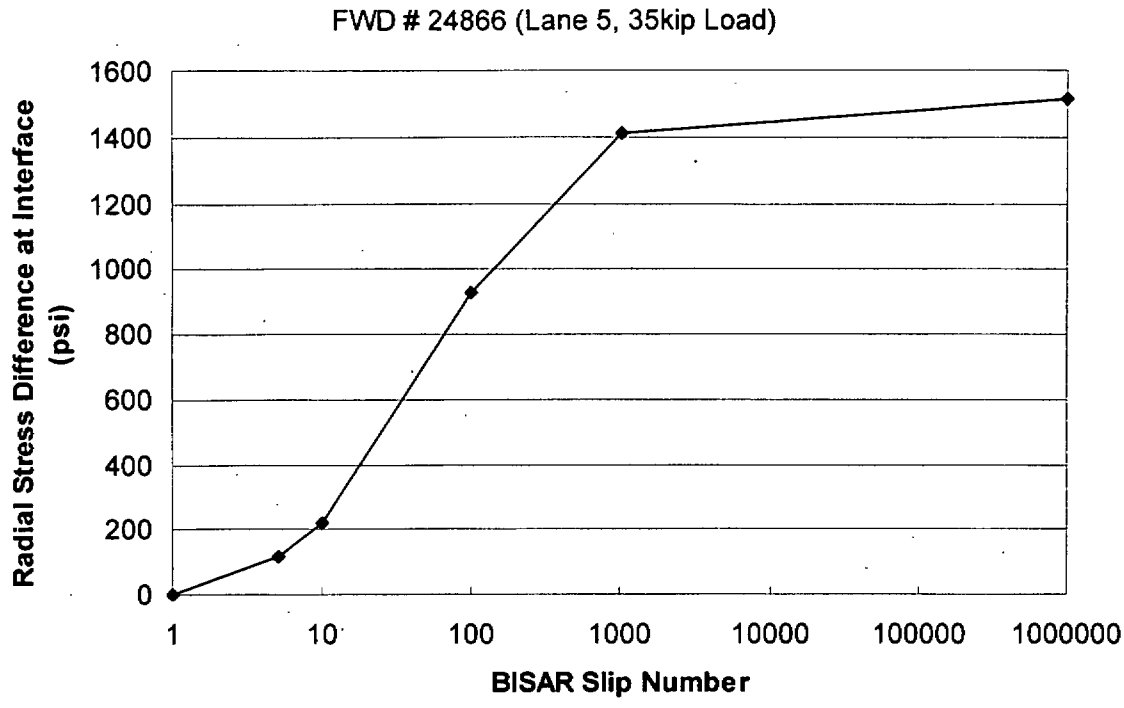

Figure J.3. FWD #24866 Radial Stress Difference vs. BISAR Slip Number

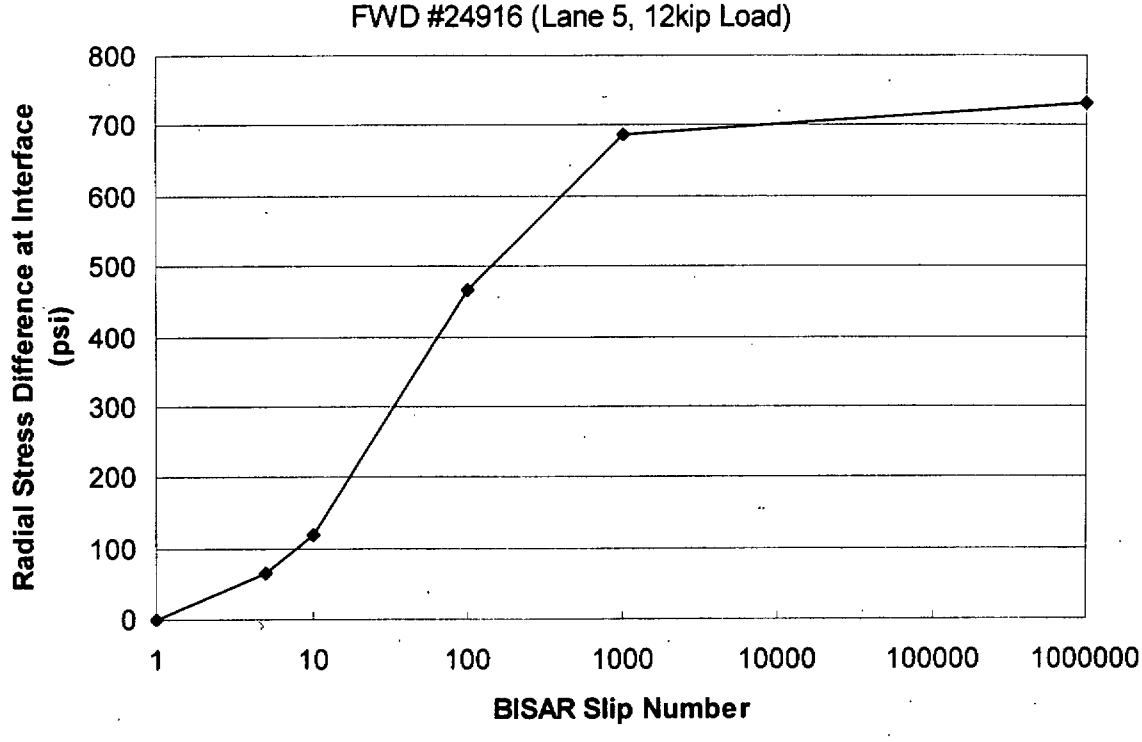

Figure J.4. FWD # 24916 Radial Stress Difference vs. BISAR Slip Number

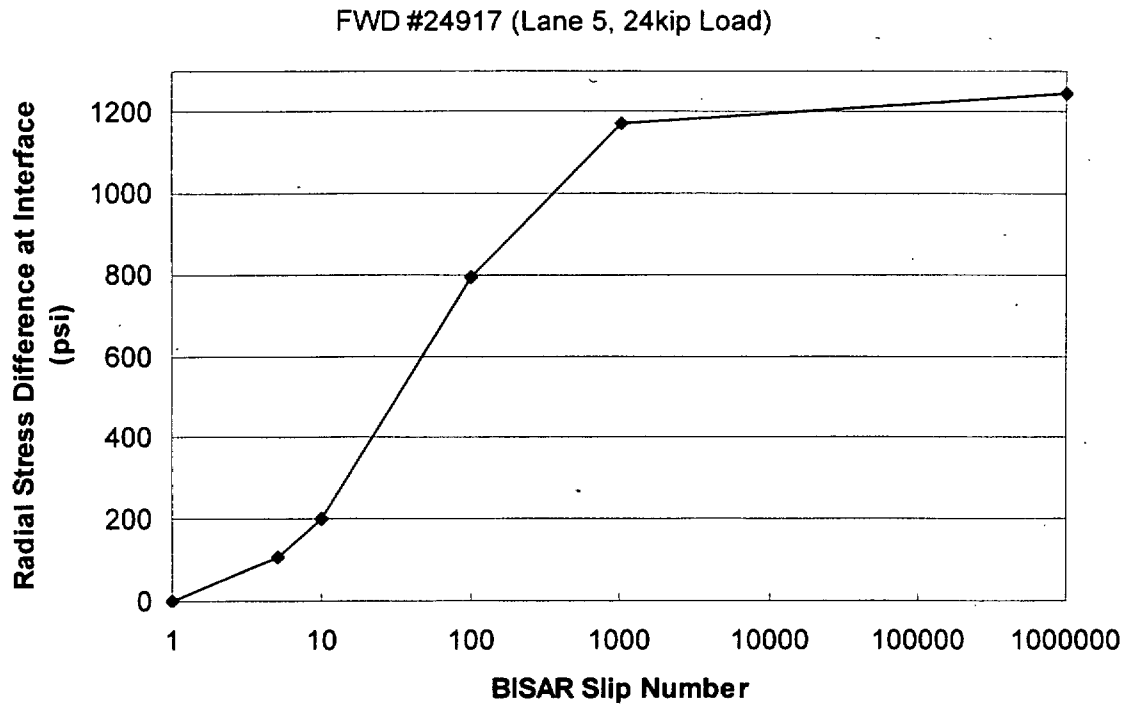

Figure J.5. FWD #24917 Radial Stress Difference vs. BISAR Slip Number

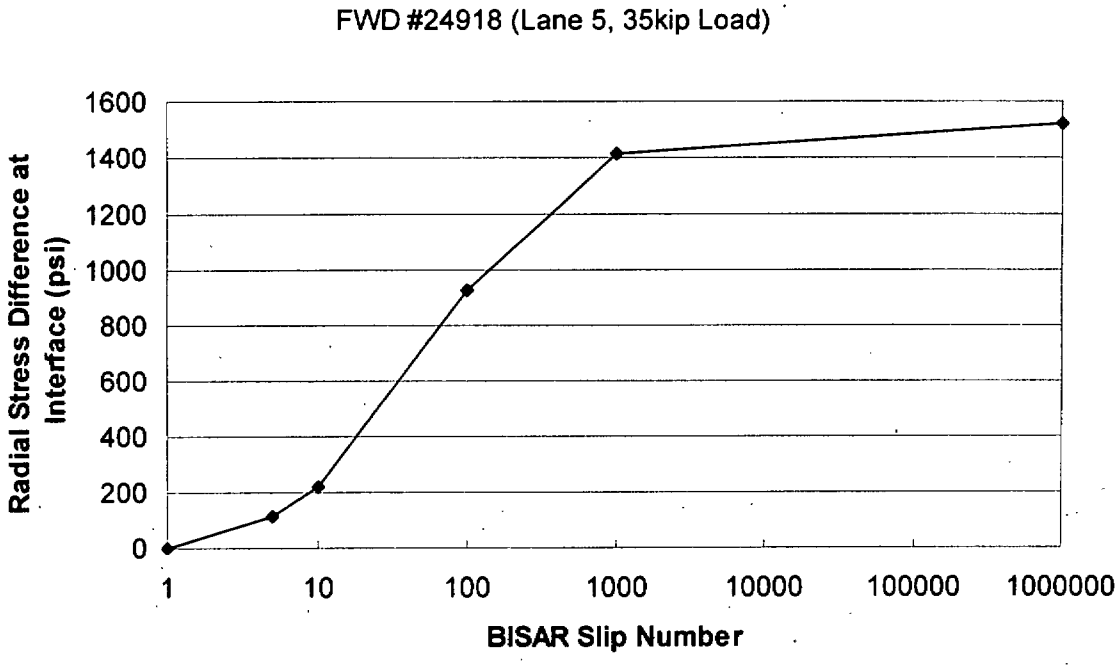

Figure J.6. FWD #24918 Radial Stress Difference vs. BISAR Slip Number

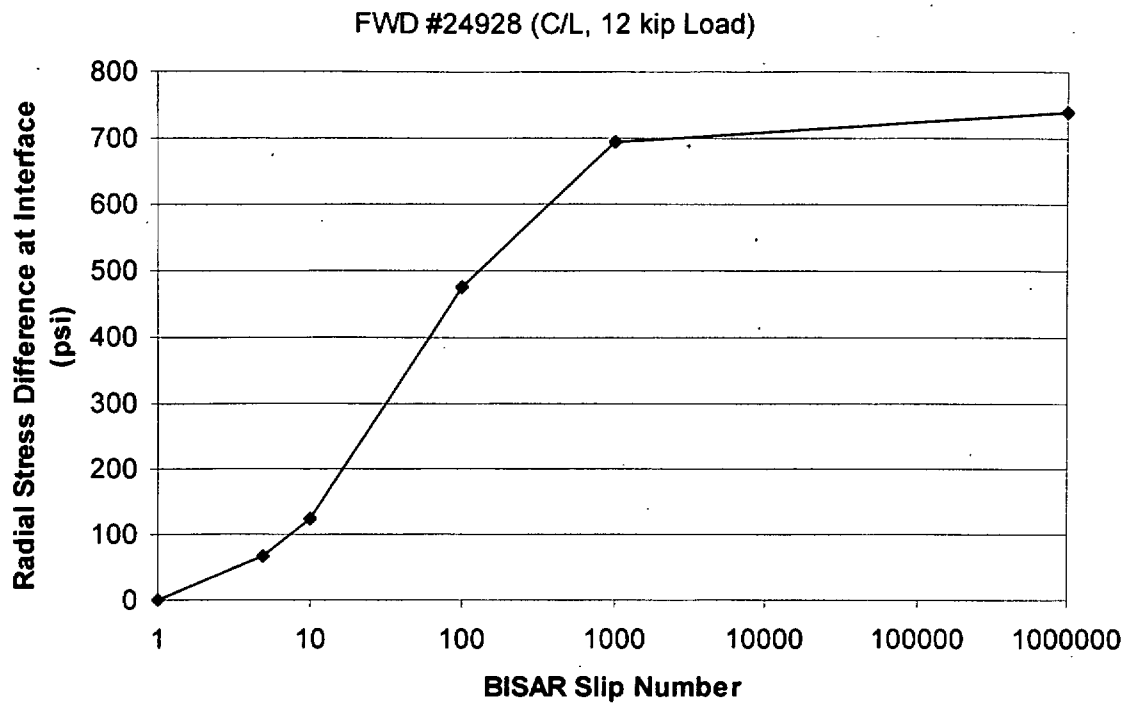

Figure J.7. FWD #24928 Radial Stress Difference vs. BISAR Slip Number

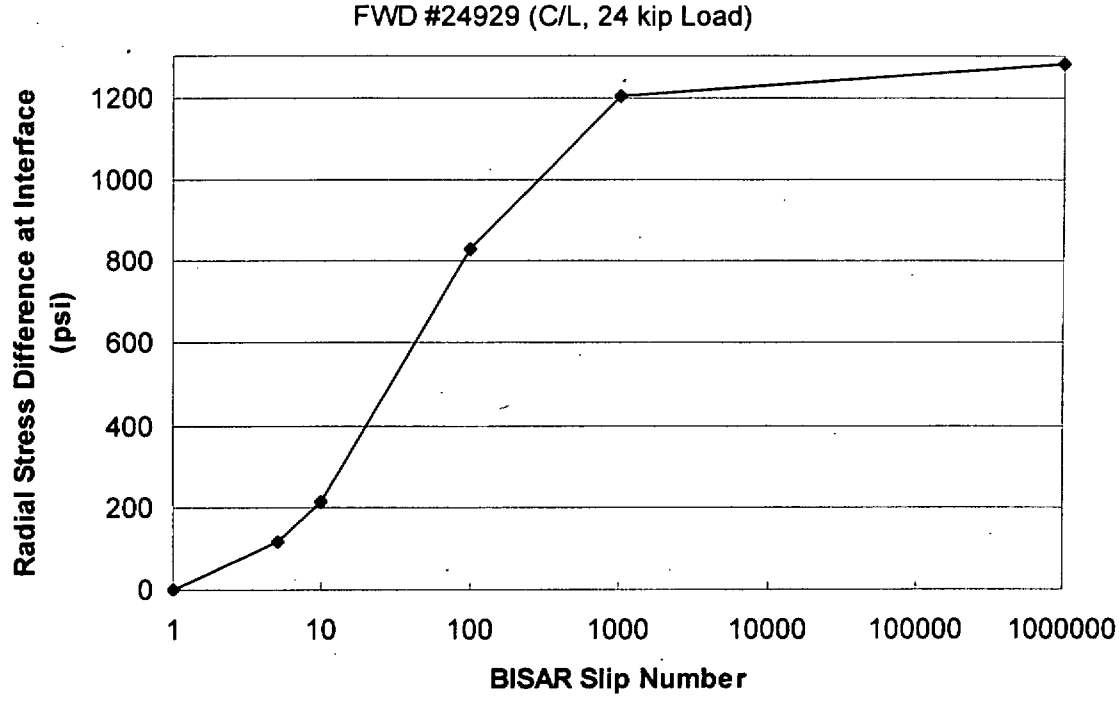

Figure J.8. FWD#24929 Radial Stress Difference vs. BISAR Slip Number

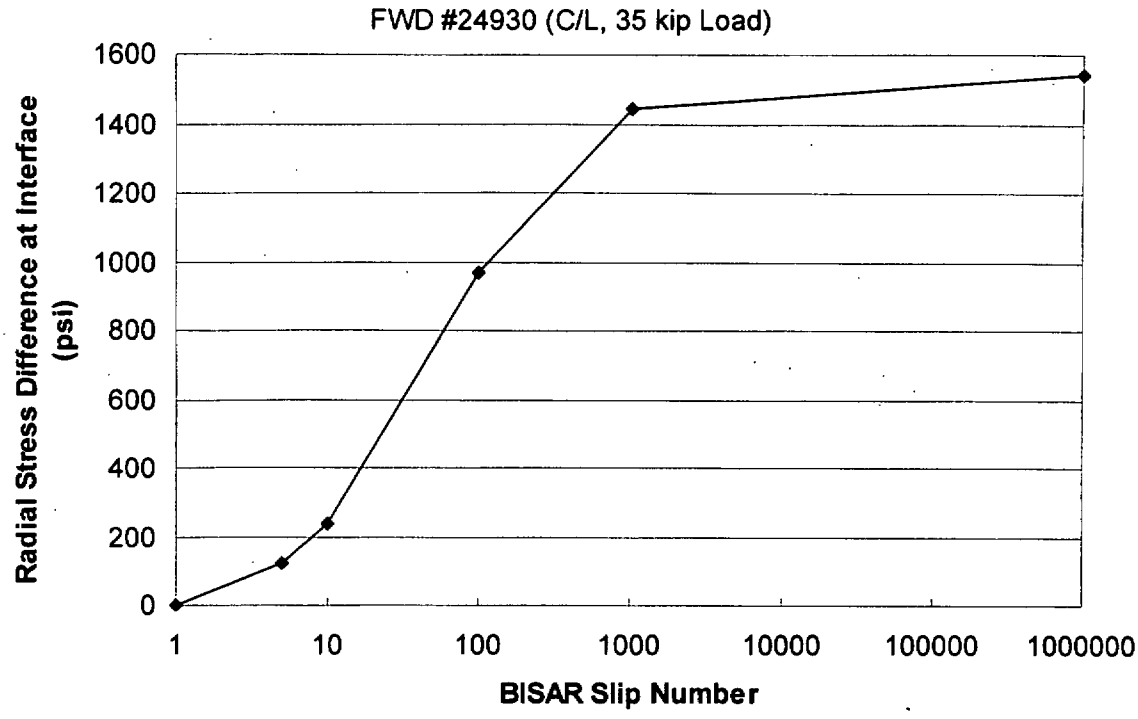

Figure J.9. FWD#24930 Radial Stress Difference vs. BISAR Slip Number

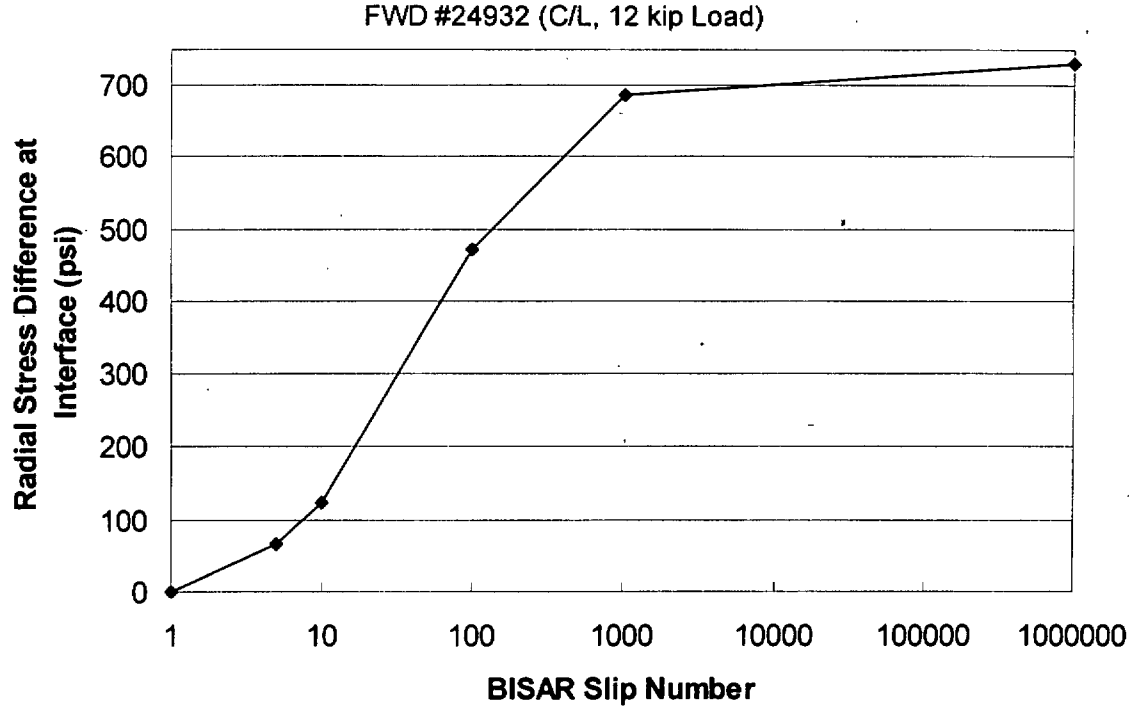

Figure J.10. FWD#24932 Radial Stress Difference vs. BISAR Slip Number

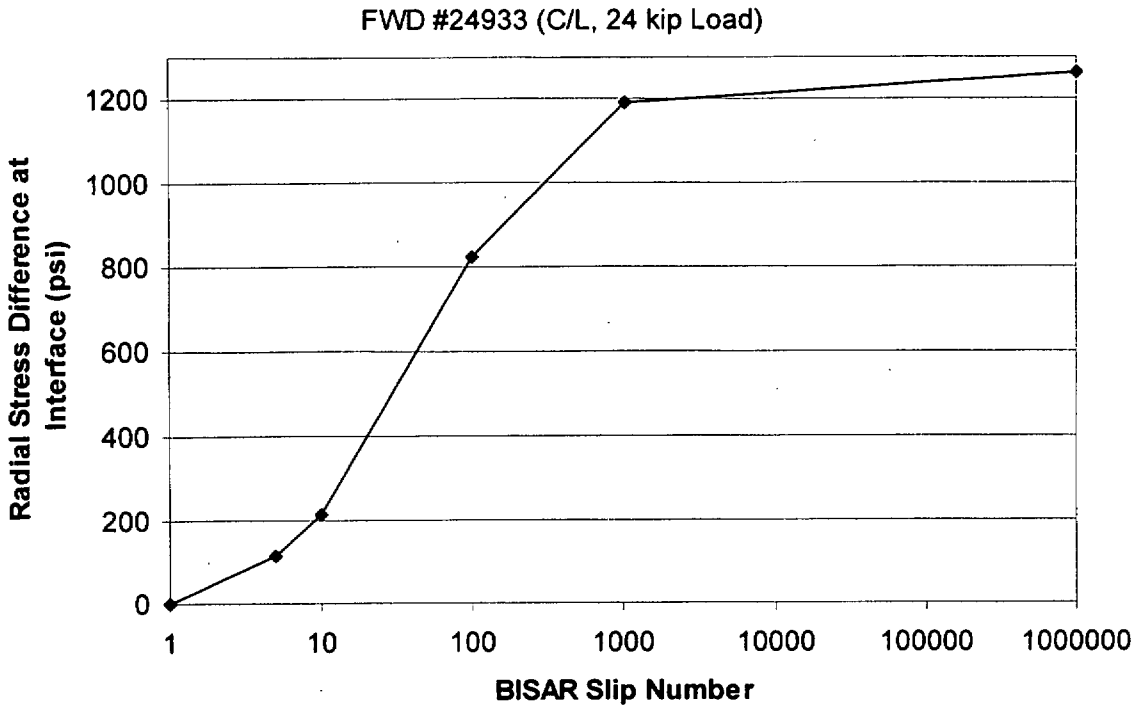

Figure J.11. FWD#24933 Radial Stress Difference vs. BISAR Slip Number

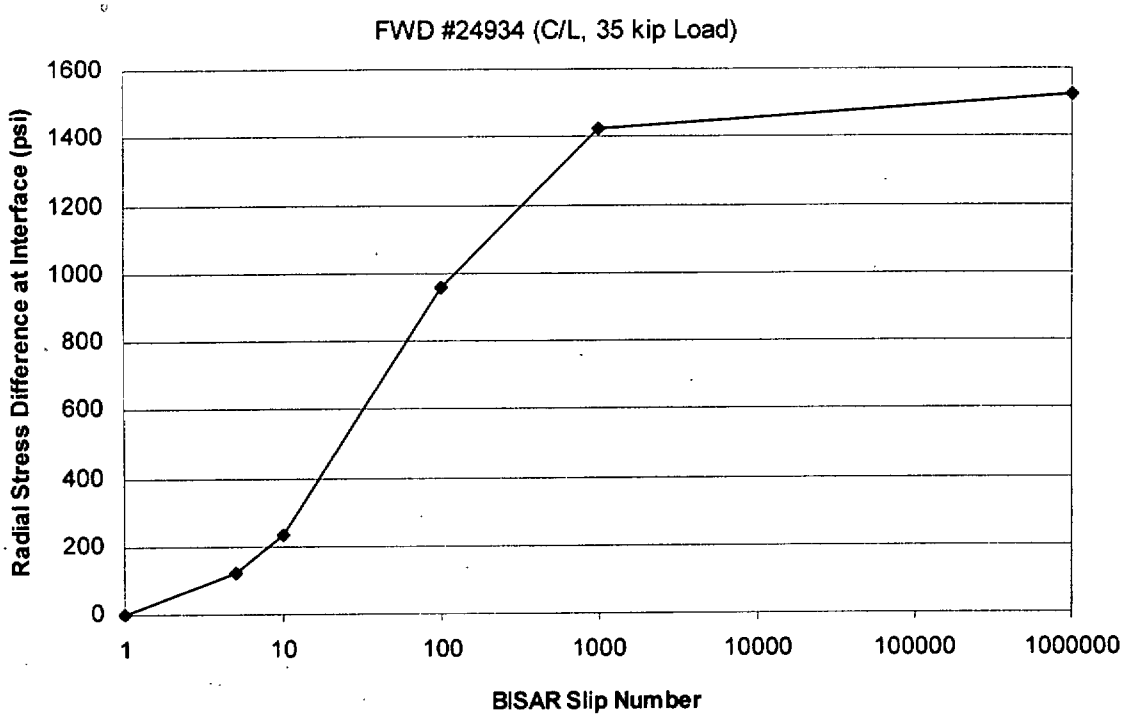

Figure J.12. FWD#24934 Radial Stress Difference vs. BISAR Slip Number